

**Characterizing the molecular mechanism of the AvrRpt2-RIN4-RPS2 defense-activation module**

Dissertation

Presented in Partial Fulfillment of the Requirements for the Degree Doctor of  
Philosophy

By

Maheen Alam,

Graduate Program in Department of Biology

SBA School of Science and Engineering  
Lahore University of Management Sciences

2021

Dissertation Committee:

Dr Syed Shahzad Ul Hussan, Ph.D. (Adviser)

Dr Ahmed Jawaad Afzal, Ph.D (Co-Adviser)

Dr Shaper Mirza, Ph.D

Dr Amir Faisal, Ph.D

## **Declaration**

The work described in this dissertation was carried out from August 2015 to June 2021 at Lahore University of Management Sciences, Pakistan and Ohio State University, USA under the supervision of Dr. Syed Shahzad Ul Hussan, Dr. Ahmed Jawaad Afzal and Dr David Mackey. I hereby declare that this submission is my own work and that, to the best of my knowledge and belief, contains no material previously published or written by another person neither has it been accepted for the award of any other degree or diploma at a university or any other institute of higher learning, except where due acknowledgment has been made in the text.

Maheen Alam

## **Dedication**

Dedicated to my mother, Yasmeen Obaid, a great human being, a loving mother and an amazing teacher. You will forever be my role model.

Dedicated to my father, Obaid Alam, for his unconditional love, support and encouragement.

Dedicated to my husband, Ahmed Jamal Waheed, for his love, support and patience throughout the challenges of graduate school and life; and without whom I would not have been able to make it.

## **Acknowledgments**

I am grateful to all the people that stood by my side and helped me throughout my graduate school journey. I would first like to thank my advisors Dr Ahmed Jawaad Afzal, Dr Syed Shahzad Ul Hussan and Dr David Mackey who made this possible. I am grateful to Dr Ahmed Jawaad Azal for giving me the opportunity to get a PhD and to work with him. I am fortunate that I was able to work in his lab and be trained by him during his time in LUMs. His passion for research and science has been a source of inspiration for me. Thank you for always believing in me, for pushing me harder and making me a better scientist. I am grateful to Dr Syed Shahzad Ul Hussan for taking me on as a graduate student and for supporting me. Thank you for always being so accommodating, supportive and understanding. I am glad that I had the opportunity to learn from him and train under him. I am truly grateful to Dr David Mackey for giving me the opportunity to work with him and for supporting me during my visit at OSU. I am indebted to him for his continued guidance, constructive feedback and support during my PhD. His approach towards research, passion for science and enthusiasm for training are truly inspirational. It has been an honor to work in his lab and to learn from him.

I am grateful to my committee members for their guidance, feedback and dedicating their time to my dissertation. I would also like to express my gratitude to all the faculty members in the Biology Department for their help and support. A very special thanks to Dr Muhammad Tariq and Dr Amir Faisal's lab for sharing their reagents, equipment and knowledge. I am grateful to Aishah Bilal for her constant help and support, but mostly her friendship.

I am thankful to my former lab (PMBG) members, Dr Muneeza Rai, Anam Siddiqui, Dr Bilal Haider, Maheen Hamayun, Amina Chaudhry and Hira Sohail for always being there for me and for believing in me. I am glad that I had a chance to work with them and to have made friends for life. I am grateful to the people that have contributed towards this project. I thankful to my current lab (BSB-LUMs) members, Amina Qadir, Saira Dar, Fareeha Hassan and Hafsa Iftikhar for their help with my research and for being so accommodating.

I am extremely grateful to the former and current Mackey lab members, Dr Mingzhe Shen, Dr Gayani Ekanayke, Dr Alex Turo, Laura Giese and Kelly Mikhail for all their help and for their friendship. I am truly grateful to Dr Mingzhe Shen who took time to train me and was always willing to help me. I am glad that our time overlapped and I was able to work with him. I would like to thank Laura Giese for managing the lab and making sure I always had what I needed. Thank

you for everything and for all your help. I am thankful to Gayani Ekanayke for her valuable feedback towards my research.

I am grateful to Dr Guo-Liang Wang's lab for sharing their reagents and equipment. A very special thanks to Dr Mazin Magzoub for inviting me to work in his lab and for supporting me during my stay at NYU-AD. It was a pleasure to work with him and his lab members.

I am extremely grateful to Priscila M Rodriguez Garcia for her constant help and support. Thank you for always being there for me, for encouraging me and helping me get to the end of my journey. I would also like to thank Annie Ashraf, Ankita Das, Swetha Rajasekaran, Sanket Walujkar and Zhongxia Yi for their help, support and encouragement, and mostly for their friendship.

Lastly, but most importantly, I am deeply grateful to my husband for his extraordinary support, love and patience. His encouragement and support made sure that I give everything it takes to finish what I started. I would like to thank my family, my parents and brother, for their unconditional love and encouragement throughout my life. Thank you for always believing in me.

## Table of Contents

|  |      |
|--|------|
| Acknowledgments.....   | 44   |
| Table of Contents .....  | 66   |
| List of Tables .....   | 99   |
| List of Figures.....   | 1010 |
| Abstract: .....  | 1313 |
| Chapter 1: Introduction to Plant immunity and RPM1 interacting protein 4 (RIN4).....   | 1515 |
| Chapter 2. Function of AvrRpt2-induced, defense suppressive fragments of RIN4 in RPS2 regulation.....  | 2222 |
| 2.1. Introduction:.....  | 2222 |
| 2.2. Results:.....   | 2525 |
| 2.2.1. Non membrane tethered RIN4 derivatives cause an RPS2-dependent HR-like cell death response.....   | 2525 |
| 2.2.2. Membrane tethered ACP3 derivative is able to suppress RPS2 in <i>N. benthamiana</i> .....   | 2727 |
| 2.2.3. Non-membrane tethered derivative, ACP2, fails to suppress RPS2 and is able to activate ACP3-suppressed RPS2.....                                  | 3030 |
| 2.2.4. ACP2 activates RPS2 suppressed by ACP3 when present in the cytosol.....   | 3333 |
| 2.3. Discussion:.....  | 3636 |
| Chapter 3. RIN4 homologs from important crop species differentially regulate the Arabidopsis NB-LRR immune receptor, RPS2 .....                          | 3939 |
| 3.1. Introduction .....  | 3939 |
| 3.2. Results .....   | 4141 |
| 3.2.1. RIN4 homologs are present in important crop species .....   | 4141 |
| 3.2.2. RIN4 homologs localize at the plasma membrane.....  | 4343 |
| 3.2.3. RIN4 homologs differ in their ability to suppress RPS2 .....  | 4747 |
| 3.2.4. Polymorphic amino acid residues present in the RIN4 homologs that might correlate with the (in)ability of the RIN4 homologs to suppress RPS2..... | 5555 |

|   |                        |
|---|------------------------|
| 3.2.5. AvrRpt2-mediated cleavage of YFP-AcV5-RIN4 <sup>ΔARCS1</sup> derivatives generates soluble and membrane-tethered cleavage products ..... | <a href="#">5656</a>   |
| 3.2.6. AvrRpt2-mediated cleavage of homologs results in the activation of RPS2 .....  | <a href="#">5959</a>   |
| 3.3. Discussion:.....   | <a href="#">6363</a>   |
| Chapter 4: Fragments of RIN4 produced by AvrRpt2 differ in their ability to suppress RPS2...  | <a href="#">6666</a>   |
| 4.1. Introduction: .....  | <a href="#">6666</a>   |
| 4.2. Results .....  | <a href="#">6969</a>   |
| 4.2.1. Fragments of RIN4 produced by AvrRpt2 differ in their ability to suppress RPS2 ....  | <a href="#">6969</a>   |
| 4.2.2. YFP-AcV5-AtRIN4 <sup>INT</sup> is unable to activate YFP-AtRIN4 <sup>CLV3</sup> suppressed RPS2 .....                                    | <a href="#">7373</a>   |
| 4.2.3. Non-membrane tethered AtRIN4 fragments fail to reactivate RPS2 suppressed by homologous Flag-AtRIN4 <sup>CLV3</sup> fragments. ....      | <a href="#">7777</a>   |
| 4.2.4. Homologous RIN4 <sup>INT</sup> derivatives are capable of activating RPS2-HA suppressed by Flag-AtRIN4 <sup>CLV3</sup> .....             | <a href="#">8181</a>   |
| 4.2.5. Homologous RIN4 <sup>INT</sup> derivatives are capable of activating RPS2-HA suppressed by homologous Flag-RIN4 <sup>CLV3</sup> .....    | <a href="#">8383</a>   |
| 4.3. Discussion .....   | <a href="#">8585</a>   |
| Chapter 5. RPS2 remains at the membrane during ectopic and AvrRpt2-induced activation .....   | <a href="#">8888</a>   |
| 5.1. Introduction: .....  | <a href="#">8888</a>   |
| 5.2. Results .....  | <a href="#">9090</a>   |
| 5.2.1. RPS2-YFP-HA and RPS2-HA are functionally comparable for cell death induction and RIN4-suppression in <i>Nicotiana benthamiana</i> . .... | <a href="#">9191</a>   |
| 5.2.2. RPS2 remains at the membrane during ectopic and AvrRpt2-induced activation .....   | <a href="#">9292</a>   |
| 5.3. Discussion .....   | <a href="#">9696</a>   |
| Conclusion: .....   | <a href="#">9898</a>   |
| Chapter 6 Methodology .....   | <a href="#">9999</a>   |
| 6.1. Plants and growth conditions .....   | <a href="#">9999</a>   |
| 6.2. Plasmid construction.....  | <a href="#">9999</a>   |
| 6.3. <i>Agrobacterium</i> -mediated transient expression .....  | <a href="#">102102</a> |
| 6.4. Confocal microscopy analysis.....  | <a href="#">102102</a> |
| 6.5. Protein extraction and SDS-PAGE .....  | <a href="#">103103</a> |

|   |                        |
|---|------------------------|
| <b>6.6. Subcellular fractionation</b> .....                 | <a href="#">103103</a> |
| <b>6.7. Quantification of hypersensitive response</b> ..... | <a href="#">104104</a> |
| <b>6.8. Protein alignment</b> .....                         | <a href="#">104104</a> |
| <b>6.9. Palmitoylation prediction</b> .....                 | <a href="#">104104</a> |
| <b>References:</b> .....                                    | <a href="#">106106</a> |

## List of Tables

|   |                        |
|---|------------------------|
| Table 3.1. Regions of AtRIN4 known to participate in immune regulation are well conserved in the homologous RIN4 proteins.. | <a href="#">4343</a>   |
| Table 3.2. Predicted C-terminal palmitoylation target sites within the RIN4 homologs..                                      | <a href="#">4444</a>   |
| Table 3.3 Polymorphic amino acids present in RIN4 homologs under study. .   | <a href="#">5656</a>   |
| Table 6.1 Oligonucleotides used in this study.....  | <a href="#">101401</a> |

## List of Figures

|   |                      |
|---|----------------------|
| Figure 1.1. Plant innate immunity.....  | <a href="#">1616</a> |
| Figure 1.2. RIN4 amino acid sequence.....   | <a href="#">1818</a> |
| Figure 1.3. AvrB and AvrRpm1 mediated phosphorylation of RIN4 results in the activation of RPM1.....  | <a href="#">2020</a> |
| Figure 1.4. AvrRpt2 mediated cleavage of RIN4 results in the activation of ETI in Arabidopsis.....  | <a href="#">2020</a> |
| Figure 2.1. Regulation of RPS2 by RIN4 in Arabidopsis.....  | <a href="#">2424</a> |
| Figure 2.2. Non-membrane-tethered derivatives of RIN4 cause an RPS2-dependent cell death response in Col-0.....   | <a href="#">2626</a> |
| Figure 2.3. Expression of a non-membrane tethered derivative, CCC>AAA, in the presence of full length RIN4 elicits an RPS2 dependent cell death in <i>Arabidopsis</i> plants..... | <a href="#">2727</a> |
| Figure 2.4. Cell death in <i>N. benthamiana</i> induced by different titers of agrobacteria expressing RPS2 and its suppression by ACP3.....                                      | <a href="#">2828</a> |
| Figure 2.5. Membrane tethering of RIN4 is required for RPS2 suppression.....  | <a href="#">3030</a> |
| Figure 2.6. Flag-ACP2 is capable of activating Flag-ACP3 suppressed RPS2-HA.....  | <a href="#">3333</a> |
| Figure 2.7. In the absence of the pathogen ACP2 is sufficient to activate ACP3 suppressed RPS2.....   | <a href="#">3434</a> |
| Figure 2.8. ACP2 activates RPS2 suppressed by ACP3 when present in the cytosol.....   | <a href="#">3636</a> |
| Figure 3.1. <i>In silico</i> analysis of RIN4 homologs from important crop plants.....  | <a href="#">4242</a> |
| Figure 3.2. Schematic diagram of RIN4 derivatives used in this study.....   | <a href="#">4646</a> |
| Figure 3.3. RIN4 homologs localize at the plasma membrane.....  | <a href="#">4747</a> |
| Figure 3.4. RIN4 homologs localize at the plasma membrane.....  | <a href="#">4949</a> |
| Figure 3.5. YFP-AtRIN4FL and YFP-Acv5-AtRIN4 <sup>ΔRCS1</sup> are comparable in their ability to suppress RPS2.....   | <a href="#">5050</a> |
| Figure 3.6. RIN4 homologs differ in their ability to regulate RPS2.....   | <a href="#">5252</a> |
| Figure 3.7. YFP-Acv5-MdRIN4 <sup>ΔRCS1</sup> suppresses RPS2-HA expressed in <i>N. benthamiana</i> .....  | <a href="#">5353</a> |
| Figure 3.8. YFP-Acv5-RIN4 <sup>ΔRCS1</sup> derivatives differ in their ability to suppress RPS2-HA introduced at a low or high titre in <i>N. benthamiana</i> .....               | <a href="#">5555</a> |

|   |                      |
|---|----------------------|
| Figure 3.9. AvrRpt2-mediated cleavage of the RIN4 homologs generates soluble, internal fragments. ....  | <a href="#">5858</a> |
| Figure 3.10. AvrRpt2-mediated cleavage of YFP-AcV5-RIN4 <sup>ΔRCSI</sup> derivatives generates fragments that is no longer membrane localized. ....       | <a href="#">5959</a> |
| Figure 3.11. Overexpression of AvrRpt2 in <i>N. benthamiana</i> results HR like cell death response.....  | <a href="#">6060</a> |
| Figure 3.12. AvrRpt2-mediated cleavage of the RIN4 homologs activates RPS2.....   | <a href="#">6262</a> |
| Figure 4.1. AvrRpt2 mediated cleavage of RIN4 results in the activation of ETI in Arabidopsis.....  | <a href="#">6767</a> |
| Figure 4.2. Schematic diagram of RIN4 derivatives used in this chapter. ....  | <a href="#">6868</a> |
| Figure 4.3. The YFP-RIN4 <sup>CLV3</sup> fragments are plasma membrane-localized and are capable of suppressing RPS2 in <i>N. benthamiana</i> . ....      | <a href="#">7070</a> |
| Figure 4.4. The YFP-AcV5-RIN4 <sup>INT</sup> fragments are soluble and fail to suppress RPS2 in <i>N. benthamiana</i> .....                               | <a href="#">7373</a> |
| Figure 4.5. Flag-AtACP2 and YFP-AcV5-AtRIN4 <sup>INT</sup> derivatives fail to activate YFP-AtRIN4 <sup>CLV3</sup> suppressed RPS2. ....                  | <a href="#">7575</a> |
| Figure 4.6. Homologous YFP-AcV5-RIN4 <sup>INT</sup> derivatives fail to activate RPS2 suppressed by homologous YFP-RIN4 <sup>CLV3</sup> derivatives. .... | <a href="#">7676</a> |
| Figure 4.7. Schematic diagram of RIN4 derivatives used in this chapter. ....  | <a href="#">7777</a> |
| Figure 4.8. The Flag-RIN4 <sup>CLV3</sup> fragments are capable of suppressing RPS2 in <i>N. benthamiana</i> .....  | <a href="#">7979</a> |
| Figure 4.9. Non-membrane tethered AtRIN4 fragments fail to activate RPS2 suppressed by homologous Flag-AtRIN4 <sup>CLV3</sup> fragments.. ....            | <a href="#">8181</a> |
| Figure 4.10. Homologous RIN4 <sup>INT</sup> derivatives are capable of activating RPS2-HA suppressed by Flag-AtRIN4 <sup>CLV3</sup> .....                 | <a href="#">8383</a> |
| Figure 4.11. Homologous RIN4 <sup>INT</sup> activate RPS2 suppressed by Homologous Flag-RIN4 <sup>CLV3</sup> . ....                                       | <a href="#">8484</a> |
| Figure 5.1. RPS2-YFP-HA and RPS2-HA are functionally comparable for cell death induction and RIN4-suppression in <i>N. benthamiana</i> .....              | <a href="#">9292</a> |
| Figure 5.2. RPS2 remains membrane-localized during ectopic and AvrRpt2-induced activation.....  | <a href="#">9494</a> |

Figure 5.3. Ectopically active and AcV5-AtRIN4<sup>11-211</sup> suppressed RPS2-YFP-HA are predominantly membrane localized in *N. benthamiana* cells..... [9595](#)

## Abstract:

The ability of pathogens to cause disease and hosts to resist pathogen invasion are components of an ongoing arms race. Plants rely on a multi-layered immune system to guard against pathogenic invasion. Detection of microbe associated molecular patterns (MAMPs), triggers the first layer of immunity called MAMP-triggered immunity (MTI). However, pathogens suppress this first layer by deploying virulence factors, including type three secreted effector (TTSE) proteins, in the host cell. In addition to suppressing MTI, these effectors potentially trigger a second layer of immunity, effector triggered immunity (ETI), through the activation of disease resistance (R) proteins. Plants utilize intracellular resistance (R) proteins to recognize pathogen effectors either by direct interaction or indirectly via effector-mediated perturbations of host components. RPM1-INTERACTING PROTEIN4 (RIN4) is a plant immune regulator that mediates the indirect activation of multiple, independently evolved R-proteins by multiple, unrelated effector proteins. One of these, RPS2 (RESISTANT TO *P. SYRINGAE*2), is activated upon cleavage of Arabidopsis (At)RIN4 by the *Pseudomonas syringae* effector AvrRpt2.

AvrRpt2 is a cysteine protease that, in order to promote pathogenicity, causes cleavage of RIN4. Two of the resulting fragments, namely AvrRpt2 cleavage product (ACP) 2 and ACP3, are potent suppressors of MTI. In resistant Arabidopsis plants, cleavage of RIN4 by AvrRpt2 elicits the activation of RPS2, which in turn activates an immune response. The currently favored model for RPS2 activation states that RPS2 is activated post AvrRpt2 mediated elimination of RIN4. However this model does not reconcile with the hypothesized link between the virulence activity of AvrRpt2 and the activation of RPS2. In this study we have demonstrated that in the presence of wild type RIN4, non-membrane tethered derivatives of RIN4 activate RPS2. Additionally we demonstrate that both ACP2 and ACP3 take up new roles in RPS2 regulation. While the membrane-tethered fragment, ACP3, retains the ability to suppress RPS2, the non-membrane tethered fragment, ACP2, fails to suppress RPS2 expressed in *Nicotiana benthamiana*. Furthermore we report that ACP2 is able to activate RPS2 suppressed by ACP3 fragment and that this activation occurs when ACP2 is present in the cytosol. These results link the AvrRpt2-induced cleavage fragments of RIN4 to the activation of RPS2.

To further gain insight into the AvrRpt2-RIN4-RPS2 defense-activation module, we compared the function of AtRIN4 with RIN4 homologs present in a diverse range of plant species. We selected seven homologs containing conserved features of AtRIN4, including two NOI (Nitrate induced) domains, each containing a predicted cleavage site for AvrRpt2, and a C-terminal palmitoylation site predicted to mediate membrane tethering of the proteins. Palmitoylation-mediated tethering of AtRIN4 to the plasma membrane and cleavage by AvrRpt2 are required for suppression and activation of RPS2, respectively. We have demonstrated that while all seven homologs localized at the plasma membrane, only four suppressed RPS2 when transiently expressed in *N. benthamiana*. All seven homologs were cleaved by AvrRpt2 and, for those homologs that were able to suppress RPS2, cleavage relieved suppression of RPS2. Further, we demonstrated that the membrane-tethered, C-terminal AvrRpt2-generated cleavage fragment is sufficient for the suppression of RPS2. Lastly, we show that the membrane localization of RPS2 is unaffected by its suppression or activation status.

## Chapter 1: Introduction to Plant immunity and RPM1 interacting protein 4 (RIN4)

The ability of pathogens to cause disease and hosts to resist pathogen invasion are components of an ongoing arms race. Plants, like animals, are susceptible to a wide range of bacterial, viral and fungal infections. However unlike animals, plants lack a multitude of mobile immune cells and hence rely on passive and active defenses to protect themselves against the invading pathogen (Dodds and Rathjen 2010; Toruno et al. 2019). Physical barriers such as the waxy cuticle, cell wall and stomates protect against pathogen invasion by hindering their entry into the cells (Chisholm et al. 2006; Toruno et al. 2019). In addition to the physical barriers, plants have developed a sophisticated multi-layered innate immune system that protects them against pathogens post-invasion (Dangl and McDowell 2006).

This multilayered immune system comprises of two branches (Figure 1.1); the first layer recognizes conserved microbial features known as microbe/pathogen associated molecular patterns (MAMPs or PAMPs), which are presented to the host during infection (Figure 1.1) (Dangl and McDowell 2006).

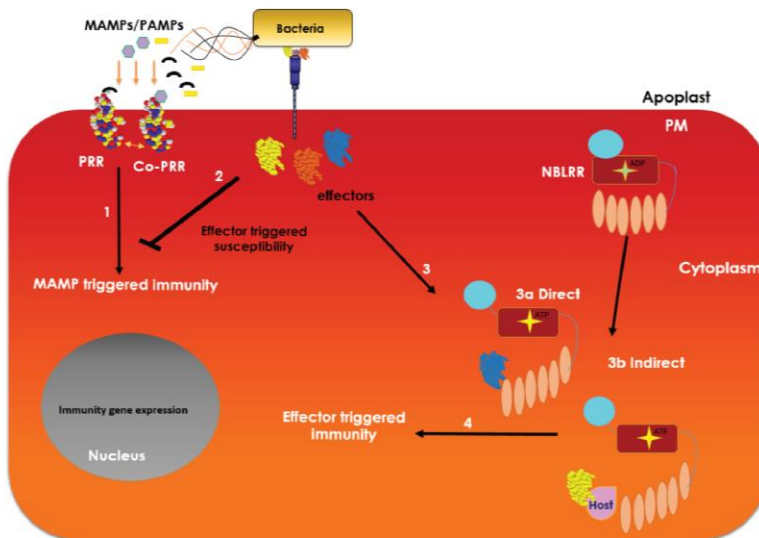


**Figure 1.1. Plant innate immunity.** (1) Pathogens such as bacteria express MAMPs/PAMPs during colonization of the plant cell. Host cell detects these molecules through PRR's which in turn elicits MTI, (2) To counter MTI, pathogens deliver effector proteins in the plant cell. This leads to a disease state called ETS, (3) Plants however, detect these effectors using intracellular receptors or resistance (R) proteins, 3a Detection of effectors by the R proteins can occur directly, 3b R proteins can also detect effector mediated modification of a host virulence target, (4) Detection of effectors by the R proteins results in the activation of ETI.

Pattern recognition receptors, receptor like kinases (RLKs) present on the surface of the plant cell, detect and bind to MAMPs, such as lipopolysaccharides, flagellin or chitin, which in turn leads to the activation of first layer of immunity, MAMP triggered immunity (MTI) (Figure 1.1) (Chisholm et al. 2006; Dangl and McDowell 2006; Toruno et al. 2019). MTI outputs include cell wall fortification, reactive oxygen species (ROS) production, activation of defense hormones and transcriptional reprogramming all of which restricts the growth of the pathogen (Chisholm et al. 2006; Dangl and McDowell 2006; Tahir et al. 2019).

MTI usually stops the infection, however in order to promote pathogenesis many pathogens have evolved to suppress MTI (Chisholm et al. 2006; Dangl et al. 2013). For instance the Gram-negative bacteria use a needle like apparatus, the type three secretion system (TTSS), to inject effector proteins into the plant cytosol to cause a disease like state known as effector triggered susceptibility (ETS) (Figure 1.1) (Dangl et al. 2013; Dangl and McDowell 2006). The secretion of these effectors comes with the risk to the pathogen as these proteins can be detected by a second group of receptors present within the plant cell (Figure 1.1) (Dangl et al. 2013; Tahir et al. 2019). These intracellular receptors known as the resistance (R) proteins specifically recognize the secreted effectors resulting in the activation of the second layer of immunity, the effector triggered immunity (ETI) (Figure 1.1) (Dangl and McDowell 2006). ETI results in a robust immune response, which usually culminates in programmed cell death (PCD) or hypersensitive response (HR) at the site of infection (Figure 1.1) (Chisholm et al. 2006; Dangl and McDowell 2006).

R proteins predominantly belong to the nucleotide binding and leucine rich repeat (NLRs) family of receptors that are capable of detecting effectors from a wide range of pathogens (Dangl et al. 2013). Initially, it was widely accepted that the R proteins directly recognize the effector proteins

(Dangl and McDowell 2006). This receptor-ligand model was supported by the fact that most of the effector proteins were small and localized with the corresponding R proteins in plant cells (Figure 1.1) (Dangl and McDowell 2006; van der Hoorn and Kamoun 2008). Direct mode of interaction between a few NLR and effector proteins has been determined (Dodds et al. 2006; van der Hoorn and Kamoun 2008). However for a majority of such combinations a physical interaction has not been determined and in those cases the effector recognition by the R protein is thought to be indirect (Dangl and McDowell 2006; van der Hoorn and Kamoun 2008). The indirect mode of detection is explained by the guard hypothesis which states that the effector targets and modifies a host protein (guardee), independent of the R protein, and this modification is then recognized by the corresponding R protein (guard) leading to the activation of an immune response (Figure 1.1) (Dangl and Jones 2001; van der Hoorn and Kamoun 2008). This indirect perception enables the plant cell to detect a wide range of effectors produced by a variety of pathogens. A well characterized example of a host effector target, that regulates both PTI and ETI in *Arabidopsis* is RPM1 interacting protein 4 (RIN4) (Figure 1.2) (Afzal et al. 2011; Chisholm et al. 2006; Chung et al. 2011; Chung et al. 2014; Dangl and McDowell 2006; Mackey et al. 2003; Toruno et al. 2019).

RIN4 is a small intrinsically unstructured protein that contains two NOI (Nitrate induced) domains (with no known function) and is tethered to the membrane due to the palmitoylation of the C-terminal cysteine residues (Figure 1.2) (Afzal et al. 2013; Toruno et al. 2019). The importance of RIN4 to plant immunity is evident from the fact that it is targeted by five unrelated effectors, AvrRpm1, AvrB, AvrRpt2, HopF2 and HopZ3 secreted by *Pseudomonas syringae* (Lee et al. 2015; Mackey et al. 2003; Mackey et al. 2002; Redditt et al. 2019; Wilton et al. 2010). In the absence of the pathogen *Arabidopsis* RIN4 negatively regulates MTI (Afzal et al. 2011; Mackey et al. 2002). The effectors that target RIN4 promote virulence, at least in part, by enhancing its negative regulation of MTI (Kim et al. 2005b). For example HopF2 promotes growth of *P. syringae* in the presence of RIN4 in *Arabidopsis* plants. This activity of HopF2 may be dependent on its putative ADP-ribosyltransferase activity (Wilton et al. 2010).



**Figure 1.2. RIN4 amino acid sequence.** Wild type RIN4 (211 amino acids) contains two domains of unknown function (NOI) and a predicted palmitoylation site of three cysteine residues present near the C-terminal end. RIN4 is targeted by *P. syringae* T3E, AvrRpt2, which cleaves RIN4 at RCS1 and RCS2.

Two sequence-unrelated effectors, AvrB and AvrRpm1, mediate hyper-phosphorylation of RIN4 by increasing the expression of *Arabidopsis* RIN4 interacting protein kinase (RIPK) (Chung et al. 2011; Desveaux et al. 2007; Mackey et al. 2002). These effectors modify RIN4 in order to interfere with its ability to regulate PTI (Chung et al. 2014). Detection of a MAMP, flg22 (flagellin peptide) triggers the accumulation of RIN4 phosphorylated at Serine (S) 141 which in turn activates MTI (Chung et al. 2014). AvrB and AvrRpm1 act with a host kinase to phosphorylate RIN4 at Threonine 166 (Thr166), which is present in the C-NOI conserved motif (Y/FTXXF) (Figure 1.3) (Chung et al. 2011). Phosphorylation at Thr166 is epistatic to phosphorylation at S141 (Chung et al. 2014). Therefore AvrB and AvrRpm1 promote bacterial virulence by suppressing PTI responses activated by RIN4 phosphorylated at S141 (Chung et al. 2014). AvrRpm1 also promotes phosphorylation of RIN4 at Thr166 through its ADP-ribosyltransferase activity (Redditt et al. 2019). AvrRpm1 dependent ADP-ribosylation of RIN4 also results in the association of the modified RIN4 with EXO70 (an exocyst subunit), which in turn inhibits the secretion of compounds that regulate MTI (Redditt et al. 2019).

A fourth effector, AvrRpt2, is a cysteine protease that results in the cleavage of RIN4 at a conserved motif, VPXFGXW, present in the RIN4 cleavage site (RCS) 1 and 2, in the N-NOI and the C-NOI respectively (Figure 1.2) (Axtell and Staskawicz 2003; Chisholm et al. 2005; Kim et

al. 2005a; Mackey et al. 2003). Cleavage of RIN4 at these sites results in the generation of three fragments termed AvrRpt2 cleavage product 1 (ACP1, AtRIN4<sup>1-10</sup>), ACP2 (AtRIN4<sup>11-152</sup>) and ACP3 (AtRIN4<sup>153-211</sup>) (Figure 1.4) (Afzal et al. 2011; Kim et al. 2005a). Two of the resulting fragments, ACP2 and ACP3, are hyperactive suppressors of MTI relative to full length AtRIN4 (Afzal et al. 2011). Hence AvrRpt2 targets RIN4 to promote bacterial virulence by inhibiting MTI. Taken together these findings indicate that effector induced modifications of RIN4 result in MTI suppression.

In addition to regulating MTI, RIN4 also regulates ETI through effector-induced activation of R proteins in *Arabidopsis*. AtRIN4 associates with two plasma membrane localized NLRs, RPM1 and RPS2 in *Arabidopsis* (Axtell and Staskawicz 2003; Mackey et al. 2003; Mackey et al. 2002). In the absence of the pathogen, RIN4 maintains the accumulation of RPM1 and negatively regulates both RPM1 and RPS2 (Figure 1.3 and 1.4) (Mackey et al. 2003; Mackey et al. 2002). Perturbation of RIN4, particularly phosphorylation at Thr166 residue caused by AvrRpm1 and AvrB elicits the activation of RPM1 (Figure 1.3) (Chung et al. 2011; Liu et al. 2011; Mackey et al. 2002); whereas AvrRpt2 mediated cleavage of RIN4 elicits the activation of RPS2 (Figure 1.4) (Axtell and Staskawicz 2003; Day et al. 2005; Kim et al. 2005a; Mackey et al. 2003). Taken together these findings establish RIN4 as a hub that regulates both branches of immunity in *Arabidopsis*.

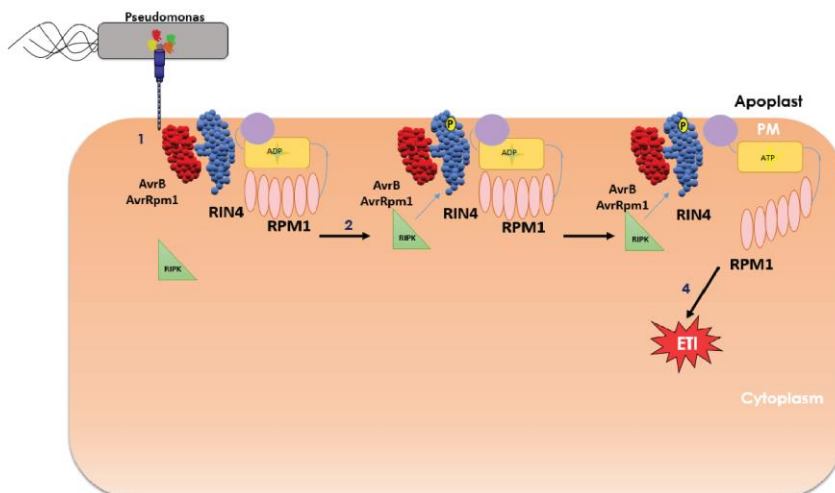


**Figure 1.3. AvrB and AvrRpm1 mediated phosphorylation of RIN4 results in the activation of RPM1.** (1) *P. syringae* secretes the effectors in plant cytosol using the T3SS, (2) AvrB and AvrRpm1 induce RIPK to hyper-phosphorylate RIN4, (3) Effector mediated perturbation of RIN4 elicit RPM1 activation and (4) Activated RPM1 elicits an ETI response.

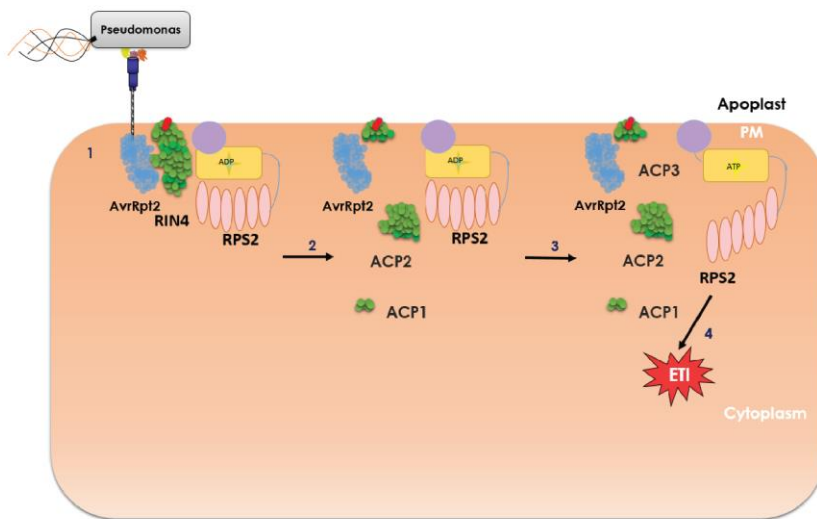


**Figure 1.4. AvrRpt2 mediated cleavage of RIN4 results in the activation of ETI in Arabidopsis.** (1) *P. syringae* secretes AvrRpt2 in plant cytosol using the T3SS, (2) AvrRpt2, once activated inside the host cell, results in the cleavage of RIN4, (3) Cleavage of RIN4 by AvrRpt2 activates RPS2 and (4) Activated RPS2 then elicits ETI.

Although recent studies provide detailed information about the host targets of the pathogen effectors, the exact mechanisms by which they regulate host defenses remains unclear. Similarly in case of RIN4, even though progress is being made towards understanding how it functions in Arabidopsis, little is known about how effector induced perturbations of RIN4 activate NLR mediated ETI. Our research presented here aims towards understanding the molecular mechanism of AvrRpt2-RIN4-RPS2 defense activation module. In this study we have demonstrated that membrane attachment of RIN4 is required for RPS2 suppression. We have also demonstrated that AvrRpt2 induced cleavage fragments are involved in RPS2 regulation. Based on our findings we

propose a new model for RPS2 activation, where the cleavage of RIN4 by AvrRpt2 results in the generation of two fragments, with ACP3 still capable of suppressing RPS2 and ACP2 capable of overcoming this suppression to activate RPS2. We further extend our findings to understand the role of RIN4 homologs in regulating RPS2. Finally we have determined that similar to RIN4 suppressed RPS2, both ectopically and effector activated RPS2 remain membrane localized. Collectively our results have contributed towards understanding how AvrRpt2 mediated cleavage of RIN4 activates RPS2.

## Chapter 2. Function of AvrRpt2-induced, defense suppressive fragments of RIN4 in RPS2 regulation

### 2.1. Introduction:

RIN4 is a multifunctional protein that regulates both MTI and ETI in Arabidopsis (Afzal et al. 2011; Chung et al. 2014; Mackey et al. 2003). In the absence of the pathogen RIN4 negatively regulates MTI (Mackey et al. 2003). RLCK-mediated perception of flg22, a peptide MAMP from within the flagellin protein, subsequently results in phosphorylation of RIN4 at S141, which relieves suppression of MTI by RIN4 permitting stronger activation of MTI outputs (Chung et al. 2014). Multiple effectors secreted by *Pseudomonas syringae* target RIN4 to promote virulence partly by enhancing its negative regulation of MTI (Chung et al. 2014; Kim et al. 2005b; Lee et al. 2015). For example, in order to promote virulence, AvrB and AvrRPM1, two sequence unrelated effectors secreted by *P. syringae*, cause hyper-phosphorylation of RIN4 (Chung et al. 2011; Chung et al. 2014). The effectors act with a host kinase to specifically increase the levels of RIN4 phosphorylated at Threonine (Thr) 166 (Chung et al. 2011; Liu et al. 2011). Phosphorylation of RIN4 at Thr166 is epistatic to S141 phosphorylation (Chung et al. 2014). Therefore the effectors contribute towards pathogen virulence by phosphorylating RIN4 to maintain its suppression of MTI. Another example is of AvrRpt2, a cysteine protease secreted by *P. syringae*, that cleaves RIN4 at the conserved motif VPXFGXW, known as RCS1 and RCS2 (RIN4 cleavage sites), in the N and the C-NOI domains respectively (Axtell and Staskawicz 2003; Chisholm et al. 2005; Kim et al. 2005a; Takemoto and Jones 2005). Cleavage of RIN4 by AvrRpt2 at these sites results in the generation of three fragments, namely ACP1 (AtRIN4<sup>1-10</sup>), ACP2 (AtRIN4<sup>11-152</sup>) and ACP3 (AtRIN4<sup>153-211</sup>) (Afzal et al. 2011; Chisholm et al. 2005; Kim et al. 2005a). Two of these fragments, ACP2 and ACP3 persist post cleavage and are hyperactive suppressors of MTI in comparison to full length RIN4 (Afzal et al. 2011). Therefore AvrRpt2 promotes virulence by generating fragments of RIN4 that further inhibit MTI.

RIN4 physically associates with and suppresses RPS2, an NLR protein present in Arabidopsis (Day et al. 2005; Mackey et al. 2003). The C-terminal cysteine residues are predicted to serve as a site for palmitoylation and membrane attachment of RIN4 (Day et al. 2005; Takemoto and Jones 2005). Membrane localization of RIN4 is correlated with its ability to suppress RPS2 (Figure 2.1a)

(Day et al. 2005). In the absence of RIN4, ectopic activation of RPS2, defined as activation occurring in the absence of an effector, results in seedling lethality (Figure 2.1b) (Day et al. 2005; Mackey et al. 2003). In *Arabidopsis* species that have RPS2, AvrRpt2-mediated cleavage of RIN4 elicits the activation of RPS2 resulting in ETI (Figure 2.1c) (Mackey et al. 2003). Taken together this indicates that the interaction between RIN4 and RPS2 results in the suppression of the NLR protein and cleavage of RIN4 by the effector results in the complete activation of RPS2. However, to this date, the mechanism of RPS2 activation in the presence of the effector remains unknown.

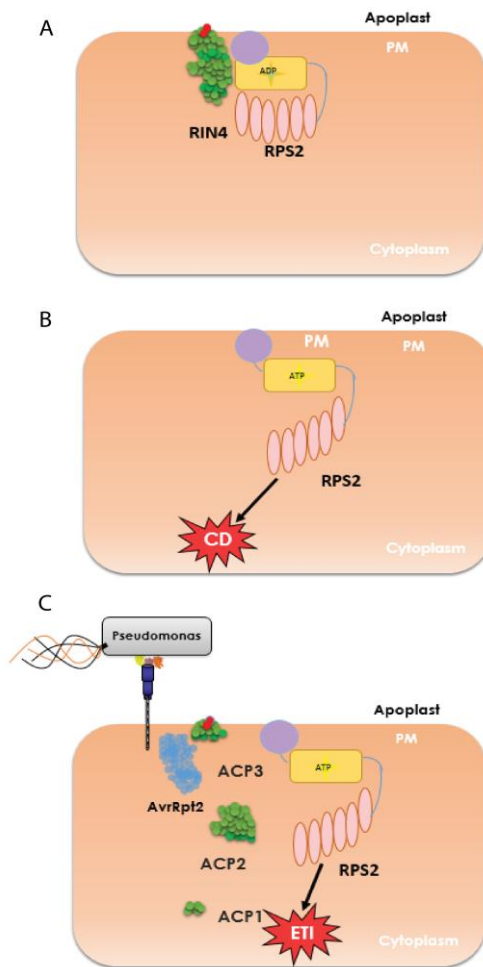


**Figure 2.1. Regulation of RPS2 by RIN4 in Arabidopsis.** (A) RIN4, when tethered at the membrane, negatively regulates RPS2. (B) In the absence of RIN4, RPS2 becomes ectopically active leading to cell death. (C) AvrRpt2, once inside the host cell, results in the cleavage of RIN4 which elicits RPS2 activation.

The generally accepted model for RPS2 activation states that RPS2 activates signaling upon perception of AvrRpt2-mediated elimination of RIN4. We have previously demonstrated that the non-membrane tethered (lacking the terminal cysteine residues required for palmitoylation) derivatives of RIN4, in comparison to wild type RIN4 are more potent suppressors of MTI (Afzal et al. 2011). These derivatives, when expressed in the presence of the full length RIN4, also activate a cell death response which is similar to an NLR mediated immune response (Afzal et al. 2011). The expression of these non-membrane tethered derivatives in the presence of wild type RIN4 resembles the scenario where both the soluble, ACP2, and membrane tethered, ACP3, fragments are generated by AvrRpt2. Thus, we speculate that post AvrRpt2 mediated cleavage of RIN4, the production of non-membrane tethered fragment, ACP2, might elicit RPS2 activation in the presence of the membrane tethered fragment, ACP3. However there is no evidence that links the AvrRpt2-induced cleavage fragments of RIN4 to RPS2 activation.

Recently, it has been demonstrated that AvrRpt2-mediated cleavage of MdRIN4 results in the activation of an independently evolved NLR-protein, Mr5 in apple (Prokhorchik et al. 2020). In the absence of the pathogen, AtRIN4 prevents ectopic activation of RPS2 in *Arabidopsis* and *Nicotiana benthamiana* plants (Day et al. 2005; Mackey et al. 2003). However, MR5 is not ectopically active when expressed by itself in *N. benthamiana* plants (Prokhorchik et al. 2020). Interestingly MdACP3 is sufficient to activate MR5 expressed in *N. benthamiana* plants (Prokhorchik et al. 2020). This indicates that in case of Apple the ACP3 fragment generated upon RIN4 cleavage is sufficient for the activation of Mr5 protein. Therefore we hypothesized that AvrRpt2-induced, defense suppressive fragments of RIN4 might also be involved in RPS2 regulation.

In this chapter we report that in the presence of full length RIN4, non-membrane tethered derivatives of RIN4 result in the activation of RPS2. We further report that two cleavage fragments, ACP2 and ACP3 differ in their ability to regulate RPS2 expressed in *N. benthamiana*. The membrane tethered, ACP3 fragment is able to suppress RPS2, while the non-membrane

tethered ACP2 fragment is unable to suppress RPS2 activation. Furthermore we report that ACP2 is able to activate RPS2 suppressed by ACP3 fragment. Taken together these results link the AvrRpt2-induced cleavage fragments of RIN4 to the activation of RPS2.

## **2.2. Results:**

### **2.2.1. Non membrane tethered RIN4 derivatives cause an RPS2-dependent HR-like cell death response**

The CCC motif present near the carboxy-terminal end of RIN4 serves as a site for palmitoylation (Takemoto and Jones 2005). Palmitoylation of the terminal cysteine residues is responsible for membrane localization of RIN4. We have previously shown that derivatives of RIN4 (177 $\Delta$ 211 and CCC>AAA) that lack the terminal cysteine residues, either due to deletion of the last 35 amino acids or mutation of the C-terminal cysteine residues to alanine, are no longer membrane localized (Afzal et al. 2011). Inducible expression of these derivatives in wild type Arabidopsis plants elicits a cell death response that resembles HR elicited by NLR proteins (Afzal et al. 2011). We have also shown that in mutant plants that lack both RPM1 and RPS2, these derivatives fail to induce cell death (Afzal et al. 2011). Based on this we speculated that the cell death response activated upon the induction of these derivatives might be dependent on the activation of either RPM1 or RPS2.

To determine whether the cell death activated by the expression of the non-membrane tethered derivatives is dependent on these NLR proteins, transgenic lines expressing dex-inducible RIN4FL, 177 $\Delta$ 211 and CCC>AAA were established in *rpm1-3* or *rps2-101C* single mutant or *rpm1rps2* double mutant Arabidopsis plants (Figure 2.2a). Figure 2.2b and c show that expression of either 177 $\Delta$ 211 or CCC>AAA in the *rpm1* background resulted in macroscopic cell death. However expression of 177 $\Delta$ 211 or CCC>AAA in either *rps2* or *rpm1rps2* double mutant plants failed to elicit cell death (Figure 2.2b and c). The difference in cell death cannot be attributed to the differential expression of 177 $\Delta$ 211 or CCC>AAA. As shown in figure 2.2d, 177 $\Delta$ 211 is detected in both the *rpm1* and *rps2* backgrounds. However, the CCC>AAA derivative could not be detected in the *rpm1* background, likely due to the stronger cell death response it elicits in comparison to 177 $\Delta$ 211. Taken together these results indicate that expression of non-membrane tethered derivatives of RIN4 elicits an RPS2-dependent cell death response in Arabidopsis plants (Figure 2.3).

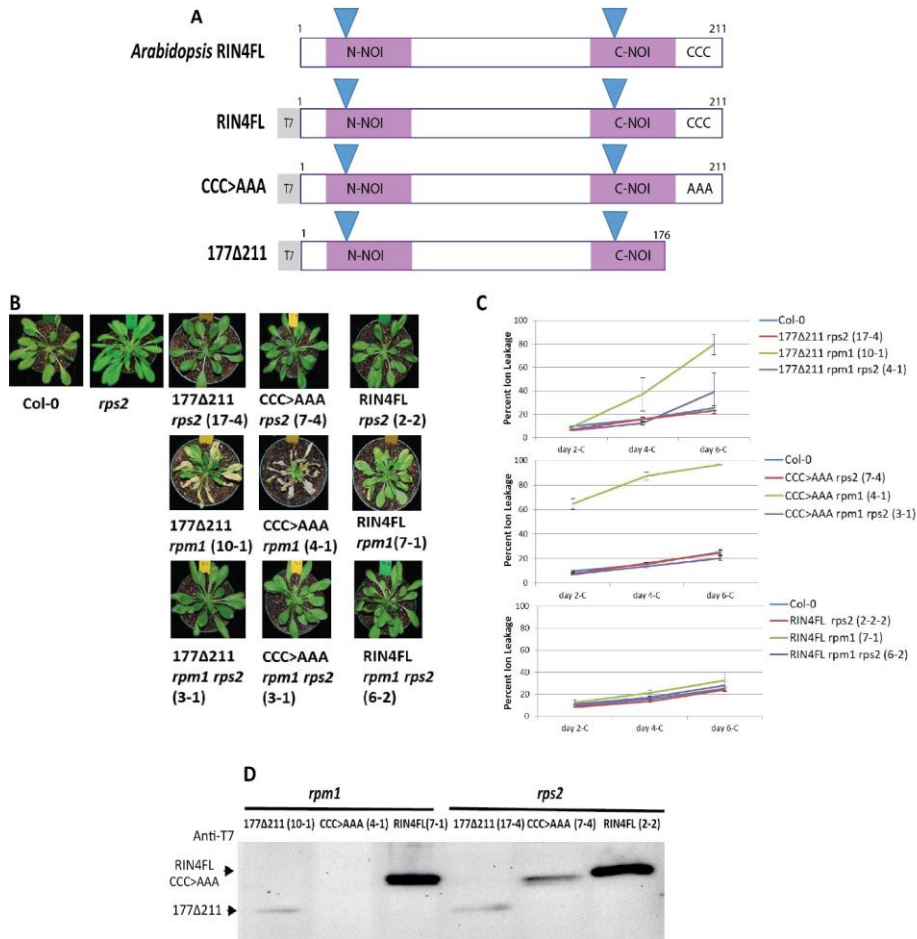


**Figure 2.2. Non-membrane-tethered derivatives of RIN4 cause an RPS2-dependent cell death response in Col-0.** (A) RIN4 derivatives used in this assay included Wt RIN4, RIN4FL, CCC>AAA (mutation of acylation site Cysteines to Alanines), 177Δ211 (deletion of 35 C-terminal residues). RIN4 derivatives under the control of a Dex-inducible promoter were used to generate stable transgenic lines. The dexamethasone inducible constructs had an N-terminal T7-tag (gray box). (B) Expression of 177Δ211 and CCC>AAA in Col-0 causes a cell death response in *rpm1* but not in *rps2* plants. Pictures showing plant phenotypes were taken 72 hours post Dexamethasone spray. (C) Cell death in **b** was quantified through ion leakage. Leaf discs from Col-0, *rpm1*, *rps2*

and *rpm1 rps2* plants were collected 2 days post dexamethasone induction, immersed in sterile water and conductivity of the bath solution was measured at the indicated time points. Data represents 1 of 3 independent experiments with at least 3 technical replicates per transgenic line. Error bars represent standard error of the mean (SEM). **(D)** Anti-T7 Western Blot confirming protein accumulation of CCC>AAA and 177Δ211 in *rpm1* and *rps2*. CCC>AAA is undetectable in *rpm1* due to excessive cell death. Arrows indicate positions of individual RIN4 derivatives.

Formatted: Font: Not Bold  
Formatted: Font: Italic

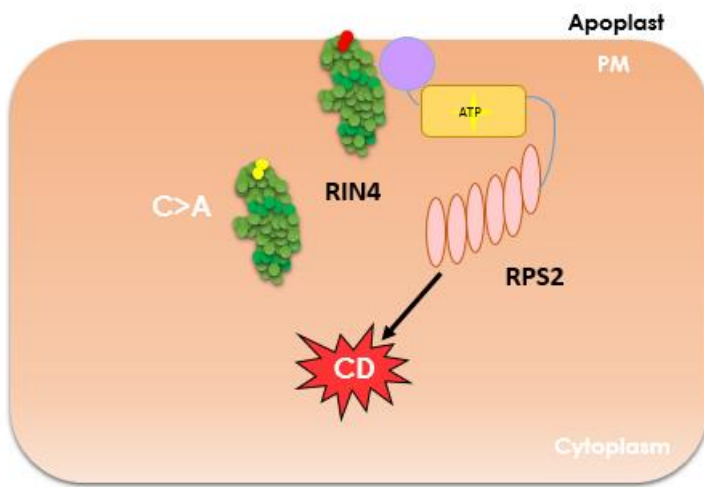


**Figure 2.3. Expression of a non-membrane tethered derivative, CCC>AAA, in the presence of full length RIN4 elicits an RPS2 dependent cell death in *Arabidopsis* plants.**

### 2.2.2. Membrane tethered ACP3 derivative is able to suppress RPS2 in *N. benthamiana*

Membrane localization of RIN4 correlates with its ability to suppress RPS2 (Day et al. 2005). Since the ACP3 cleavage fragment remains membrane localized, due to the presence of the C-terminal palmitoylation group, we hypothesized that this fragment might also be able to suppress RPS2. For this purpose we expressed Flag-ACP3 along with RPS2-HA in the heterologous system, *N. benthamiana* (Figure 2.4). We used *N. benthamiana* for the expression of our constructs because it has been widely used to determine protein expression and localization and to understand the biochemical interactions between different plant proteins, including RIN4 and RPS2 (Day et al. 2005; Tai et al. 1999).

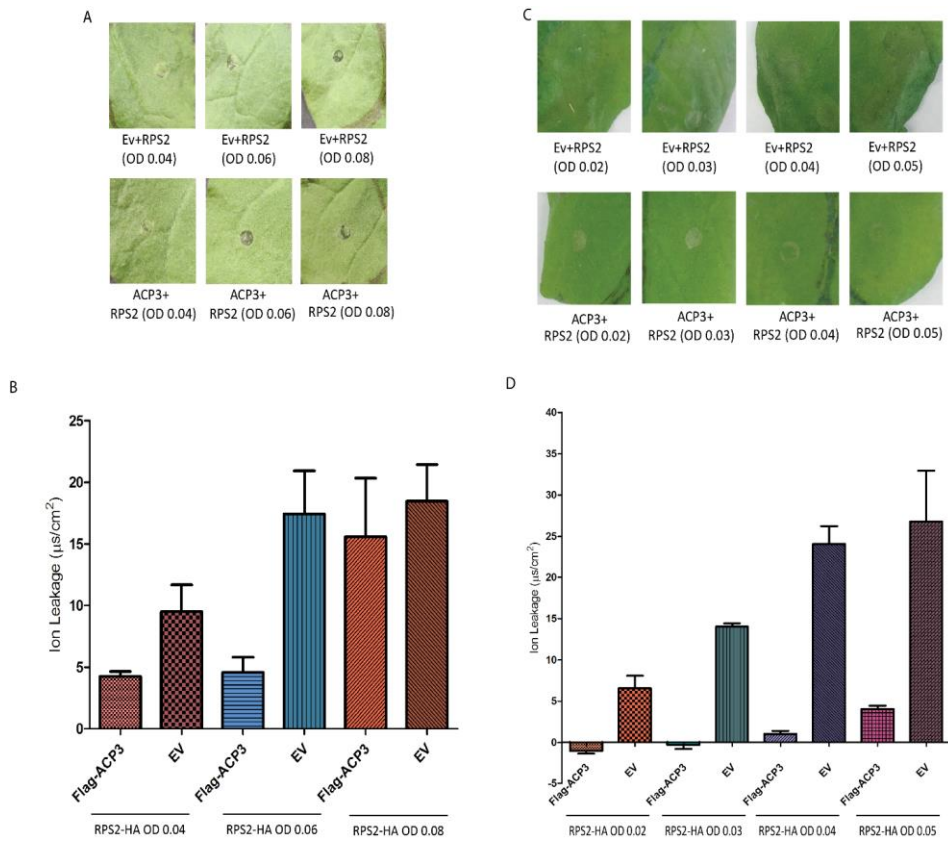


**Figure 2.4. Cell death in *N. benthamiana* induced by different titers of agrobacteria expressing RPS2 and its suppression by ACP3. A&B- ACP3 fails to suppress RPS2-HA expressed at a high titer. (A)** ACP3 and empty vector (OD<sub>600</sub> 0.6) were co-infiltrated with RPS2-HA (OD<sub>600</sub> 0.04, 0.06 and 0.08) in *N. benthamiana*. Macroscopic RPS2-induced cell death was observed at 48 HPI. Empty vector failed to suppress RPS2-HA. ACP3 suppressed RPS2-HA expressed at and of OD<sub>600</sub> 0.04, and 0.06; while it failed to suppress RPS2 expressed at an OD<sub>600</sub> of 0.08. **(B)** Cell death was quantified based on electrolyte leakage. Three leaf discs for each combination, as in panel A, were collected, immersed in sterile water, and conductivity of the bath solution was measured at 96 HPI. Error bars represent SEM. **C&D- ACP3 suppresses RPS2-HA introduced at a low titre in *N. benthamiana*.** (C) ACP3 and/or empty vector (OD<sub>600</sub> 1.0) were

co-infiltrated with RPS2-HA ( $OD_{600}$  0.02, 0.03, 0.04 and 0.05) in *N. benthamiana*. Macroscopic RPS2-induced cell death was observed at 48 HPI. ACP3 suppressed RPS2 expressed at a lower titer, while empty vector failed to suppress RPS2. **(D)** Cell death was quantified based on electrolyte leakage. Three leaf discs for each combination, as in panel C, were collected, immersed in sterile water, and conductivity of the bath solution was measured at 72 HPI. Error bars represent SEM.

Similar to previous reports, Flag-ACP3 failed to suppress activation of RPS2-HA expressed with a high titer of Agrobacteria (Figure 2.4a and b) (Day et al. 2005). Since ACP3 localizes at the membrane and contains a partially truncated C-NOI domain we speculated that it might be able to suppress RPS2 expressed at a low titer. Figure 2.4c and d show that Flag-ACP3 is able to suppress RPS2 expressed at low titers. It was observed that RPS2 expressed at  $OD_{600}$  0.04 gives robust cell death and is consistently suppressed by Flag-ACP3. Thus, we chose to use  $OD_{600}$  of 0.04 for RPS2 to test for its suppression by ACP3 fragment.

To determine RPS2 suppression, Flag-RIN4 derivatives ( $OD_{600}$  0.6) (Figure 2.5a) were co-infiltrated with RPS-HA ( $OD_{600}$  0.04) in *N. benthamiana*. Flag-RIN4Fl suppresses RPS2-HA while the empty vector fails to suppress RPS2-HA expressed in *N. benthamiana* (Figure 2.5 b and c). Similar to Flag-RIN4Fl, Flag-ACP3 was also able to suppress RPS2-HA expressed at an OD of 0.04 (Figure 2.5b and c). Even though Flag-ACP3 accumulates to a significantly lower level compared to Flag-RIN4Fl it retained the ability to suppress RPS2 (Figure 2.5d). Taken together these results indicate that Flag-ACP3 is sufficient to suppress RPS2-HA expressed at a lower titer. This also indicates that ACP3 fragment generated in the presence of AvrRpt2 might participate in AvrRpt2-mediated activation of RPS2.

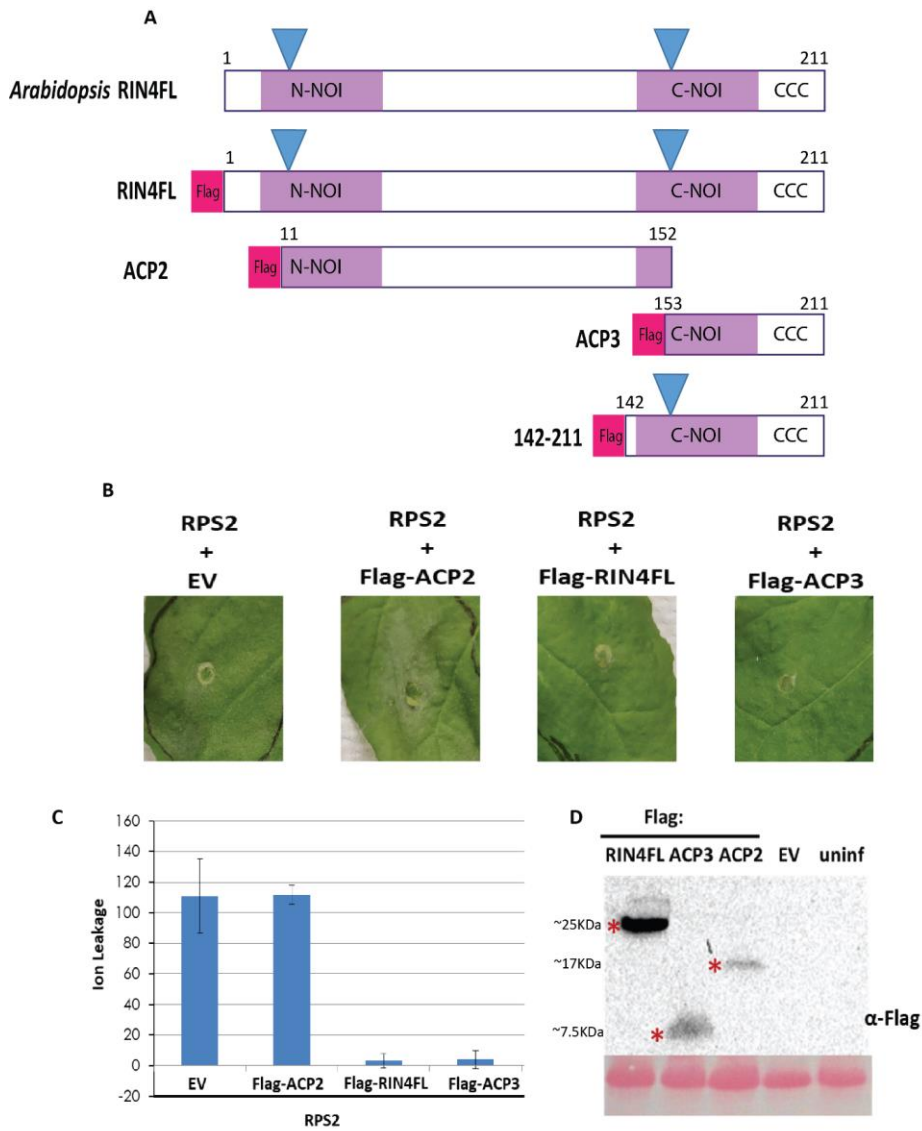


**Figure 2.5. Membrane tethering of RIN4 is required for RPS2 suppression.** (A) 35S-driven RIN4 derivatives used for transient experiments had an N-terminal Flag-tag. (B) Flag-RIN4 derivatives ( $OD_{600}$  0.6) were co-infiltrated with RPS2-HA ( $OD_{600}$  0.04) in *N. benthamiana*.

Macroscopic HR on leaves of *N. benthamiana* plants was observed 48 hours post infiltration (HPI). Similar to full length RIN4, ACP3 was able to suppress RPS2; while ACP2 and empty vector failed to suppress RPS2. (C) Cell death in **B** was quantified using ion leakage. Three leaf discs for each Flag-RIN4 derivative co-infiltrated with RPS2 were collected 48 HPI, immersed in sterile water and conductivity of the bath solution was measured at 48 HPI. (D) Anti-Flag immunoblot conducted on samples collected 48 HPI shows that in comparison to Flag-RIN4Fl the cleavage fragments accumulate to a lower level. Even so, ACP3 mediated suppression of RPS2 is equivalent to RPS2 suppressed by RIN4Fl. Therefore the ability of the derivatives to regulate RPS2 does not correlate with insufficient expression level. Panel below show ponceau stain for RuBisCO used as loading control

### **2.2.3. Non-membrane tethered derivative, ACP2, fails to suppress RPS2 and is able to activate ACP3-suppressed RPS2**

Non-membrane tethered derivatives of RIN4 fail to suppress RPS2 (Figure 2.2a and b). Since ACP2 is also reported to accumulate in the soluble fraction (Afzal et al. 2011), we speculated that it might not be able to suppress RPS2. To test this hypothesis we expressed Flag-ACP2 (Figure 2.5a) derivative along with RPS2-HA at an OD of 0.04 in *N. benthamiana*. Figure 2.5a and b show that while Flag-RIN4FL suppresses, the Flag-ACP2 derivative failed to suppress RPS2-HA expressed in *N. benthamiana*.

Based on our results we conclude that while the membrane tethered fragment, ACP3, retains the ability to suppress RPS2, the soluble fragment, ACP2, fails to suppress RPS2 expressed in *N. benthamiana*. Generation of ACP2 and ACP3 by AvrRpt2 resembles the scenario where the non-membrane tethered derivatives are expressed in the presence of wild type RIN4. As shown in figure 2.2b and c expression of either 177 $\Delta$ 211 or CCC>AAA derivatives in the presence of RIN4Fl results in the activation of RPS2. We speculate that similar to these non-membrane tethered derivatives, the ACP2 fragment might be able to overcome the ACP3 mediated suppression of RPS2.

To test this, we co-expressed Flag-ACP2 and Flag-ACP3 along with RPS2-HA in *N. benthamiana*. Figure 2.6a and b show that similar to Flag-RIN4Fl, Flag-ACP3 was also able to suppress RPS2-

HA; while both Flag-ACP2 and empty vector failed to suppress RPS2-HA. Interestingly Flag-ACP2 was able to overcome Flag-ACP3 mediated suppression of RSP2-HA (Figure 2.6a and b).

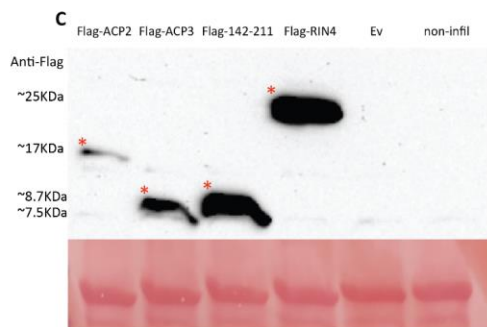
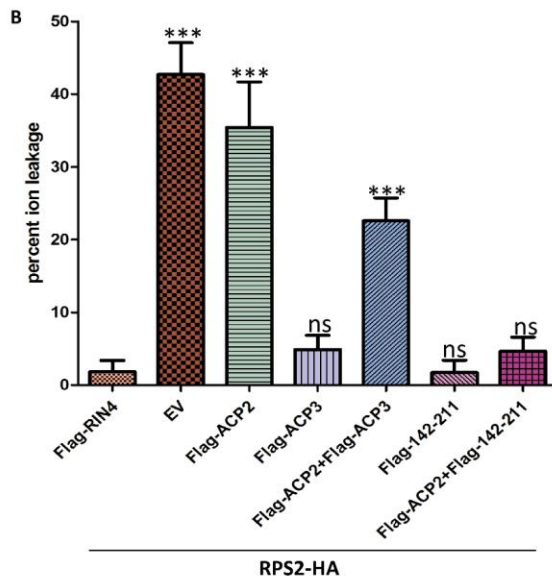
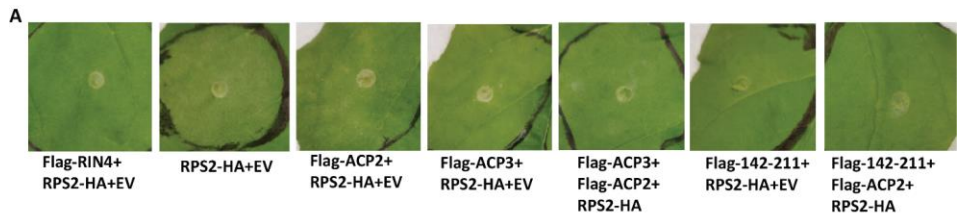


**Figure 2.6. Flag-ACP2 is capable of activating Flag-ACP3 suppressed RPS2-HA.** (A) Flag-RIN4 derivatives and empty vector (OD<sub>600</sub> 0.6) were co-expressed with RPS2-HA (OD<sub>600</sub> 0.04) in *N. benthamiana*. Macroscopic HR was observed 48 HPI. Similar to Flag-RIN4Fl, Flag-ACP3 and Flag-142-211 were able to suppress RPS2; while Flag-ACP2 and empty vector failed to suppress RPS2. Flag-ACP2 was able to activate Flag-ACP3 suppressed RPS2, while it failed to activate Flag-142-211 suppressed RPS2. (B) Cell death in A was quantified using ion leakage. Three leaf discs for each combination were collected 48 HPI, immersed in sterile water and conductivity of the bath solution was measured at 96 HPI. Data was gathered from 3 independent experiments. Error bars represent SEM. Student's t-test, at 95% confidence limits, was used for comparison with Flag-AtRIN4Fl (ns, not significant; \*\*\*P<0.0001). (C) Anti-Flag immunoblot conducted on samples collected 72 HPI shows that Flag-RIN4Fl and Flag-142-211 accumulate to a similar level, while the cleavage fragments accumulated to a lower level. Even so, ACP3 mediated suppression of RPS2 is equivalent to RPS2 suppressed RIN4Fl and ACP2 is able to overcome this suppression. Therefore the ability of the derivatives to regulate RPS2 does not correlate with insufficient expression level. Panel below show ponceau stain for RuBisCO used as loading control.

A derivative of RIN4 with an intact C-NOI domain, 142-211 (Figure 2.5a), was also able to suppress RPS2 expressed in *N. benthamiana* (Figure 2.6a and b). In comparison to ACP3, Flag-ACP2 failed to activate RPS2 suppressed by 142-211 (Figure 2.6a and b). This indicated that ACP2 is sufficient to activate RPS2 suppressed by a membrane tethered fragment, ACP3, generated by AvrRpt2. Even though, in comparison to Flag-RIN4Fl, Flag-ACP2 accumulates to a lower level (Figure 2.5d), its ability to activate ACP3 suppressed RPS2 does not correlate with insufficient expression level. Taken together results from our experiments are consistent with a model where cleavage of RIN4 by AvrRpt2 activates RPS2 through the generation of the non-membrane tethered, ACP2, fragment (Figure 2.7).

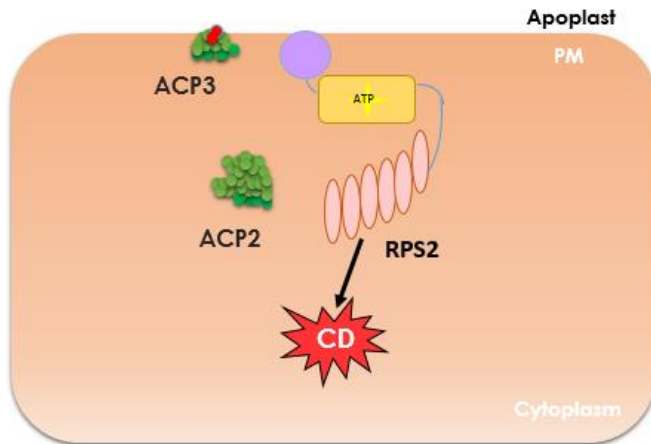


**Figure 2.7. In the absence of the pathogen ACP2 is sufficient to activate ACP3 suppressed RPS2.** While the membrane tethered fragment, ACP3, has the ability to suppress RPS2, the soluble fragment, ACP2, is able to overcome this suppression. Similarly, in the presence of the effector, ACP3 might retain the ability to weakly suppress RPS2, however the release of ACP2 from RIN4 might trigger RPS2 activation leading to ETI.

#### **2.2.4. ACP2 activates RPS2 suppressed by ACP3 when present in the cytosol.**

The non-membrane tethered, ACP2, fragment is reported to accumulate in the soluble fraction (cytosol and nucleus). In order to determine the functional significance of ACP2 localization and its ability to activate ACP3 suppressed RPS2, we generated derivatives of ACP2 carrying a nuclear localization signal (NLS, YFP-NLS-ACP2), nuclear export signal (NES, YFP-NES-ACP2) or a Shuffled Nuclear Export Signal (SNE, YFP-SNE-ACP2) (Figure 2.8a). We expressed these derivatives in *N. benthamiana* to determine their localization. Figure 2.8b shows that full length RIN4 co-localized at the membrane with an RFP fused plasma membrane GTPase, OsRac1 (Figure 2.8b). While YFP-NES-, YFP-NLS- and YFP-SNE-tagged ACP2 derivatives localized in the cytosol, nucleus, and in both locations, respectively (Figure 2.8b).

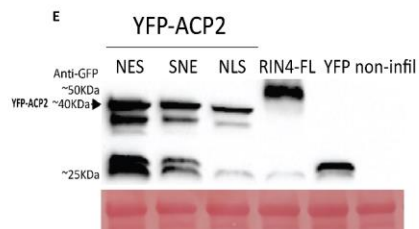
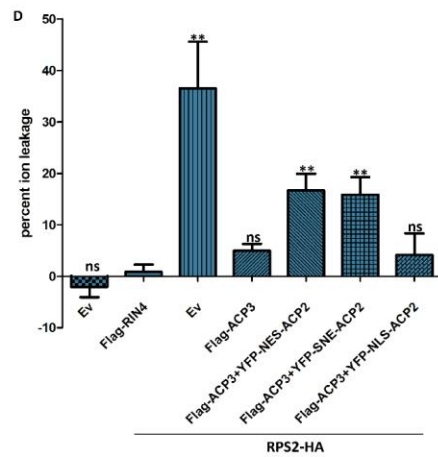
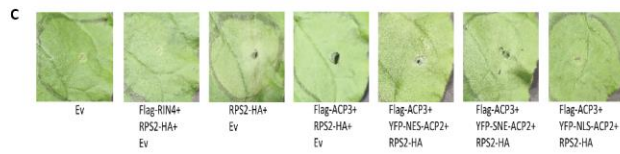
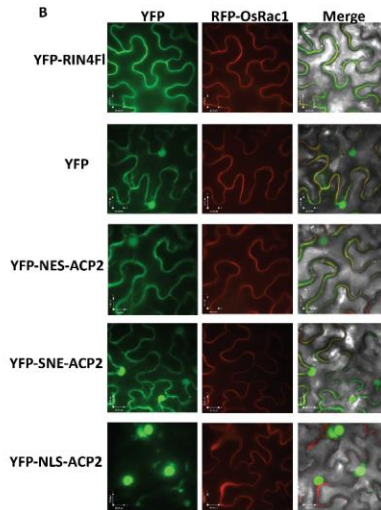
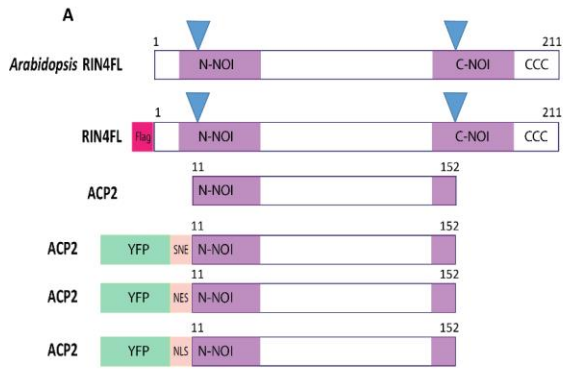


**Figure 2.8. ACP2 activates RPS2 suppressed by ACP3 when present in the cytosol.** (A) 35S-driven RIN4 derivatives used for transient experiments had an N-terminal YFP-tag and either a nuclear localization signal (NLS), nuclear export signal (NES) or a Shuffled Nuclear Export Signal (SNE). (B) YFP tagged RIN4 derivatives (OD<sub>600</sub> 0.6) were co-infiltrated with RFP-OsRac1 (OD<sub>600</sub> 0.6) in *N. benthamiana*. Fluorescent signal was observed at 72 hours post infiltration (HPI) using confocal microscopy (Scale bar: 25 μM). YFP-RIN4Fl localized at the membrane, while the free YFP protein localized in the cytosol and the nucleus. YFP-NES-ACP2 localized in the cytosol, YFP-NLS-ACP2 localized in the nucleus and YFP-SNE-ACP2 localized in both the cytosol and nucleus. (C) ACP2 derivatives (OD<sub>600</sub> 0.6) were co-expressed with Flag-ACP3 (OD<sub>600</sub> 0.6) and RPS2-HA (OD<sub>600</sub> 0.04) in *N. benthamiana*. Macroscopic HR on leaves of *N. benthamiana* plants was observed 48 hours post infiltration (HPI). Similar to full length RIN4, ACP3 was able to suppress RPS2; while empty vector failed to suppress RPS2. Both YFP-SNE-ACP2 and YFP-NES-ACP2 activated ACP3 suppressed RPS2; while YFP-NLS-ACP2 failed to activate ACP3 suppressed RPS2. (D) Cell death in C was quantified using ion leakage. Three leaf discs for each combination were collected 48 HPI, immersed in sterile water and conductivity of the bath solution was measured at 96 HPI. Data was gathered from 4 independent experiments. Error bars represent SEM. Student's t-test, at 95% confidence limits, was used for comparison with Flag-AtRIN4Fl (ns, not significant; \*\*P<0.01). (E) Anti-GFP immunoblot conducted on samples collected at 72 HPI shows that NLS and SNE tagged ACP2 accumulate to comparable levels in *N. benthamiana*. Panel below show ponceau stain for RuBisCO used as loading control.

In order to determine the role of the ACP2 derivatives in RPS2 regulation, we co-expressed these derivatives with Flag-ACP3 and RPS2-HA in *N. benthamiana*. Figure 2.8-d and e show that both Flag-RIN4Fl and Flag-ACP3 suppress RPS2 while the empty vector fails to suppress RPS2. Interestingly both YFP-NES-ACP2 and YFP-SNE-ACP2 were able to overcome ACP3 mediated suppression of RPS2 (Figure 2.8c and d), while YFP-NLS-ACP2 failed to overcome this suppression. Expression levels of the proteins do not account for their (in)ability to activate ACP3-suppressed RPS2 (Figure 2.8e). These results indicate that ACP2 is only able to overcome ACP3 mediated suppression of RPS2 when it is predominantly present in the cytosol.

### 2.3. Discussion:

Understanding the molecular mechanism by which the pathogen encoded effectors trigger an NLR mediated immune response will not only provide insight into the function of these plant immune receptors but also enhance our efforts to breed and engineer disease resistant crop plant. A well-studied example of an NLR activation in the presence of the effector is the activation of Arabidopsis RPS2 by the *P. syringae* T3E, AvrRpt2. The widely accepted model for RPS2 activation states that RPS2 activates signaling upon perception of AvrRpt2-mediated elimination of RIN4. We demonstrate that in Arabidopsis plants, expression of non-membrane tethered derivatives of RIN4, in the presence of wild type RIN4, resulted in the activation of RPS2. This indicates that activation of RPS2 occurred in the presence of a RIN4 derivative and therefore does not require elimination of RIN4.

Membrane localization of RIN4 is required for RPS2 suppression. Specifically the C-terminal half of RIN4 is sufficient for suppressing RPS2 expressed in *N. benthamiana* (Day et al. 2005). Similarly we have demonstrated that a derivative with an intact C-NOI domain, 142-211, was also able to suppress RPS2 expressed in *N. benthamiana*. We have further demonstrated that the membrane tethered cleavage fragment, ACP3, is also capable of suppressing RPS2 expressed at a low titer. This indicates that ACP3 generated upon cleavage by AvrRpt2 might maintain suppression of RPS2 in *Arabidopsis*. Suppression of RPS2 by ACP3 is in contrast to the regulation of an NLR protein, MR5, by RIN4 in apple. AvrRpt2 mediated cleavage of MdRIN4 triggers the activation of MR5; however the MdACP3 fragment generated post cleavage is required for MR5 activation (Prokchorchik et al. 2020). It was further reported that, in the absence of the effector, MdACP3 is sufficient for MR activation (Prokchorchik et al. 2020). Both RPS2 and MR5 belong to the same CC-NLR class of proteins; however they have evolved independently to recognize AvrRpt2 mediated cleavage of RIN4 (Prokchorchik et al. 2020). It is clear that these non-homologous proteins are differently regulated by RIN4 in their respective species.

We further show that the AvrRpt2-induced cleavage fragments of RIN4, ACP2 and ACP3, differentially regulate RPS2. While the membrane tethered derivative, ACP3, retained the ability to suppress, the non-membrane tethered derivatives, ACP2, failed to suppress RPS2. We also demonstrate that ACP2, when co-expressed with ACP3 and RPS2, overcomes the ACP3-mediated suppression of RPS2. However when ACP2 is co-expressed with a RIN4 derivative that has an

intact C-NOI domain, 142-211, it fail to activate RPS2. This indicates that ACP2 specifically triggers activation of ACP3-suppressed RPS2. Furthermore we have demonstrated that ACP2 activates ACP3 suppressed RPS2 when it is present in the cytosol. Therefore we propose a new model for RPS2 activation, where the cleavage of RIN4 by AvrRpt2 results in the generation of two fragments that coordinately activate RPS2 (Figure 2.6).

AvrRpt2 promotes *P. syringae* growth in Arabidopsis plants lacking RPS2. AvrRpt2 is reported to suppress MTI responses including expression of the pathogenesis-related (PR) gene and promotes auxin/indole acetic acid protein (Aux/IAA) turnover which promotes *P. syringae* pathogenicity (Cui et al. 2013; Kim et al. 2005b). AvrRpt2-mediated cleavage of fragments of RIN4 are also potent suppressors of MTI outputs (Afzal et al. 2011). Specifically ACP2 suppresses callose deposition associated with cell wall reinforcement, while both fragments promote bacterial growth (Afzal et al. 2011). Thus AvrRpt2 makes a stronger and distinct contribution to promoting *P. syringae* pathogenicity by targeting RIN4. In resistant species however, RPS2 has evolved to 'guard' RIN4, as AvrRpt2 mediated cleavage of RIN4 is detected by RPS2 which in turn leads to its activation. Specifically the production of a locally-concentrated but non-membrane tethered fragment, ACP2, elicits the activation of RPS2. On the whole this model best fits to the guard hypothesis that the virulence promoting perturbation of RIN4 by AvrRpt2 results in the activation of RPS2.

## **Chapter 3. RIN4 homologs from important crop species differentially regulate the Arabidopsis NB-LRR immune receptor, RPS2**

This chapter is adapted from Alam, et al., 2021 RIN4 homologs from important crop species differentially regulate the Arabidopsis NB-LRR immune receptor, RPS2. *Plant cell reports*. In press

### **3.1. Introduction**

Plants have evolved a sophisticated innate immune system to defend themselves against invading pathogens. Although plants lack mobile immune cells, they have developed immune receptors that recognize pathogen molecules (Jones and Dangl 2006). Pathogen recognition by plant cells relies on membrane-localized and intracellular receptors (Bonardi et al. 2012; Macho and Zipfel 2015; Monteiro and Nishimura 2018). The former are typically activated by microbe-associated molecular patterns (MAMPs), such as lipopolysaccharides, flagellin or chitin, leading to MAMP triggered immunity (MTI) (Chisholm et al. 2006; Glowacki et al. 2011; Khan et al. 2016; Zipfel 2014). Most of the intracellular receptors, known as resistance (R) proteins, belong to the nucleotide binding and leucine rich repeat (NLRs) family of receptors (Bonardi et al. 2012; Chiang and Coaker 2015; Chisholm et al. 2006; Monteiro and Nishimura 2018). Perception by NLRs, of effector proteins from potential pathogens, including the type three effectors (T3Es) translocated from gram negative bacteria into host cells, leads to effector triggered immunity (ETI) that frequently culminates in a hypersensitive response characterized by programmed cell death (PCD) (Chiang and Coaker 2015; Dodds and Rathjen 2010; Jones and Dangl 2006; Monteiro and Nishimura 2018).

NLRs can detect effector proteins either directly or indirectly. Many pathogens have been reported to possess hundreds of effector proteins (Jones and Dangl 2006); whereas plants have more limited allelic diversity at the R loci and these alleles are maintained by balancing selection (Bergelson et al. 2001; Van der Hoorn 2002). This excess of effectors relative to R-proteins, as well as selective pressure favoring effector variants that evade detection, limits the effectiveness of direct recognition of effectors. Indirect detection, which is based on perception of an effector-induced perturbation within a host cell, allows plants to use their limited repertoire of NLRs to detect a larger number of effectors, as the effectors converge on a finite set of host targets (Dangl and McDowell 2006). Because indirect recognition is often triggered by perturbations resulting from

the virulence activity of effectors, effectors are constrained in their ability to retain function while evading detection.

A well characterized example of a host protein that mediates indirect recognition of effectors is RPM1 interacting protein 4 (RIN4). AtRIN4 is a small, intrinsically unstructured protein that contains two NOI (Nitrate induced) domains (with no known biochemical function) and is localized at the plasma membrane because of the palmitoylation of its C-terminal cysteine residues (Afzal et al. 2013; Day et al. 2005; Desveaux et al. 2007; Takemoto and Jones 2005; Toruno et al. 2019). The AtRIN4 protein is targeted by five unrelated *Pseudomonas syringae* effectors, AvrRpm1, AvrB, AvrRpt2, HopF2 and HopZ3 (Lee et al. 2015; Mackey et al. 2003; Mackey et al. 2002; Redditt et al. 2019; Wilton et al. 2010). In the absence of effector-targeting, RIN4 negatively regulates MTI (Kim et al. 2005b). The effectors that target RIN4 promote virulence, at least in part, by enhancing its negative regulation of MTI. For example, AvrRpt2 is a cysteine protease that cleaves AtRIN4 at conserved motifs, VPXFGXW, present at the N-terminal side of both NOI domains (Axtell and Staskawicz 2003; Chisholm et al. 2005; Kim et al. 2005a; Takemoto and Jones 2005). Two of the resulting fragments, termed AvrRpt2-cleavage product 2 (ACP2, AtRIN4<sup>11-152</sup>) and ACP3 (AtRIN4<sup>153-211</sup>) are hyperactive suppressors of MTI, relative to full length AtRIN4 (Afzal et al. 2011). AtRIN4 associates with two plasma-membrane localized NLRs, RPM1 and RPS2, and its perturbation by AvrRpm1, AvrB, or AvrRpt2 elicits their partial or full activation (Axtell and Staskawicz 2003; Chung et al. 2011; Day et al. 2005; Kim et al. 2009; Mackey et al. 2003; Mackey et al. 2002). These findings establish AtRIN4 as a hub at the nexus of MTI, effector-induced suppression of MTI, and effector-induced activation of ETI in *Arabidopsis*.

RIN4 homologs with N-terminal and C-terminal NOI domains and a putative C-terminal palmitoylation site exist in a wide variety of plant species, including mosses, monocots and dicots (Afzal et al. 2013). Several of these RIN4 homologs, including those from lettuce (*Lactuca sativa*), tomato (*Solanum lycopersicum*), soybean (*Glycine max*), barley (*Hordeum vulgare*) and apple (*Malus domestica*), regulate plant immunity (Gill et al. 2012; Jeuken et al. 2009; Luo et al. 2009; Mazo-Molina et al. 2020; Prokhorchik et al. 2020; Selote and Kachroo 2010b). Soybean contains four RIN4 homologs, each of which contains a putative C-terminal palmitoylation site and are plasma membrane localized (Selote and Kachroo 2010b). Similar to AtRIN4, GmRIN4a and

GmRIN4b negatively regulate basal immunity; silencing of either homolog resulted in enhanced resistance to virulent strains of *P. syringae* (Selote and Kachroo 2010a; Selote and Kachroo 2010b). Also similar to AtRIN4, GmRIN4a and GmRIN4b are targeted by the effectors AvrB, AvrRpm1 and AvrRpt2, possibly to enhance negative regulation of MTI (Ashfield et al. 2014; Selote and Kachroo 2010b). However, unlike the recognition of AvrB or AvrRpm1 by a single R-protein (RPM1) in *Arabidopsis*, AvrB and AvrRpm1 are recognized in resistant soybean cultivars by two independently evolved R-proteins, Rpg1b and Rpg1r, respectively (Ashfield et al. 2014; Selote and Kachroo 2010b). Although AvrRpt2 elicits an effective defense response on some soybean cultivars (Whalen et al. 1991), the relationship of GmRIN4 homologs to RPS2 is unknown. More recently, it has been demonstrated that AvrRpt2-mediated cleavage of SIRIN4 and MdrIN4 results in the activation of two independently evolved NLR-proteins, Ptr1 in tomato and Mr5 in apple (Mazo-Molina et al. 2020; Prokchorchik et al. 2020). AtRIN4 prevents ectopic activation, defined as that occurring in the absence of effector-activation, of RPS2 in unchallenged *Arabidopsis* and *N. benthamiana* plants (Day et al. 2005; Mackey et al. 2003). By contrast, MR5 is not ectopically active, but ACP3 is sufficient to activate it (Prokchorchik et al. 2020). Collectively, these findings indicate that a variety of NLR-proteins distinctly monitor the status of RIN4. Conservation of RIN4 in crop species leads to the hypothesis that those RIN4 homologs are able to regulate the activity of RPS2. Since AvrRpt2-like effectors with the capacity to specifically cleave RIN4 are found in a diverse collection of plant pathogens (Eschen-Lippold et al. 2016; Mazo-Molina et al. 2020; Prokchorchik et al. 2020), understanding the ability of RIN4 homologs to function with RPS2 could enable the development of crops resistant to a variety of pathogens.

In this study, we show that, similar to AtRIN4, RIN4 homologs from seven crop species all localize at the plasma membrane. Despite this common localization, the RIN4 homologs differ in their ability to suppress RPS2. We also demonstrate that all RIN4 homologs are cleaved by AvrRpt2 and, for those capable of suppressing RPS2, this cleavage results in RPS2 activation.

## **3.2. Results**

### **3.2.1. RIN4 homologs are present in important crop species**

While RIN4 homologs are present in plant species dating as far back as moss, only a few of them have been reported to regulate innate immunity in their respective host species (Afzal et al. 2013;

Jeuken et al. 2009; Mazo-Molina et al. 2020; Prokchorchik et al. 2020; Selote and Kachroo 2010b). We initially performed protein blast using AtRIN4 as a query to identify seven RIN4 homologs in notable annual and perennial crop plants including *G. max* (soybean, GmRIN4), *L. sativa* (lettuce, LsRIN4), *M. domestica* (apple, MdRIN4), *O. sativa* (rice, OsRIN4), *P. persica* (peach, PpRIN4), *S. lycopersicum* (tomato, SIRIN4) and *S. tuberosum* (potato, StRIN4). The regions of AtRIN4 known to participate in immune regulation (Figure 3.1a), including the N-NOI and C-NOI domains present at the N- and C-terminal regions of the proteins, respectively (Afzal et al. 2011; Day et al. 2005), were well conserved in the homologous proteins (Figure 3.1b, Table 3.1).

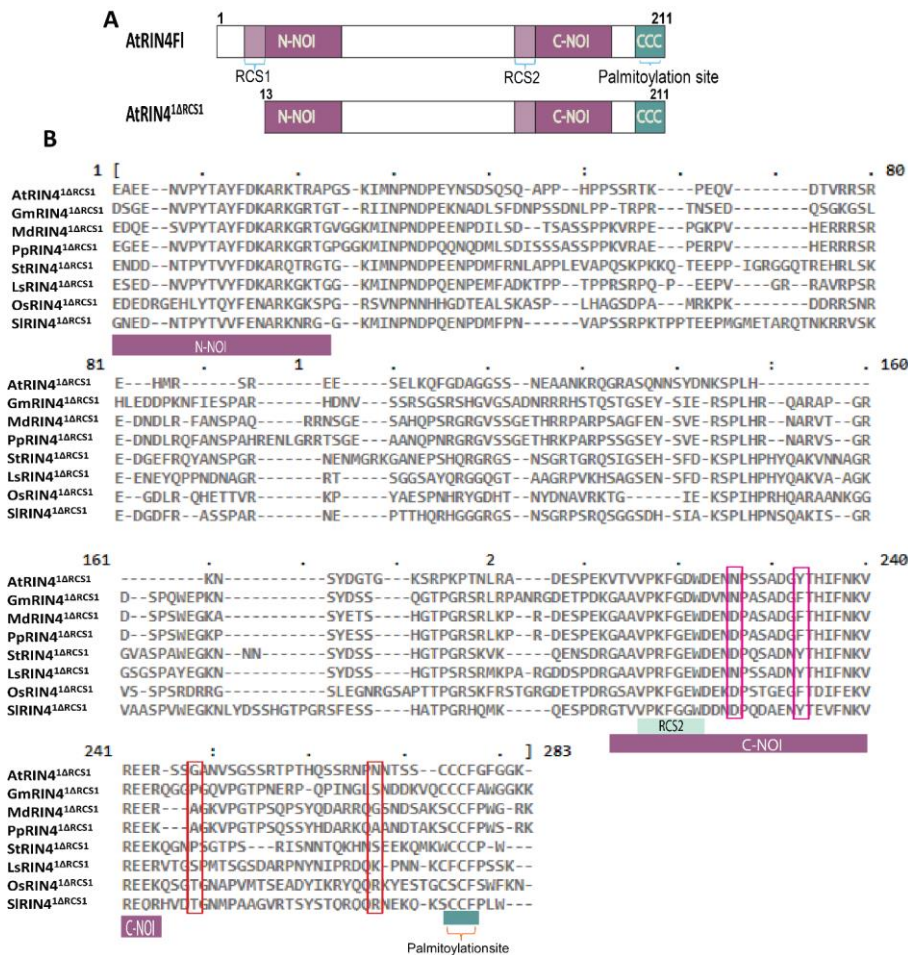


**Figure 3.1. *In silico* analysis of RIN4 homologs from important crop plants. (A)** Schematic representations of wild type AtRIN4 and its 1ΔRCS1 derivative. Indicated are the NOI (Nitrate induced) domains of unknown function, the AvrRpt2-cleavage sites (RCS1 & RCS2) present at the N-terminal side of the NOI domains, and the C-terminal palmitoylation motif with targeted cysteine residues (shown in green). **(B)** Alignment of the amino acid sequence of AtRIN4<sup>1ΔRCS1</sup> and 1ΔRCS1 derivatives of homologs from various plant species, Arabidopsis (At), Soybean (Gm), Peach (Pp), Potato (St), Lettuce (Ls), Rice (Os) and Tomato (St). Indicated are conserved domains, including the N-NOI, RCS2/C-NOI domains, and the C-terminal cysteine residues predicted to serve as sites for palmitoylation.

| Species                              | NCBI ID         |            | Cultivar specific ID   | Length    |             |          | N-NOI (AA 13-34) |             |          | RCS1**   |          | C-NOI (AA 145-176) |             |          | RCS2       |          | C-terminal cysteine residues |   |
|--------------------------------------|-----------------|------------|--|-----------|-------------|----------|------------------|-------------|----------|----------|----------|--------------------|-------------|----------|------------|----------|------------------------------|---|
|                                      |                 | %identity* |  | %identity | %similarity | Position | %identity        | %similarity | Position | Sequence | Position | %identity          | %similarity | Position | Sequence   | Position | No.                          |   |
| <i>Arabidopsis thaliana</i>          |                 |            | RP1M1 interacting protein 4 NP_189143.2                        | 211 AA    |             |          | 13-34 AA         |             |          | 6-12 AA  | VPKFGNW  | 145-176 AA         |             |          | 148-154 AA | VPKFGDW  | 203-205 AA                   | 3 |
| <i>Glycine max</i> (Soybean)         | NM_00125304.4.2 | 99%        | Cultivar: Faisal Soybean. RP1M1 interacting protein 4 MW438284 | 246 AA    | 47.392%     | 55.92%   | 14-36 AA         | 68.18%      | 72.72%   | 7-13 AA  | VPKFGNW  | 177-208 AA         | 81.25%      | 84.37%   | 182-188 AA | VPKFGDW  | 237-239 AA                   | 3 |
| <i>Malus domestica</i> (Apple)       | NM_00129390.5.1 | 97%        | Cultivar: Kandhari. RP1M1 interacting protein 4 MW438285       | 241 AA    | 48.81%      | 54.97%   | 14-36 AA         | 72.72%      | 72.72%   | 7-13 AA  | VPKFGNW  | 175-206 AA         | 78.12%      | 84.37%   | 178-184 AA | VPKFGDW  | 234-235 AA                   | 2 |
| <i>Prunus persica</i> (Peach)        | XM_00720116.5.2 | 100%       | Cultivar: A-668. RP1M1 interacting protein 4 MW438286          | 249 AA    | 45.97%      | 53.55%   | 14-35 AA         | 81.81%      | 81.81%   | 7-13 AA  | VPKFGNW  | 183-214 AA         | 75%         | 84.37%   | 186-192 AA | VPKFGDW  | 242-243 AA                   | 2 |
| <i>Solanum tuberosum</i> (Potato)    | XM_00633995.6.2 | 98%        | Cultivar: FSD-white. RP1M1 interacting protein 4 MW438287      | 252 AA    | 44.54%      | 54.02%   | 13-34 AA         | 63.63%      | 72.72%   | 6-12 AA  | VPKFGNW  | 189-220 AA         | 71.87%      | 81.25%   | 192-198 AA | VPRFGDW  | 248-250 AA                   | 3 |
| <i>Lactuca sativa</i> (Lettuce)      | GQ497782.1      | 100%       | Cultivar: Grand Rapids. RP1M1 interacting protein 4 MW438288   | 243 AA    | 46.91%      | 55.92%   | 13-34 AA         | 66.66%      | 76.19%   | 7-13 AA  | VPKFGNW  | 177-208 AA         | 81.25%      | 87.5%    | 180-186 AA | VPRFGDW  | 236, 238 AA                  | 2 |
| <i>Oryza sativa</i> (Rice)           | XM_01577269.3.2 | 100%       | Cultivar: Basmati-385. RP1M1 interacting protein 4 MW438289    | 242 AA    | 33.17%      | 45.49%   | 13-36 AA         | 50%         | 63.63%   | 6-12 AA  | VPKFGSW  | 173-204 AA         | 59.37%      | 78.12%   | 176-182 AA | VPKFGDW  | 234, 236 AA                  | 2 |
| <i>Solanum lycopersicum</i> (Tomato) | XM_00424236.2.4 | 100%       | Cultivar: Nagina. RP1M1 interacting protein 4 MW438290         | 250 AA    | 42.18%      | 51.18%   | 13-33 AA         | 52.38%      | 61.9%    | 6-12 AA  | VPKFGNW  | 184-215 AA         | 65.62%      | 75%      | 187-193 AA | VPKFGDW  | 245-246 AA                   | 2 |

**Table 3.1. Regions of AtRIN4 known to participate in immune regulation are well conserved in the homologous RIN4 proteins.** Key features of RIN4, including the N- and C-NOI domains, RCS2, and the C-terminal cysteine residues, are conserved in the homologs under study.

The C-NOI domains of the homologs show greater sequence conservation relative to the N-NOI domain, consistent with previously published data (Table 3.1) (Afzal et al. 2013). The N-terminal portion of both NOI domains within the homologs also contains a consensus AvrRpt2 cleavage site (RCS: VPXFGXW, Table 3.1). Lastly, each homolog also contains two or three cysteine residues near its C-terminus, within a predicted palmitoylation target site (Table 3.2) that is crucial for membrane localization of AtRIN4 (Day et al. 2005; Kim et al. 2005a; Takemoto and Jones 2005).

| ID     | Amino acid Position | Peptide         | Score* | Cutoff* |
|--------|---------------------|-----------------|--------|---------|
| AtRIN4 | 203                 | NPNNTSSCCFGFGG  | 7.505  | 2.412   |
|        | 204                 | PNNTSSCCFGFGGK  | 8.766  | 2.412   |
|        | 205                 | NNTSSCCFGFGGK-  | 7.703  | 3.717   |
| GmRIN4 | 237                 | SNDDKVQCCFAWGG  | 4.268  | 2.412   |
|        | 238                 | NDDKVQCCFAWGGK  | 10.306 | 2.412   |
|        | 239                 | DDKVQCCFAWGGKK  | 7.585  | 3.717   |
| MdRIN4 | 234                 | SNDSAKSCFPWGRK  | 9.673  | 2.412   |
|        | 235                 | NDSAKSCFPWGRK-  | 3.94   | 3.717   |
| PpRIN4 | 242                 | ANDTAKSCFPWSRK  | 8.416  | 2.412   |
|        | 243                 | NDTAKSCFPWSRK-  | 3.783  | 3.717   |
| StRIN4 | 248                 | EEKMKWCCCPW---  | 6.036  | 2.412   |
|        | 249                 | EKQMKWCCCPW---- | 14.343 | 2.412   |
|        | 250                 | KQMKWCCCPW----- | 6.297  | 3.717   |
| LsRIN4 | 236                 | DQKPNNKCFPFSSK  | 13.857 | 10.722  |
| OsRIN4 | 234                 | RKYESTGCSCFSWFK | 11.341 | 10.722  |
| SIRIN4 | 245                 | RNEKQKSCFPLW--  | 5.495  | 2.412   |
|        | 246                 | NEKQKSCFPLW---  | 11.151 | 10.722  |

**Table 3.2. Predicted C-terminal palmitoylation target sites within the RIN4 homologs.** The table shows the palmitoylation prediction score for cysteine residues near the C-terminus of the

homologous RIN4 proteins. Arabidopsis (At), Soybean (Gm), Peach (Pp), Potato (St), Lettuce (Ls), Rice (Os) and Tomato (St). \*Score for the individual cysteine residues (shown in red) indicates the potential of S-palmitoylation at that residue. \*\*A score above the Cutoff indicates a putative palmitoylation site.

### 3.2.2. RIN4 homologs localize at the plasma membrane

Based on the putative palmitoylation target sites, we predicted that, like AtRIN4, the RIN4 homologs would also localize at the plasma membrane. In order to test their membrane localization, derivatives lacking the first 12 or 13 amino acids and containing instead an N-terminal YFP- and AcV5-tag were constructed (YFP-AcV5-RIN4<sup>ΔRCS1</sup>; for the structure of this and all protein derivatives used in this chapter, see Figure 3.2).

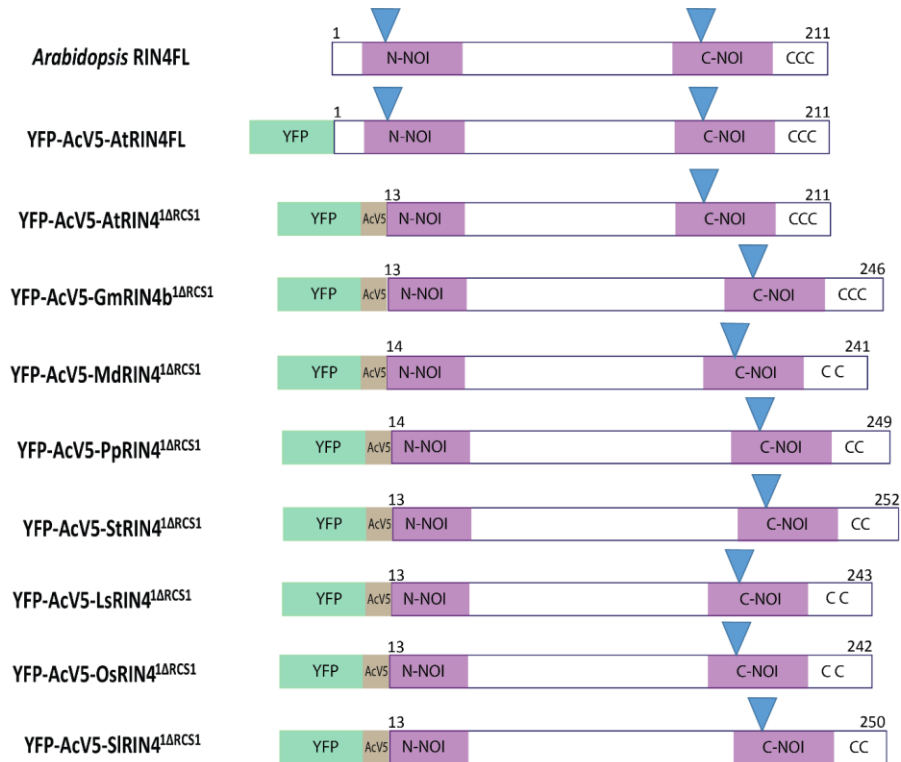
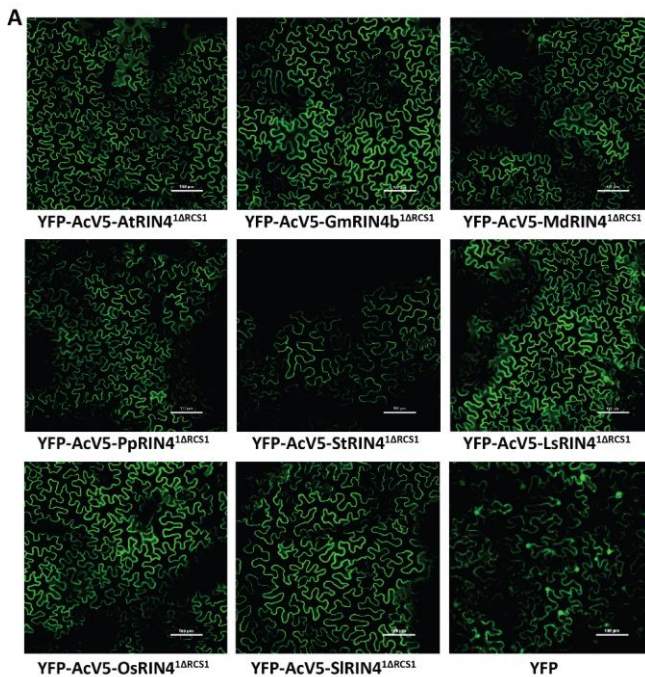


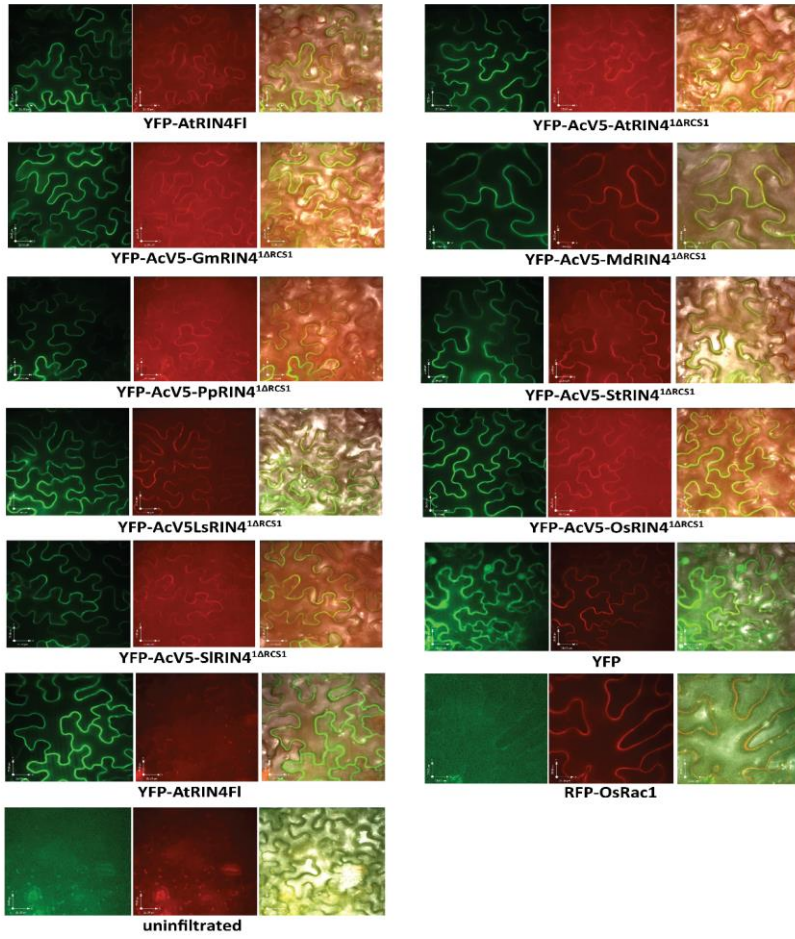
**Figure 3.2. Schematic diagram of RIN4 derivatives used in this study.** Within RIN4 derivatives: Green rectangles indicate YFP tag, brown squares indicate AcV5 epitopes, purple rectangles indicate NOI domains, and blue triangles indicate RCS2.

When expressed in *N. benthamiana* using *Agrobacterium*-mediated infiltrations, fluorescent microscopy indicated that these derivatives all localized to the cell periphery, consistent with the predicted plasma membrane localization and in contrast to free YFP protein, which localized to the cytosol and the nucleus (Figure 3.3a). Furthermore the YFP-RIN4 derivatives co-localized with RFP fused OsRac1, a small plasma membrane GTPase (Figure 3.4a). Subcellular fractionation confirmed that, similar to AtRIN4, all the YFP-tagged derivatives of the RIN4 homologs accumulated in the microsomal membrane fraction while free YFP protein accumulated in the soluble fraction (Figure 3.3b and Figure 3.4b). Together, these observations indicate that, like AtRIN4, the homologs under study all localize to the plasma membrane.





A



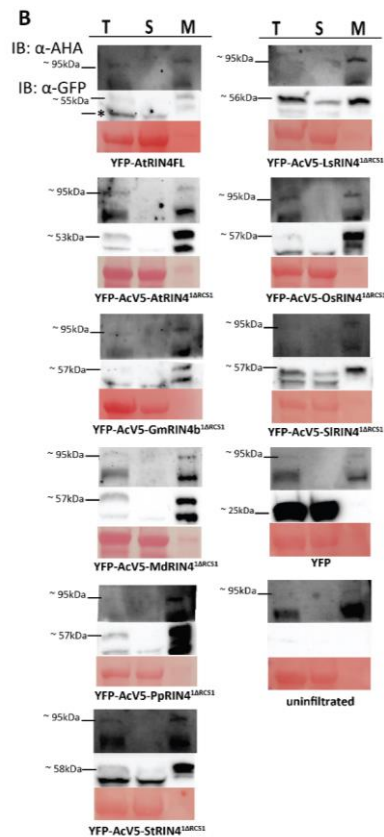


**Figure 3.4. RIN4 homologs localize at the plasma membrane.** (A) Homologous YFP-AcV5-RIN4<sup>1ARCS1</sup> derivatives (OD<sub>600</sub> 0.6) were co-infiltrated with RFP-OsRac1 (OD<sub>600</sub> 0.6) in *N. benthamiana* plants. Fluorescent signal was observed at 48 hours post infiltration (HPI) using confocal microscopy (Scale bar: 25  $\mu$ M). All RIN4 homologs co-localized at the membrane with OsRac1, while free YFP protein localized in the cytosol and nuclei. Arabidopsis (At), Soybean (Gm), Apple (Md), Peach (Pp), Potato (St), Lettuce (Ls), Rice (Os) and Tomato (St). (B) Plant samples obtained from 72 HPI were fractionated into total (T), soluble (S) and membrane (M) fractions. AHA, was used as a membrane protein marker. YFP-AcV5-RIN4<sup>1ARCS1</sup> homologs accumulated in the membrane fraction, while the free YFP protein accumulated in the soluble

fraction. Panels below show ponceau stain of RuBisCO as a soluble protein marker. IB, immunoblot. Molecular masses indicate the predicted mobility of the protein(s) of interest.

### 3.2.3. RIN4 homologs differ in their ability to suppress RPS2

Plasma membrane localization of AtRIN4 is crucial for the suppression of RPS2-induced cell death in *N. benthamiana* and *Arabidopsis* (Afzal et al. 2011; Day et al. 2005). Despite the shared localization of all of the RIN4 homologs, only a subset were able to suppress RPS2 when co-expressed transiently in *N. benthamiana*. The ability of full-length (FL) AtRIN4 to suppress RPS2 was matched by YFP-AcV5-AtRIN4<sup>1ΔRCS1</sup> (Figure 3.5).

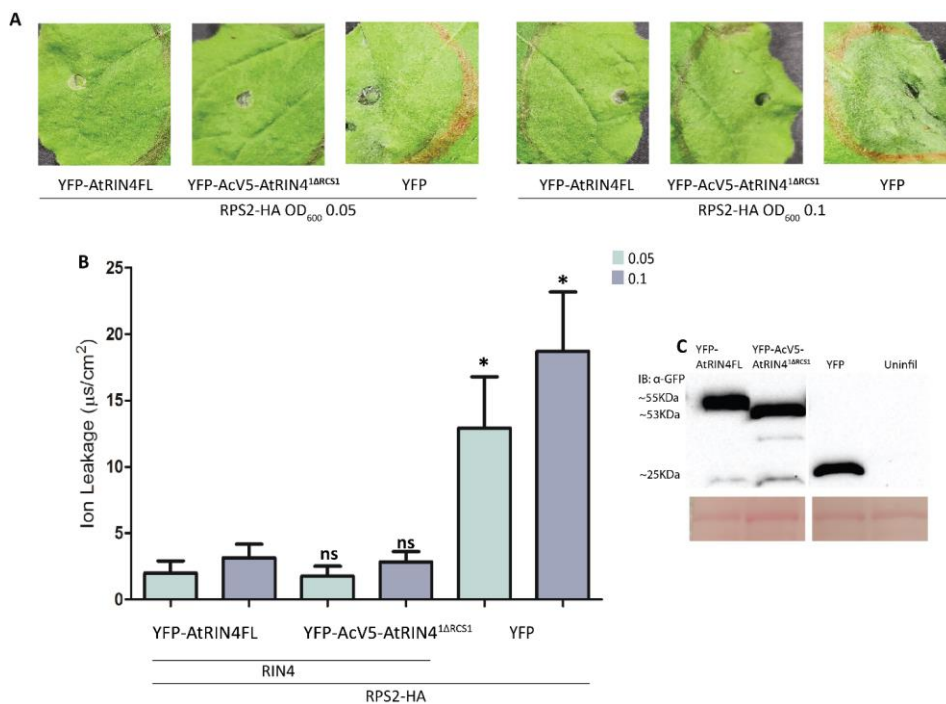


**Figure 3.5. YFP-AtRIN4FL and YFP-AcV5-AtRIN4<sup>1ΔRCS1</sup> are comparable in their ability to suppress RPS2.** (A) The indicated YFP-AtRIN4 derivatives or free YFP (OD<sub>600</sub> 1.0) and RPS2-HA (OD<sub>600</sub> 0.05 or OD<sub>600</sub> 0.1) were co-infiltrated in *N. benthamiana* and macroscopic cell death was observed at 48 HPI. (B) Cell death was quantified based on electrolyte leakage. Three leaf

discs for each AtRIN4 derivative co-infiltrated with RPS2 were taken, immersed in sterile water, and conductivity of the bath solution was measured at 72 HPI. Data collected from 4 independent experiments show that the  $\Delta$ ARCS1 region was not required for the suppression of RPS2. Error bars represent SEM. Student's t-test, at 95% confidence limits, was used for comparison with YFP-AtRIN4FL (ns, not significant; \*P < 0.05). (C) Anti-GFP immunoblot conducted on samples from 72 HPI shows that YFP-AtRIN4 derivatives accumulated to comparable levels in *N. benthamiana*. Panel below shows ponceau stain for RuBisCO used as loading control. Molecular masses indicate the predicted mobility of the protein(s) of interest.

Similar to YFP-AcV5-AtRIN4 $\Delta$ ARCS1, the YFP-AcV5-RIN4 $\Delta$ ARCS1 versions from soybean, peach, potato and apple also suppressed RPS2 (Figure 3.6a and b and Figure 3.7).

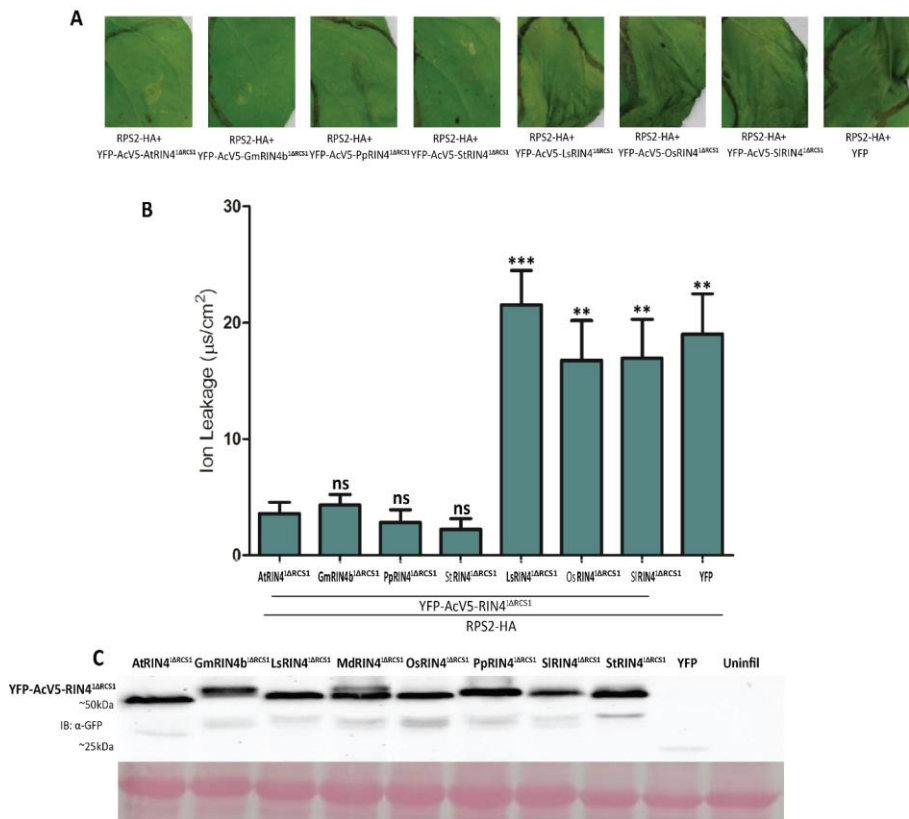


**Figure 3.6. RIN4 homologs differ in their ability to regulate RPS2.** YFP-AcV5-RIN4<sup>ΔRCS1</sup> derivatives (OD<sub>600</sub> 1.0) and RPS2-HA (OD<sub>600</sub> 0.1) were transiently expressed in *N. benthamiana*. **(A)** Macroscopic RPS2-induced cell death was observed at 48 HPI. YFP failed to suppress RPS2-HA (far right panel). Similar to YFP-AcV5-AtRIN4<sup>ΔRCS1</sup>, the YFP-AcV5-RIN4<sup>ΔRCS1</sup> versions from soybean, peach and potato also suppressed RPS2-HA. In contrast, the YFP-AcV5-RIN4<sup>ΔRCS1</sup> versions from lettuce, rice and tomato failed to suppress RPS2-HA. **(B)** Cell death was quantified based on electrolyte leakage. Three leaf discs for each YFP-AcV5-RIN4<sup>ΔRCS1</sup> homolog co-infiltrated with RPS2-HA were collected, immersed in sterile water, and conductivity of the bath solution was measured at 72 HPI. Data was gathered from 5 independent experiments. Error bars represent SEM. Student's t-test, at 95% confidence limits, was used for comparison with AtRIN4<sup>ΔRCS1</sup> (ns, not significant; \*\*P<0.01; \*\*\*P<0.001). **(C)** Anti-GFP immunoblot conducted on samples from 72 HPI show that YFP-AcV5-RIN4<sup>ΔRCS1</sup> homologs accumulated to a comparable level in *N. benthamiana*. Panels below show ponceau stain for RuBisCO used as loading control. Molecular masses indicate the predicted mobility of the protein(s) of interest.

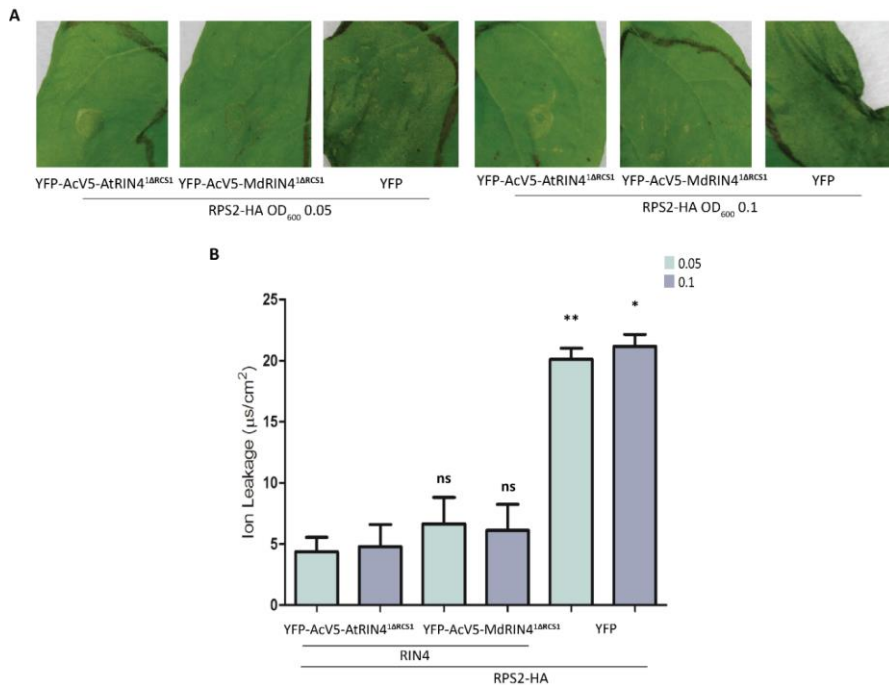


**Figure 3.7. YFP-AcV5-MdRIN4<sup>1ΔRCS1</sup> suppresses RPS2-HA expressed in *N. benthamiana*.**

(A) RPS2-HA (OD<sub>600</sub> 0.05 or 0.1) was co-infiltrated with either YFP-AcV5-AtRIN4<sup>1ΔRCS1</sup> or YFP-AcV5-MdRIN4<sup>1ΔRCS1</sup> derivatives (OD<sub>600</sub> 1.0) in *N. benthamiana*. Macroscopic RPS2-induced cell death was observed at 48 HPI. (B) Cell death was quantified based on electrolyte leakage. Three leaf discs for each combination, as in panel A, were collected, immersed in sterile water, and conductivity of the bath solution was measured at 72 HPI. Data was collected from 2 independent experiments. Error bars represent SEM. Student's t-test, at 95% confidence limits, was used for comparison with YFP-AcV5-AtRIN4<sup>1ΔRCS1</sup> (\*P < 0.05; \*\*P < 0.01).

In contrast, the YFP-AcV5-RIN4<sup>1ΔRCS1</sup> versions from lettuce, rice and tomato failed to suppress RPS2. The differences in RPS2-suppression were unlikely due to insufficient expression of the RIN4 derivatives relative to RPS2 because the same pattern was observed when RPS2 was expressed to lower or higher levels through the use of different titers of *Agrobacterium* (Figure 3.7 and 3.8). Also, the ability of the derivatives to suppress RPS2 did not correlate with their expression level (Figure 3.6c). Taken together, these results indicate that plasma membrane-localized homologs of RIN4 homologs can be divided into two groups based on their ability to suppress RPS2.

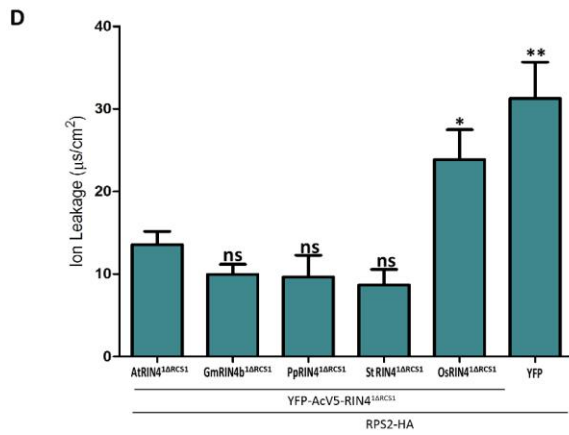
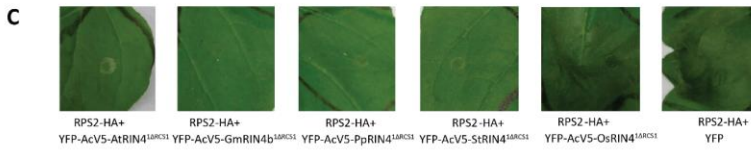
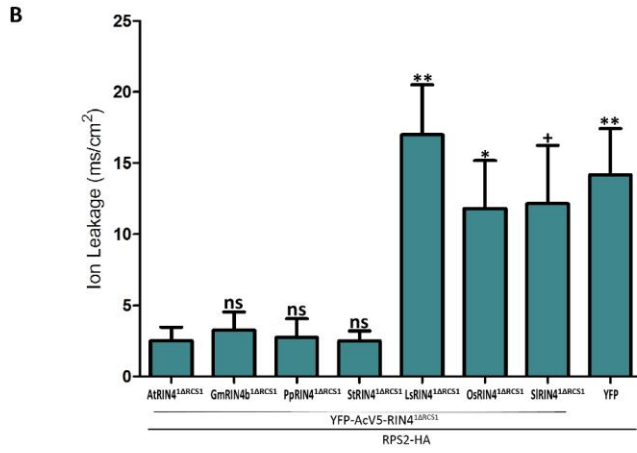


**Figure 3.8. YFP-Acv5-RIN4<sup>1ARCS1</sup> derivatives differ in their ability to suppress RPS2-HA introduced at a low or high titre in *N. benthamiana*.** (A) YFP-Acv5-RIN4<sup>1ARCS1</sup> derivatives (OD<sub>600</sub> 1.0) and RPS2-HA (OD<sub>600</sub> 0.05) were transiently expressed in *N. benthamiana*. Macroscopic RPS2-induced cell death was observed at 48 HPI. Similar to YFP-Acv5-AtRIN4<sup>1ARCS1</sup>, the YFP-Acv5-RIN4<sup>1ARCS1</sup> versions from soybean, peach and potato also suppressed RPS2-HA. While the YFP-Acv5-RIN4<sup>1ARCS1</sup> versions from lettuce, rice and tomato failed to suppress RPS2. (B) Cell death was quantified based on electrolyte leakage. Three leaf discs for each combination, as in panel A, were collected, immersed in sterile water, and conductivity of the bath solution was measured at 72 HPI. Data represents 5 independent experiments. Error bars represent SEM. Student's t-test, at 95% confidence limits, was used for comparison with AtRIN4<sup>1ARCS1</sup> (ns, not significant; \*P < 0.05; \*\*P<0.01; †P=0.0516 borderline significant). (C) YFP-Acv5-RIN4<sup>1ARCS1</sup> derivatives (OD<sub>600</sub> 1.0) and RPS2-HA (OD<sub>600</sub> 0.4) were transiently expressed in *N. benthamiana*. Macroscopic RPS2-induced cell death was observed at 48 HPI. Free YFP protein and YFP-Acv5-OsRIN4<sup>1ARCS1</sup> failed to suppress RPS2-HA. While similar to YFP-Acv5-AtRIN4<sup>1ARCS1</sup>, YFP-Acv5-RIN4<sup>1ARCS1</sup> versions from soybean, peach and potato also suppressed RPS2-HA. (D) Cell death was quantified based on electrolyte leakage. Four leaf discs for each combination, as in panel C, were collected, immersed in sterile water, and conductivity of the bath solution was measured at 72 HPI. Data was collected from 4 independent experiments. Error bars represent SEM. Student's t-test, at 95% confidence limits, was used for comparison with AtRIN4<sup>1ARCS1</sup> (ns, not significant; \*P<0.05; \*\*P>0.01).

### **3.2.4. Polymorphic amino acid residues present in the RIN4 homologs that might correlate with the (in)ability of the RIN4 homologs to suppress RPS2**

Since differences in ability of RIN4 homologs to suppress RPS2 are unlikely a result of their expression level or subcellular localization, we instead suspected differences based on amino acid composition. Similarly, amino acid polymorphisms underlie differences in NLR regulation by MdRIN4 and AtRIN4 (Prokhorchik et al. 2020). Through multiple sequence alignment, using ClustalW, we identified two polymorphic amino acid residues that correlate with the (in)ability of the RIN4 homologs to suppress RPS2 (Figure 3.1b and Table 3.3). At positions corresponding to G179 and N196 in AtRIN4, the non-suppressing homologs all have an S/T or K/R residue, respectively, while distinct residues are present in the suppressing homologs. Notably, each of the

two polymorphic residues are within the ACP3 fragment of AtRIN4, which is sufficient for suppression of RPS2 (Day et al. 2005). Position 196 of AtRIN4 is part of a predicted Molecular Recognition Feature that is a potential binding sites for host proteins which might be a part of a functional protein complex (Sun et al. 2014). Based on our alignment results, we speculate that the amino acids at one or both of these positions may directly or indirectly affect interaction with and suppression of RPS2.

| Amino acid present in suppressing |          |          |          |          | Amino acid in non-suppressing |                                 |          |          |                      |
|-----------------------------------|----------|----------|----------|----------|-------------------------------|---------------------------------|----------|----------|----------------------|
| Name and position of amino acid   |          |          |          |          | Nature of amino acid          | Name and position of amino acid |          |          | Type of substitution |
| AtRIN4                            | GmRIN4   | MdRIN4   | PpRIN4   | StRIN4   |                               | LsRIN4                          | OsRIN4   | SIRIN4   |                      |
| G<br>179                          | P<br>212 | A<br>207 | A<br>215 | P<br>224 | Non-polar                     | S<br>212                        | T<br>208 | T<br>219 | Polar                |
| N<br>196                          | S<br>230 | G<br>226 | A<br>234 | S<br>243 | Neutral polar/nonpolar        | K<br>231                        | R<br>227 | R<br>238 | Polar charged basic  |

**Table 3.3 Polymorphic amino acids present in RIN4 homologs under study.** Two polymorphic amino acid residues present in the C-terminal end of the protein potentially contribute towards the differential regulation of RPS2 by the homologous RIN4 proteins. Numbers indicate amino acid position in the homologous RIN4 proteins. Arabidopsis (At), Soybean (Gm), Peach (Pp), Potato (St), Lettuce (Ls), Rice (Os) and Tomato (St).

### 3.2.5. AvrRpt2-mediated cleavage of YFP-AcV5-RIN4<sup>1ARCS1</sup> derivatives generates soluble and membrane-tethered cleavage products

AvrRpt2 is a cysteine protease that, by cleaving at VPXFGXW target sites at the N-terminal side of both NOI domains within AtRIN4 (Figure 3.1a and Figure 3.2), generates three fragments: RIN4<sup>1-10</sup> (ACP1 or CLV1), RIN4<sup>11-152</sup> (ACP2 or CLV2), and RIN4<sup>153-211</sup> (ACP3 or CLV3), (Afzal et al. 2011; Chisholm et al. 2005; Kim et al. 2005a; Takemoto and Jones 2005). AvrRpt2 cleavage sites are conserved in RIN4 homologs in a wide variety of plant species (Afzal et al. 2013; Sun et al. 2014). More recently it has been demonstrated that AvrRpt2 from *P. syringae* and *Erwinia amylovora*, when expressed in *N. benthamiana*, cleaves SIRIN4 and MdRIN4, respectively (Mazo-Molina et al. 2020; Prokchorchik et al. 2020). Thus, the conserved target site within RIN4 from distantly related plant species is cleaved by AvrRpt2 effectors from diverse bacterial pathogens.

Since the RIN4 homologs contained the AvrRpt2 cleavage sites, we hypothesized that the homologs under study would also be cleaved by AvrRpt2 to generate fragments similar to those generated upon AtRIN4 cleavage. Co-expression with the effector AvrRpt2-HA in *N. benthamiana* was used to detect AvrRpt2-cleavage of the RIN4 homologs. The YFP-AcV5-RIN4<sup>ΔRCS1</sup> derivatives can be used to track the cleavage fragment, YFP-AcV5-RIN4<sup>INT</sup>, that is released upon cleavage by AvrRpt2 within the C-NOI. Figure 3.9a shows that, similar to wild-type AtRIN4, cleavage of the YFP-AcV5-RIN4<sup>ΔRCS1</sup> derivatives by AvrRpt2-HA resulted in the relocalization of YFP-AcV5-RIN4<sup>INT</sup> to the cytosol and the nucleus (Figure 3.9a and Figure 3.10). No change in the localization of the YFP signal was observed upon co-infiltration of the YFP-AcV5-RIN4<sup>ΔRCS1</sup> derivatives with the catalytically inactive mutant, AvrRpt2<sup>C122A</sup>-HA (Figure 3.9a). The localization of the YFP-AcV5-RIN4<sup>INT</sup> fragments and the intact YFP-AcV5-RIN4<sup>ΔRCS1</sup> derivatives following exposure to AvrRpt2-HA or AvrRpt2<sup>C122A</sup>-HA, respectively, was confirmed through subcellular fractionation. AvrRpt2 cleaves the RCS2 site within each of the RIN4 homologs and generates soluble RIN4<sup>INT</sup> fragments (Figure 3.9b).

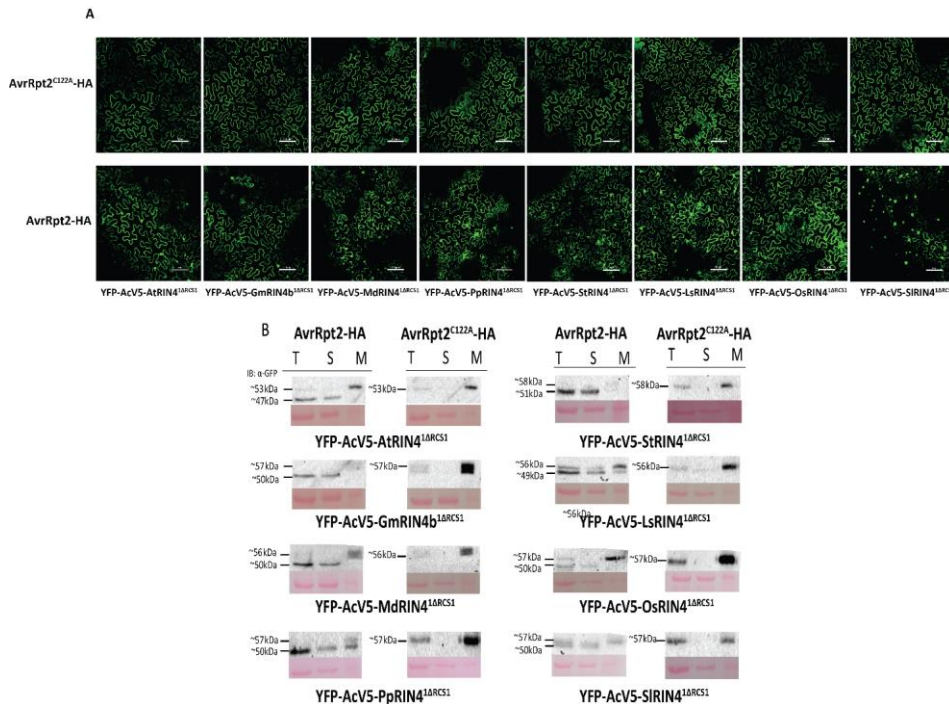


**Figure 3.9. AvrRpt2-mediated cleavage of the RIN4 homologs generates soluble, internal fragments.** (A) YFP-AcV5-RIN4<sup>ΔRCS1</sup> homologs (OD<sub>600</sub> 0.6) were co-infiltrated with either AvrRpt2-HA (OD<sub>600</sub> 0.01) or AvrRpt2<sup>C122A</sup>-HA (OD<sub>600</sub> 0.01) in *N. benthamiana* leaves. Localization of the fluorescent signal was observed at 48 HPI using confocal microscopy (Scale bar: 100 μM). Top: Membrane localization of the YFP-AcV5-RIN4<sup>ΔRCS1</sup> derivatives was unaffected by co-expression of AvrRpt2<sup>C122A</sup>-HA. Bottom: Co-expression of AvrRpt2-HA resulted in the fluorescent signal appearing in the cytosol and nuclei. (B) Anti-GFP immunoblotting was conducted on samples treated as in panel A at 48 HPI that had been fractionated into total (T), soluble (S) and membrane (M) fractions. Right: YFP-AcV5-RIN4<sup>ΔRCS1</sup> derivatives co-infiltrated with AvrRpt2<sup>C122A</sup>-HA accumulated in the membrane fraction. Left: Co-infiltration of YFP-AcV5-RIN4<sup>ΔRCS1</sup> derivatives resulted in appearance of the YFP-AcV5-RIN4<sup>INT</sup> fragments in the soluble fraction. Ponceau staining shows RuBisCO as a soluble protein marker. Molecular masses indicate the predicted mobility of the protein(s) of interest.

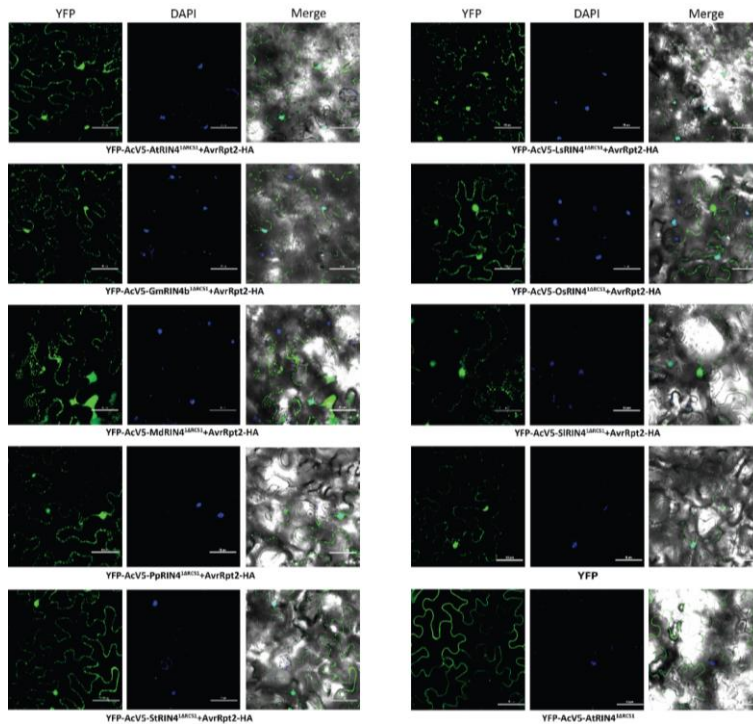


**Figure 3.10. AvrRpt2-mediated cleavage of YFP-AcV5-RIN4<sup>ΔRCS1</sup> derivatives generates fragments that is no longer membrane localized.** DAPI staining of nuclei in cells expressing YFP-AcV5-RIN4<sup>ΔRCS1</sup> homologs and AvrRpt2-HA. YFP-AcV5-AtRIN4<sup>ΔRCS1</sup> derivatives (OD<sub>600</sub> 0.6) were co-infiltrated with AvrRpt2-HA (OD<sub>600</sub> 0.01) in *N. benthamiana* leaves. Leaf tissue was stained with DAPI prior to imaging. Localization of the fluorescent signal was observed at 72 HPI using confocal-microscopy (Scale bar: 50 μM)

### 3.2.6. AvrRpt2-mediated cleavage of homologs results in the activation of RPS2

After establishing AvrRpt2-mediated cleavage of the RIN4 homologs, we next determined the ability of those homologs capable of suppressing RPS2, to mediate RPS2 activation in the presence of the effector. Similar to AtRIN4, phosphorylation and ADP-ribosylation of GmRIN4 homologs (particularly GmRIN4a and GmRIN4b) by *P. syringae* effectors, AvrB and AvrRpm1 activates the Rpg1b and Rpg1r R-proteins (Ashfield et al. 2014; Redditt et al. 2019; Selote and Kachroo 2010b). GmRIN4b was also able to restore the activation of RPM1 by AvrB or AvrRPM1 in *rin4 Arabidopsis* plants (Selote and Kachroo 2010b). Similar to the activation of RPS2 upon proteolytic cleavage of AtRIN4, it was recently demonstrated that AvrRpt2-mediated cleavage of SIRIN4 and MdRIN4 also activates the R-proteins SIPtr1 and MdMr5, respectively (Mazo-Molina et al. 2020; Prokchorchik et al. 2020). The C-terminal cleavage fragment of MdRIN4, MdACP3, was both necessary and sufficient for the activation of MR5 (Prokchorchik et al. 2020). These results indicate that effectors from different pathogens elicit NLR-mediated immune responses by targeting RIN4.

To determine if the effector-mediated cleavage of the YFP-AcV5-RIN4<sup>ΔRCS1</sup> homologs resulted in the activation of RPS2, YFP-AcV5-RIN4<sup>ΔRCS1</sup>, derivatives of homologs capable of suppressing RPS2 (and the rice derivative as a negative control) were co-infiltrated with RPS2 and/or AvrRpt2. To avoid background cell death caused by high level expression of AvrRpt2 (Figure 3.11), reminiscent of that induced upon high-level expression of AvrB in *N. benthamiana* (Chung et al. 2011), we used *Agrobacterium* at an OD<sub>600</sub> of 0.01.

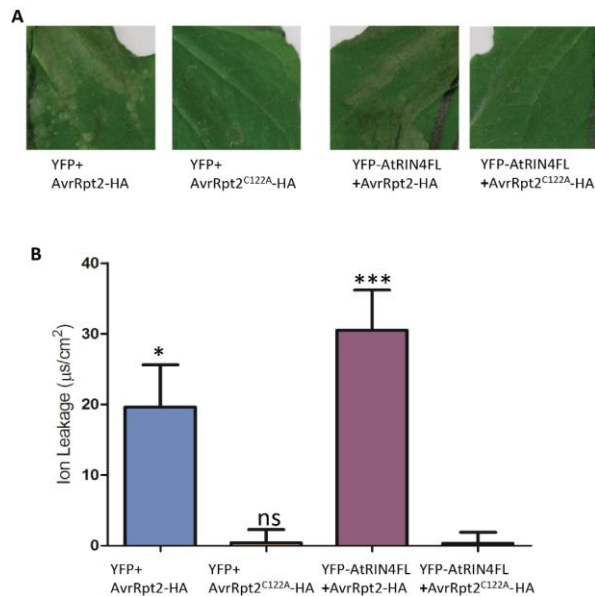


**Figure 3.11. Overexpression of AvrRpt2 in *N. benthamiana* results HR like cell death response.** (A) YFP-AtRIN4Fl and empty vector expressing YFP (OD<sub>600</sub> 0.6) were co-expressed in *N. benthamiana* with AvrRpt2-HA or AvrRpt2<sup>C122A</sup>-HA (OD<sub>600</sub> 0.05). Macroscopic HR like cell death was observed at 48 HPI. Expression of AvrRpt2-HA with either empty vector or YFP-AtRIN4Fl resulted in an HR like cell death. While no cell death was observed when empty vector or YFP-AtRIN4Fl were co-expressed with AvrRpt2<sup>C122A</sup>-HA. (B) Cell death was quantified based on electrolyte leakage. Three leaf discs for each combination, as in panel A, were taken, immersed in sterile water, and conductivity of the bath solution was measured at 72 HPI. Data was collected from 5 independent experiments. Error bars represent SEM. All combinations were compared against YFP-AtRIN4Fl derivative. Student's t-test, at 95% confidence limits, was used for comparison (ns, not significant; \*P<0.005; \*\*\*P<0.001)

Overexpression of AtRIN4 causes a delay in elimination of the full length protein by AvrRpt2, which in turn inhibits RPS2 activation (Axtell and Staskawicz 2003; Mackey et al. 2003). Similarly, when YFP-AcV5-AtRIN4 was expressed with a high titer of *Agrobacterium* (OD<sub>600</sub> of 1.0), AvrRpt2 failed to activate RPS2 (data not shown). However, YFP-AtRIN4Fl (full length)

expressed at an OD<sub>600</sub> of 0.6 was able to suppress the ectopic activation of RPS2 and permit activation of RPS2 by AvrRpt2 (Figure 3.12a and b).

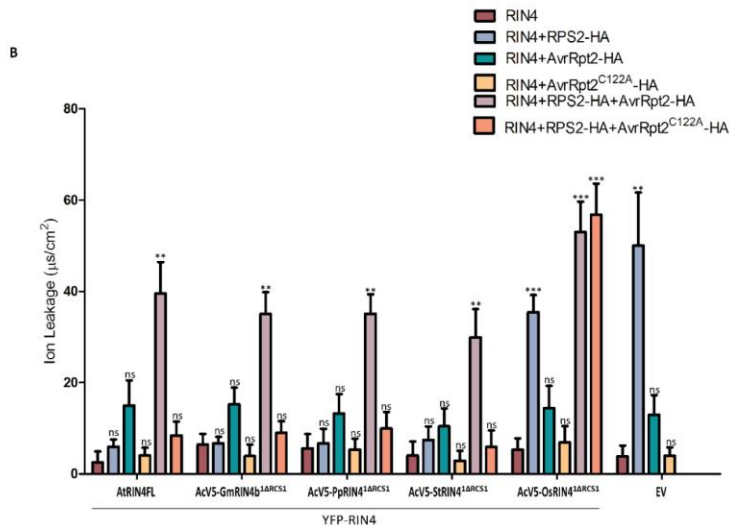
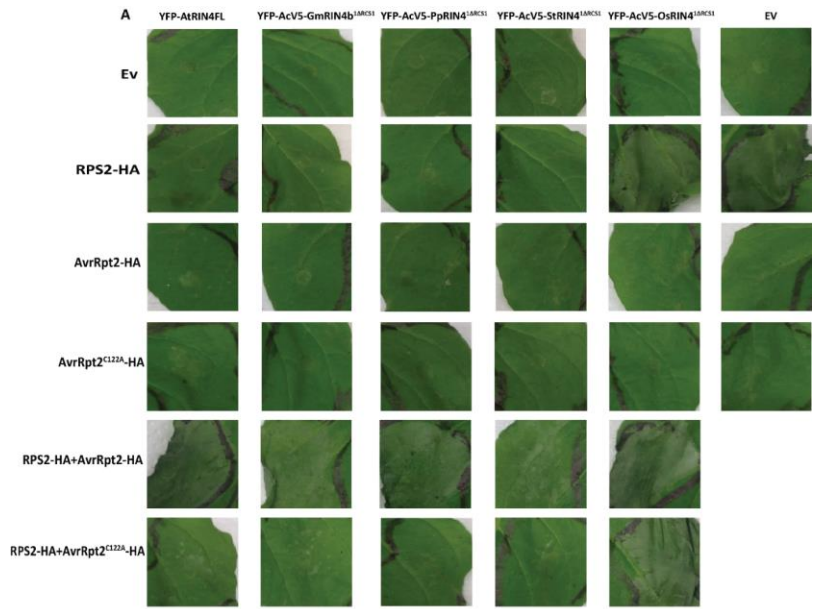


**Figure 3.12. AvrRpt2-mediated cleavage of the RIN4 homologs activates RPS2.** (A) YFP-AcV5-RIN4<sup>1ARCS1</sup> derivatives (OD<sub>600</sub> 0.6) were co-expressed in *N. benthamiana* in the indicated

combinations with RPS2-HA (OD<sub>600</sub> 0.09) and/or AvrRpt2-HA or AvrRpt2<sup>C122A</sup>-HA (OD<sub>600</sub> 0.01). Macroscopic RPS2-induced cell death was observed at 48 HPI. Similar to YFP-AtRIN4Fl, co-infiltration of YFP-AcV5-RIN4<sup>1ΔRCS1</sup> derivatives from soybean, peach and potato with AvrRpt2-HA, but not AvrRpt2<sup>C122A</sup>-HA, resulted in RPS2 dependent cell death. **(B)** Cell death was quantified based on electrolyte leakage. Three leaf discs for each combination, as in panel **A**, were taken, immersed in sterile water, and conductivity of the bath solution was measured at 72 HPI. Data was collected from 4 independent experiments. Error bars represent SEM. Within a species, all of combinations were compared against the species specific YFP-AcV5-RIN4<sup>1ΔRCS1</sup> derivative. Student's t-test, at 95% confidence limits, was used for comparison (ns, not significant; \*\*P<0.01; \*\*\*P<0.001)

Thus, for this assay, *Agrobacterium* delivering the YFP-AcV5-RIN4<sup>1ΔRCS1</sup> homologs was infiltrated at an OD<sub>600</sub> of 0.6. YFP-AcV5-RIN4<sup>1ΔRCS1</sup> homologs from soybean, peach and potato, which were able to suppress ectopic activation of RPS2, also supported the AvrRpt2-mediated activation of RPS2 (Figure 3.12a and b). This activity of AvrRpt2 was dependent on its protease activity as AvrRpt2<sup>C122A</sup> failed to overcome RPS2 suppression by any of the YFP-AcV5-RIN4<sup>1ΔRCS1</sup> homologs (Figure 3.12a and b). Thus, YFP-AcV5-RIN4<sup>1ΔRCS1</sup> homologs from soybean, peach and potato can substitute for AtRIN4 in reconstitution of the AvrRpt2-RPS2 recognition module.

### 3.3. Discussion:

AtRIN4 is a member of a highly conserved family of proteins that plays a key role in regulating innate immunity in *Arabidopsis* (Afzal et al. 2013). RIN4 homologs have been reported in plant species ranging from moss to monocots and dicots (Afzal et al. 2013). Conservation of RIN4 homologs across different plant species led to the hypothesis that the encoded proteins might respond to the effectors from plant pathogens in a manner similar to AtRIN4. RIN4 homologs typically contain the general features known to contribute to regulation of immunity, including the NOI domains with embedded AvrRpt2 cleavage sites and a C-terminal acylation motif important for membrane localization (Afzal et al. 2011; Day et al. 2005; Takemoto and Jones 2005). In this study, we have demonstrated that RIN4 homologs from several crop species have predicted C-terminal acylation motifs and, consistent with the functionality of these motifs, are localized at the

plasma membrane in *N. benthamiana*. Thus, the function of this membrane targeting strategy appears to be conserved among RIN4 proteins.

Membrane localization of AtRIN4 is required for its ability to prevent ectopic activation of RPS2 (Afzal et al. 2011; Day et al. 2005). We have demonstrated that, while derivatives of all seven RIN4 proteins used in this study localize to the plasma membrane, only those from *Arabidopsis*, soybean, peach, potato and apple are able to suppress RPS2. Since differences in ability of RIN4 homologs to suppress RPS2 are unlikely a result of their expression level or subcellular localization, we speculate that the variability in RPS2 regulation might be due to polymorphisms between RIN4 homologs.

Membrane localization of AtRIN4 is required for its ability to prevent ectopic activation of RPS2 (Afzal et al. 2011; Day et al. 2005). We have demonstrated that, while derivatives of all seven RIN4 proteins localize to the plasma membrane, only those from *Arabidopsis*, soybean, peach and potato were able to suppress RPS2. We speculated that the differential regulation of RPS2 by the RIN4 homologs results from polymorphic amino acids. It has been recently demonstrated that the differential regulation of NLR's by AtRIN4 and MdrIN4 occurs due to the presence of two key polymorphic amino acid residues present in the C-terminal end of the proteins, AtRIN4 (N158/Y165) and MdrIN4 (D186/F193) (Prokchorchik et al. 2020). However, the amino acids at these positions do not correlate with the differential ability of the RIN4 homologs to suppress RPS2. Based on our alignment data we were able to identify two polymorphic amino acids that correlated with the ability of RIN4 homologs to suppress RPS2, both of which are located in the C-terminal portion and one of which is within a MORF of the intrinsically unstructured RIN4 protein. Future investigation will examine whether these polymorphisms influence the ability of RIN4 homologs to suppress RPS2.

Similar to YFP-AcV5-AtRIN4, AvrRpt2-mediated cleavage of soybean, peach and potato YFP-AcV5-RIN4<sup>ΔRCS1</sup> derivatives resulted in the activation of RPS2. Thus, these RIN4 homologs have the ability to regulate RPS2-mediated immune response against bacterial pathogens carrying the effector AvrRpt2. Proteolysis of the YFP-AcV5-RIN4<sup>ΔRCS1</sup> derivatives by the effector, AvrRpt2, resulted in the generation of RIN4<sup>INT</sup> and RIN4<sup>CLV3</sup> fragments. We have demonstrated that these two cleavage fragments differ with respect to regulation of RPS2. The cytosolic RIN4<sup>INT</sup> fragments

are unable to suppress RPS2, while the membrane-tethered RIN4<sup>CLV3</sup> fragment retain the ability to prevent ectopic activity of RPS2. These observations raise the interesting possibility that RPS2 activation results from the combined activity of the RIN4 cleavage fragments, rather than simply the elimination of full-length RIN4.

## Chapter 4: Fragments of RIN4 produced by AvrRpt2 differ in their ability to suppress RPS2

This chapter is adapted from Alam, et al., 2021 RIN4 homologs from important crop species differentially regulate the Arabidopsis NB-LRR immune receptor, RPS2. *Plant cell reports*. In press

### 4.1. Introduction:

In order to promote pathogenesis, gram negative bacterial pathogens use a needle like apparatus, type three secretion system (TTSS) to secret effectors in the plant cytosol (Jones and Dangl 2006). Based on genomic information, it is predicted that *Pseudomonas syringae* species might secret up to 30 effectors in the plant cytosol, which collectively suppress host defenses and subsequently promote bacterial virulence (Chang et al. 2005; Coaker et al. 2006; Jones and Dangl 2006). One well studied effector secreted by *P. syringae* is AvrRpt2. AvrRpt2 is a 28 KDa cysteine protease that is secreted into the plant cytosol in an in-active state (Figure 4.1) (Coaker et al. 2006; Kim et al. 2005a).

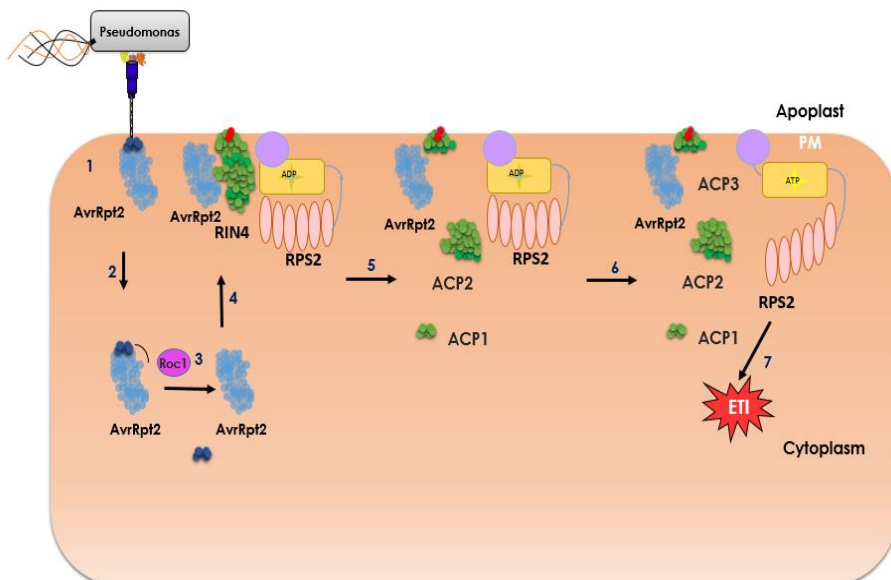


**Figure 4.1. AvrRpt2 mediated cleavage of RIN4 results in the activation of ETI in Arabidopsis:** (1) *P. syringae* secretes AvrRpt2 in plant cytosol using the T3SS, (2) AvrRpt2, once inside the host cell encounters a plant prolyl-peptidyl isomerase (PPlase), ROC1, that binds to its GPxL amino acid motif in order to activate the effector via prolyl isomerization, (3) The activated effector then auto-processes itself at the N-terminus releasing a 7 and 21 KDa fragment, (4) The 21 KDa fragment of AvrRpt2 is the active protease that localizes at the plant cell membrane, (5) Membrane localized AvrRpt2 then cleaves RIN4, (6) Cleavage of RIN4 by AvrRpt2 activates RPS2, (7) Activated RPS2 then elicits ETI.

Once inside the cytosol, AvrRpt2 encounters a plant prolyl-peptidyl isomerase (PPlase), ROC1, that binds to its GPxL amino acid motif in order to activate the effector via prolyl isomerization (Figure 4.1) (Coaker et al. 2006). The activated effector then auto-processes itself at the N-terminus releasing a 7 and 21 KDa fragment; the latter fragment is the active protease that localizes at the plant cell membrane (Figure 4.1) (Kim et al. 2005a). Membrane localized AvrRpt2 then cleaves RPM1 interacting protein 4 (RIN4) in *Arabidopsis* plants (Figure 4.1) (Chisholm et al. 2005; Coaker et al. 2006; Kim et al. 2005a; Mackey et al. 2003; Takemoto and Jones 2005).

RIN4 is a membrane localized protein that contains two sites which are similar to the AvrRpt2 processing sites (Figure 4.2) (Chisholm et al. 2005; Kim et al. 2005a). These are known as AvrRpt2 cleave site 1 (RCS1 1 (V6-W12) and RCS2 (V148-W154) (Kim et al. 2005a). Cleavage of RIN4 at these two sites by AvrRpt2 results in the generation of three fragments, namely AvrRpt2-cleavage product 1 (ACP1, AtRIN4<sup>1-10</sup>), (ACP2, AtRIN4<sup>11-152</sup>) and ACP3 (AtRIN4<sup>153-211</sup>) (Figure 4.1) (Afzal et al. 2011; Kim et al. 2005a). Two of these fragments, ACP2 and ACP3, contain a partiality truncated NOI (Nitrate induced) (Figure 4.2) domain and are potent suppressors of MTI (Afzal et al. 2011). Therefore, AvrRpt2 targets RIN4 to suppress defense response and promote bacterial virulence.

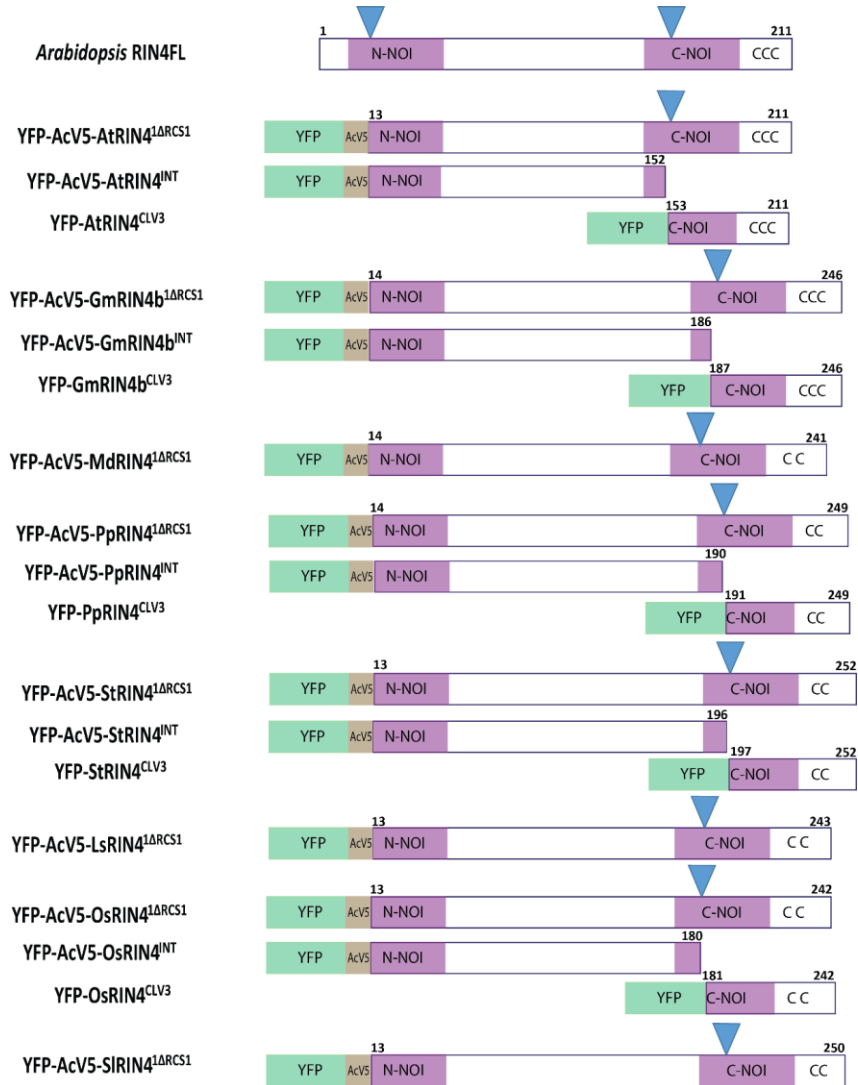


**Figure 4.2. Schematic diagram of RIN4 derivatives used in this chapter.** Within RIN4 derivatives: Green rectangles indicate YFP tag, brown squares indicate AcV5 epitopes, purple rectangles indicate NOI domains, and blue triangles indicate RCS2.

Effector mediated perturbations of RIN4 are also reported to activate ETI in Arabidopsis. For instance, AvrRpt2 mediated cleavage of RIN4 induces RPS2 activation which elicits ETI in Arabidopsis plants (Figure 4.2) (Axtell and Staskawicz 2003; Day et al. 2005; Mackey et al. 2003). We have recently demonstrated that two of the cleavage fragments, ACP2 and ACP3, play contrasting roles in RPS2 regulation (Chapter 2). Similar to full length RIN4, the membrane tethered ACP3 fragment retains the ability to suppress RPS2; while the soluble fragment ACP2, activates ACP3 suppressed RPS2. Thus, although both fragments enhance bacterial virulence in the absence of RPS2, the soluble fragment ACP2 activates plant defense in the presence of RPS2.

We have further demonstrated that RIN4 homologs from soybean, peach and potato are capable of suppressing Arabidopsis RPS2 expressed in *N. benthamiana*. Interestingly similar to AtRIN4, AvrRpt2 mediated cleavage of RIN4 homologs from soybean, peach and potato also results in RPS2 activation. Based on these results we hypothesized that, similar to AtRIN4 fragments, the homologous cleavage fragments might also be involved in RPS2 activation. The aim of this chapter was to study the effect of the homologous cleavage fragments on the activity of RPS2. For this purpose we cloned the central (RIN4<sup>INT</sup>) and C-terminal (RIN4<sup>CLV3</sup>) (Figure 4.2) fragments of RIN4 homologs and co-expressed them with RPS2 in *N. benthamiana*.

In this chapter we report that the central (RIN4<sup>INT</sup>) and C-terminal (RIN4<sup>CLV3</sup>) fragments of RIN4 generated upon AvrRpt2-cleavage differ in their regulation of RPS2. The membrane-tethered RIN4<sup>CLV3</sup> fragments, comparable to ACP3, suppress RPS2 activation. The non-membrane-tethered RIN4<sup>INT</sup> fragments, comparable to ACP2, fail to suppress RPS2. Interestingly, the homologous RIN4<sup>INT</sup> fragments are able to complement AtACP2 function by activating AtACP3 suppressed RPS2. However both AtACP2 and AtRIN4<sup>INT</sup> fail to activate RPS2 suppressed by homologous RIN4<sup>CLV3</sup> fragments. Lastly we demonstrate that similar to AtRIN4<sup>INT</sup>, the homologous RIN4<sup>INT</sup> were also able to activate RPS2 suppressed by homologous RIN4<sup>CLV3</sup> fragments.

## **4.2. Results:**

### **4.2.1. Fragments of RIN4 produced by AvrRpt2 differ in their ability to suppress RPS2**

Cleavage of AtRIN4 by AvrRpt2 serves as a trigger for the activation of RPS2 (Axtell and Staskawicz 2003; Mackey et al. 2003). After establishing that AvrRpt2-mediated cleavage of the

homologous proteins resulted in the activation of RPS2, the role of the cleavage fragments in the regulation of RPS2 activation was determined. The C-terminal cleavage fragment, AtRIN4<sup>CLV3</sup>, remains tethered at the plasma membrane because of the attached palmitoyl group (Afzal et al. 2011; Chisholm et al. 2005). Similarly, the YFP-RIN4<sup>CLV3</sup> fragments from the RIN4 homologs also localized at the membrane (Figure. 4.3a and b).

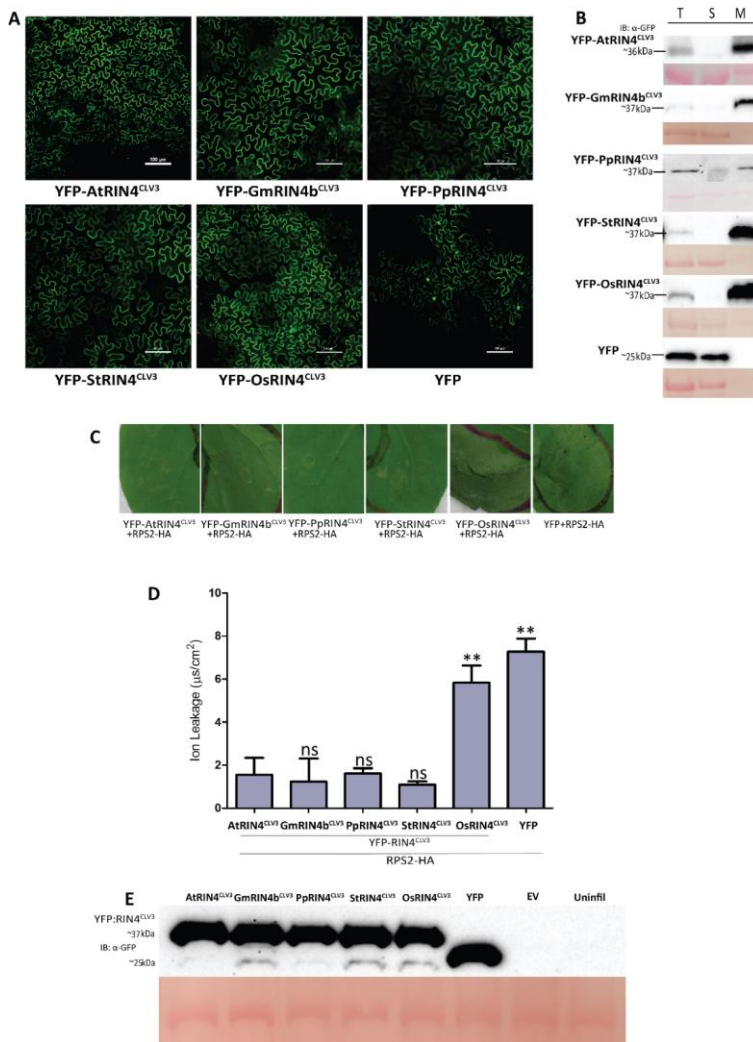


**Figure 4.3. The YFP-RIN4<sup>CLV3</sup> fragments are plasma membrane-localized and are capable of suppressing RPS2 in *N. benthamiana*.** (A) YFP-RIN4<sup>CLV3</sup> fragments (OD<sub>600</sub> 1.0) were transiently expressed in *N. benthamiana* leaves. Localization of the fluorescent signal was observed at 72 HPI using confocal-microscopy (Scale bar: 100 μM). YFP-RIN4<sup>CLV3</sup> fragments localized at the membrane, while free YFP protein localized in the cytosol and nuclei. (B) Anti-GFP immunoblotting was conducted on samples treated as in panel A at 72 HPI that had been fractionated into total (T), soluble (S) and membrane (M) fractions. YFP-RIN4<sup>CLV3</sup> fragments accumulated in the membrane fraction, while the free YFP protein accumulated in the soluble fraction. The Panel below shows ponceau stain for RuBisCO used as a soluble protein marker. (C) Co-infiltration of YFP-RIN4<sup>CLV3</sup> fragments (OD<sub>600</sub> 1.0) from Arabidopsis, soybean, peach, and potato suppressed macroscopic cell death induced by RPS2-HA (OD<sub>600</sub> 0.04) at 48 HPI in *N. benthamiana*. Free YFP protein and YFP-OsRIN4<sup>CLV3</sup> failed to suppress RPS2-HA. (D) Cell death was quantified based on electrolyte leakage. Three leaf discs for the indicated YFP-RIN4<sup>CLV3</sup> derivatives or free YFP co-infiltrated with RPS2-HA were collected, immersed in sterile water, and conductivity of the bath solution was measured at 72 HPI. Data was collected from 4 independent experiments. Error bars represent SEM. Student's t-test, at 95% confidence limits, was used for comparison with AtRIN4<sup>CLV3</sup> (ns, not significant; \*\*P>0.01). (E) Anti-GFP immunoblot conducted on samples from 72 HPI shows that YFP-RIN4<sup>CLV3</sup> fragments from the different homologs accumulated to comparable levels in *N. benthamiana*. The Panel below shows ponceau stain for RuBisCO used as loading control

When co-infiltrated in *N. benthamiana*, YFP-AtRIN4<sup>CLV3</sup> was unable to suppress RPS2 when RPS2 was expressed with *Agrobacterium* at an OD<sub>600</sub> of 0.075 (Day et al. 2005). Since the YFP-AtRIN4<sup>CLV3</sup> fragment still localizes at the plasma membrane and contains a mostly intact C-NOI domain, we speculated that it might suppress RPS2 expressed at a lower level. Indeed, Flag-AtRIN4<sup>CLV3</sup> was able to suppress RPS2 expressed at low titers (Figure 2.4). Similarly YFP-AtRIN4<sup>CLV3</sup> suppressed RPS2 that was expressed with *Agrobacterium* at an OD<sub>600</sub> of 0.04 (Figure. 4.3 c and d). Similarly, the YFP-RIN4<sup>CLV3</sup> fragment of the RIN4 homologs from soybean, peach and potato also suppressed RPS2 (Figure. 4.3c and d). The YFP-RIN4<sup>CLV3</sup> from rice, like the YFP-AcV5-RIN4<sup>ΔRCS1</sup> derivative from rice, failed to suppress RPS2 (Figure. 4.3c and d). The ability of the derivatives to suppress RPS2 did not correlate with their expression level (Figure. 4.3e).

Thus, for RIN4<sup>1ΔRCS1</sup> homologs able to suppress RPS2, the RIN4<sup>CLV3</sup> fragments are sufficient to carry out the suppression of RPS2.

We next sought to determine if, similar to the RIN4<sup>CLV3</sup> fragments, the RIN4<sup>INT</sup> fragments were able to suppress RPS2. After cleavage, the AtRIN4<sup>INT</sup> fragment is no longer tethered to the plasma membrane (Afzal et al. 2011; Kim et al. 2005a). As expected, at the YFP-AcV5-RIN4<sup>INT</sup> fragments of AtRIN4 and the RIN4 homologs localized in the soluble fraction (Figure. 4.4a and b).

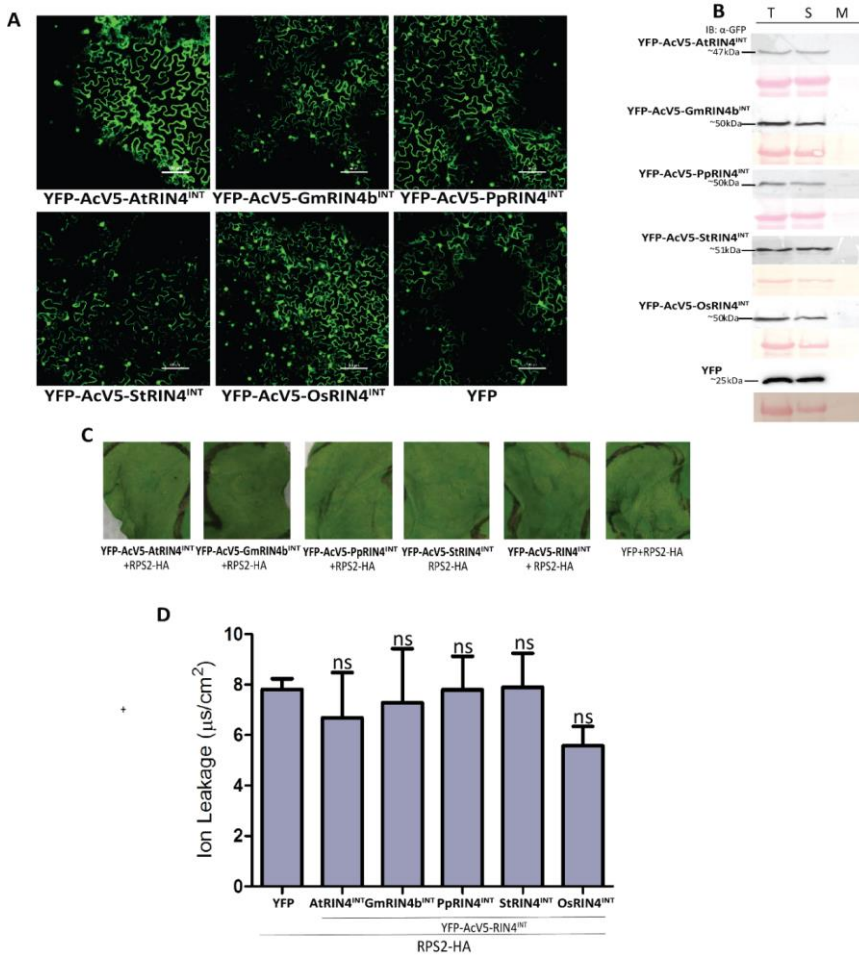


**Figure 4.4. The YFP-AcV5-RIN4<sup>INT</sup> fragments are soluble and fail to suppress RPS2 in *N. benthamiana*.** (A) YFP-AcV5-RIN4<sup>INT</sup> fragments (OD<sub>600</sub> 1.0) were transiently expressed in *N. benthamiana* plants. Localization of the fluorescent signal was observed at 72 HPI using confocal-microscopy (Scale bar: 100 μM). YFP-AcV5-RIN4<sup>INT</sup> fragments and the free YFP protein localized in the cytosol and nuclei. (B) Anti-GFP immunoblotting was conducted on samples, as in panel A, from 72 HPI that had been fractionated into total (T), soluble (S) and membrane (M) fractions. YFP-AcV5-RIN4<sup>INT</sup> fragments and the free YFP protein accumulated in the soluble fraction. The panel below shows ponceau stain for RuBisCO as a soluble protein marker. (C) Macroscopic cell death at 48 HPI of RPS2-HA (OD<sub>600</sub> 0.04) co-infiltrated with the indicated YFP-AcV5-RIN4<sup>INT</sup> fragments or free YFP (OD<sub>600</sub> 1.0) in *N. benthamiana*. (D) Cell death was quantified based on electrolyte leakage. Three leaf discs for each combination, as in panel C, were taken, immersed in sterile water, and conductivity of the bath solution was measured at 72 HPI. Data was collected from 3 independent experiments. Error bars represent SEM. Student's t-test, at 95% confidence limits, was used for comparison with YFP (ns, not significant)

AtRIN4<sup>11-152</sup> is unable to suppress RPS2 expressed with *Agrobacterium* at an OD<sub>600</sub> of 0.075 (Day et al. 2005). Even when RPS2 was expressed at the lower level, with *Agrobacterium* at an OD<sub>600</sub> of 0.04, YFP-AcV5-AtRIN4<sup>INT</sup> was unable to suppress RPS2 (Figure. 4.4c and d). Similar to YFP-AcV5-AtRIN4<sup>INT</sup>, the YFP-AcV5-RIN4<sup>INT</sup> fragments from soybean, peach and potato were also unable to suppress RPS2 (Figure. 4.4c and d). Taken together, these results indicate that the two cleavage fragments, RIN4<sup>INT</sup> and RIN4<sup>CLV3</sup>, play contrasting roles in the regulation of RPS2 activation with only the latter able to suppress RPS2.

#### **4.2.2. YFP-AcV5-AtRIN4<sup>INT</sup> is unable to activate YFP-AtRIN4<sup>CLV3</sup> suppressed RPS2**

We have recently demonstrated that in the absence of the pathogen the soluble fragment, ACP2, is able to activate RPS2 suppressed by the membrane tethered fragment, ACP3 (chapter 2). After establishing the differential regulation of RPS2 by the YFP-AtRIN4 fragments, we next sought to determine whether the YFP-AcV5-AtRIN4<sup>INT</sup> fragment was also capable of activating YFP-AtRIN4<sup>CLV3</sup> suppressed RPS2. For this purpose we co-expressed AtRIN4 derivatives, Flag-AtRIN4Fl, Flag-AtACP2, Flag-AtRIN4<sup>CLV3</sup>, YFP-AcV5-AtRIN4<sup>INT</sup> or YFP-AtRIN4<sup>CLV3</sup>, (OD<sub>600</sub> 0.6) with RPS2-HA (OD<sub>600</sub> 0.04) in *N. benthamiana* leaves (Figure 4.5a and b).

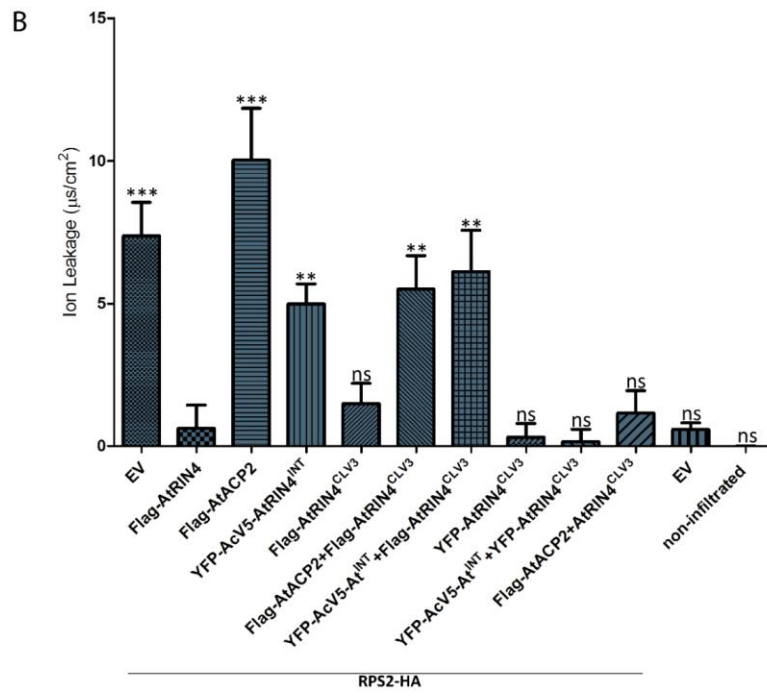


**Figure 4.5. Flag-AtACP2 and YFP-AcV5-AtRIN4<sup>INT</sup> derivatives fail to activate YFP-AtRIN4<sup>CLV3</sup> suppressed RPS2.** (A) RIN4 derivatives (Flag-AtRIN4Fl, Flag-AtACP2, Flag-AtRIN4<sup>CLV3</sup>, YFP-AcV5-AtRIN4<sup>INT</sup> or YFP-AtRIN4<sup>CLV3</sup>) and empty vector (OD<sub>600</sub> 0.6) were co-infiltrated with RPS2-HA (OD<sub>600</sub> 0.04) in *N. benthamiana* leaves. Macroscopic cell death was observed at 48 HPI. Similar to Flag-AtRIN4Fl, Flag-AtRIN4<sup>CLV3</sup> and YFP-AtRIN4<sup>CLV3</sup> suppressed RPS2-HA; while Flag-AtACP2, YFP-AcV5-AtRIN4<sup>INT</sup> and empty vector failed to suppress RPS2-HA expressed in *N. benthamiana*. Co-infiltration of either Flag-AtACP2 or YFP-AcV5-AtRIN4<sup>INT</sup> with Flag-AtRIN4<sup>CLV3</sup> resulted in activation of AtRIN4<sup>CLV3</sup> suppressed RPS2-HA. In contrast, co-infiltration of either Flag-AtACP2 or YFP-AcV5-AtRIN4<sup>INT</sup> with YFP-AtRIN4<sup>CLV3</sup> failed to activate AtRIN4<sup>CLV3</sup> suppressed RPS2-HA. (B) Cell death was quantified based on electrolyte leakage. Three leaf discs for the indicated combination co-infiltrated with RPS2-HA were collected, immersed in sterile water, and conductivity of the bath solution was measured at 96 HPI. Data was collected from 6 independent experiments. Error bars represent SEM. Student's t-test, at 95% confidence limits, was used for comparison with Flag-AtRIN4Fl (ns, not significant; \*\*P>0.01; \*\*\*P>0.001).

Similar to Flag-AtRIN4Fl, both Flag-AtRIN4<sup>CLV3</sup> and YFP-AtRIN4<sup>CLV3</sup> suppressed RPS2-HA (Figure 4.5a and b). Similar to Flag-AtACP2, YFP-AcV5-AtRIN4<sup>INT</sup> also activated Flag-AtRIN4<sup>CLV3</sup> suppressed RPS2-HA (Figure 4.5a and b). This indicates that AtRIN4<sup>INT</sup> was able to functionally complement Flag-AtACP2. Interestingly both Flag-AtACP2 and YFP-AcV5-AtRIN4<sup>INT</sup> failed to activate RPS2-HA suppressed by YFP-AtRIN4<sup>CLV3</sup> (Figure 4.5a and b). Similarly the homologous YFP-AcV5-AtRIN4<sup>INT</sup> fragments failed to activate RPS2-HA suppressed by the homologous YFP-RIN4<sup>CLV3</sup> fragments (Figure 4.6a and b). Taken together these results indicated that the addition of a bulky tag (YFP) at the N-terminus of AtRIN4<sup>CLV3</sup> hinders RPS2-HA activation.

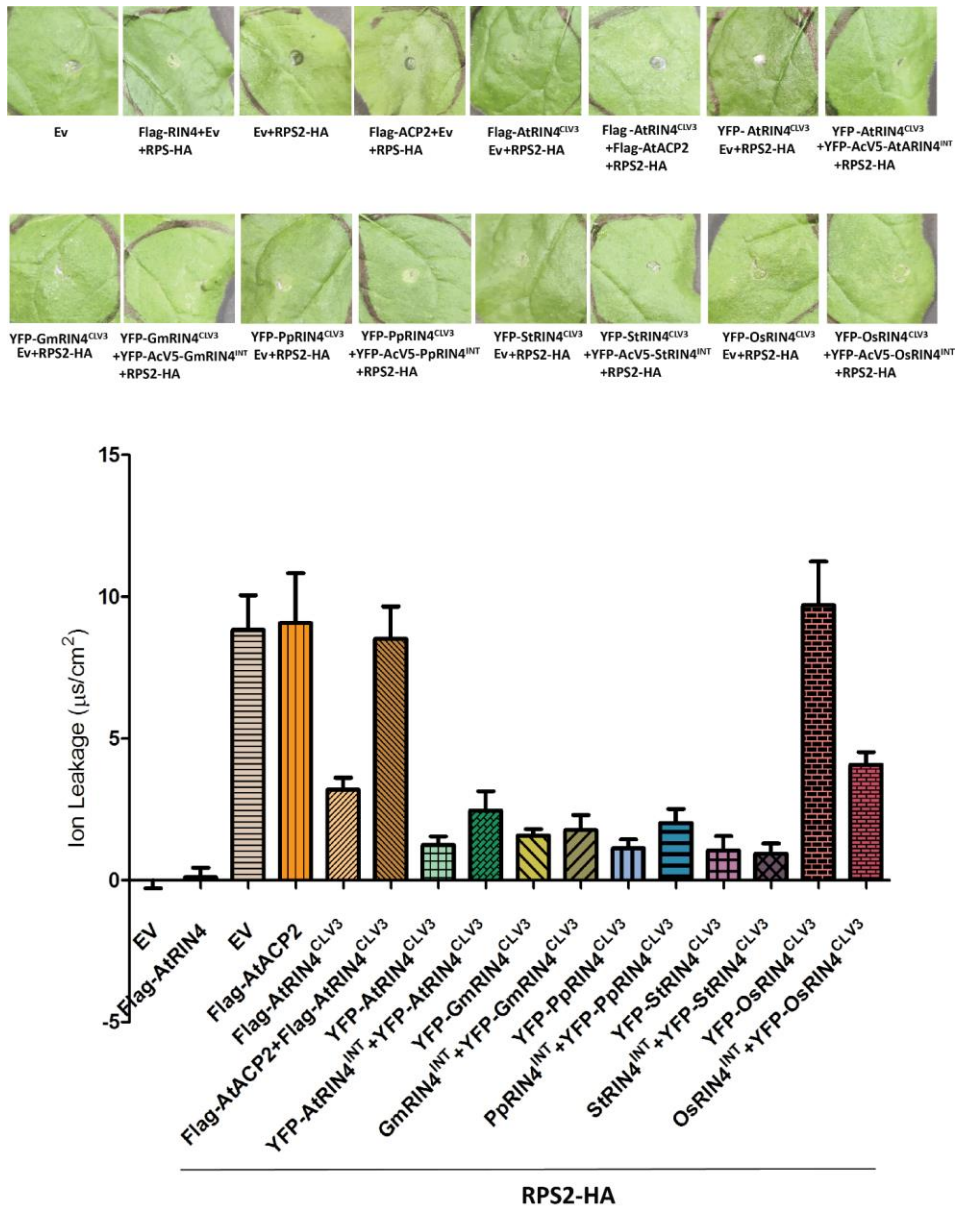
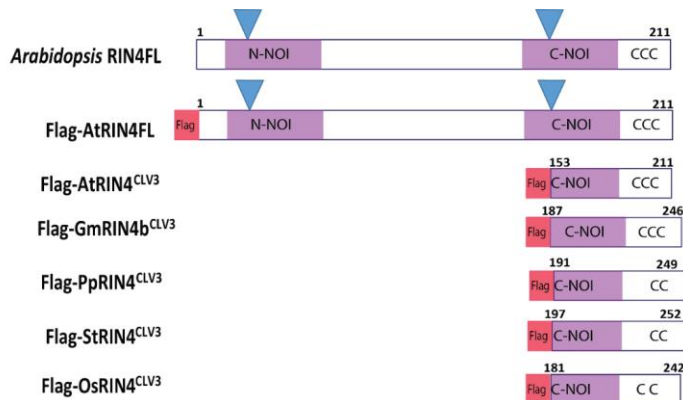


Figure 4.6. Homologous YFP-AcV5-RIN4<sup>INT</sup> derivatives fail to activate RPS2 suppressed by homologous YFP-RIN4<sup>CLV3</sup> derivatives. (A) RIN4 derivatives (Flag-AtACP2, Flag-

AtRIN4<sup>CLV3</sup>, YFP-AcV5-RIN4<sup>INT</sup> or YFP-RIN4<sup>CLV3</sup>) and empty vector (OD<sub>600</sub> 0.6) were co-infiltrated with RPS2-HA (OD<sub>600</sub> 0.04) in *N. benthamiana* leaves. Macroscopic cell death was observed at 48 HPI. Similar to Flag-AtRIN4<sup>CLV3</sup>, homologous YFP-RIN4<sup>CLV3</sup> derivatives also suppressed RPS2-HA, while the empty vector failed to suppress RPS2-HA expressed in *N. benthamiana*. Co-infiltration of Flag-AtACP2 with Flag-AtRIN4<sup>CLV3</sup> resulted in RPS2-HA activation. In contrast, co-infiltration of homologous YFP-AcV5-AtRIN4<sup>INT</sup> derivatives with YFP-AtRIN4<sup>CLV3</sup> failed to activate AtRIN4<sup>CLV3</sup> suppressed RPS2-HA. **(B)** Cell death was quantified based on electrolyte leakage. Three leaf discs for the indicated combination co-infiltrated with RPS2-HA were collected, immersed in sterile water, and conductivity of the bath solution was measured at 96 HPI. Data collected from two independent experiment. Error bars represent SEM.

#### 4.2.3. Non-membrane tethered AtRIN4 fragments fail to reactivate RPS2 suppressed by homologous Flag-AtRIN4<sup>CLV3</sup> fragments.

Since the addition of the YFP tag at the N-terminus of RIN4<sup>CLV3</sup> fragments hindered RPS2 activation by the soluble fragments we cloned these fragments with an N-terminal Flag tag (Figure 4.7).



**Figure 4.7. Schematic diagram of RIN4 derivatives used in this chapter.** Within RIN4 derivatives: Red rectangles indicate Flag tag, purple rectangles indicate NOI domains, and blue triangles indicate RCS2.

Flag-AtRIN4FI, Flag-AtRIN4<sup>CLV3</sup>, YFP-AtRIN4<sup>CLV3</sup> or homologous Flag-RIN4<sup>CLV3</sup> (OD<sub>600</sub> 0.6) were co-expressed with RPS2-HA (OD<sub>600</sub> 0.04) in *N. benthamiana* leaves (Figure 4.8a and b). Similar to Flag-AtRIN4F and YFP-AtRIN4<sup>CLV3</sup>, the homologous Flag-RIN4<sup>CLV3</sup> fragments also suppressed RPS2 (Figure. 4.8a and b); while the Flag-RIN4<sup>CLV3</sup> from rice, failed to suppress RPS2 (Figure. 4.8a and b). The ability of the derivatives to suppress RPS2 did not correlate with their expression level (Figure. 4.8c).

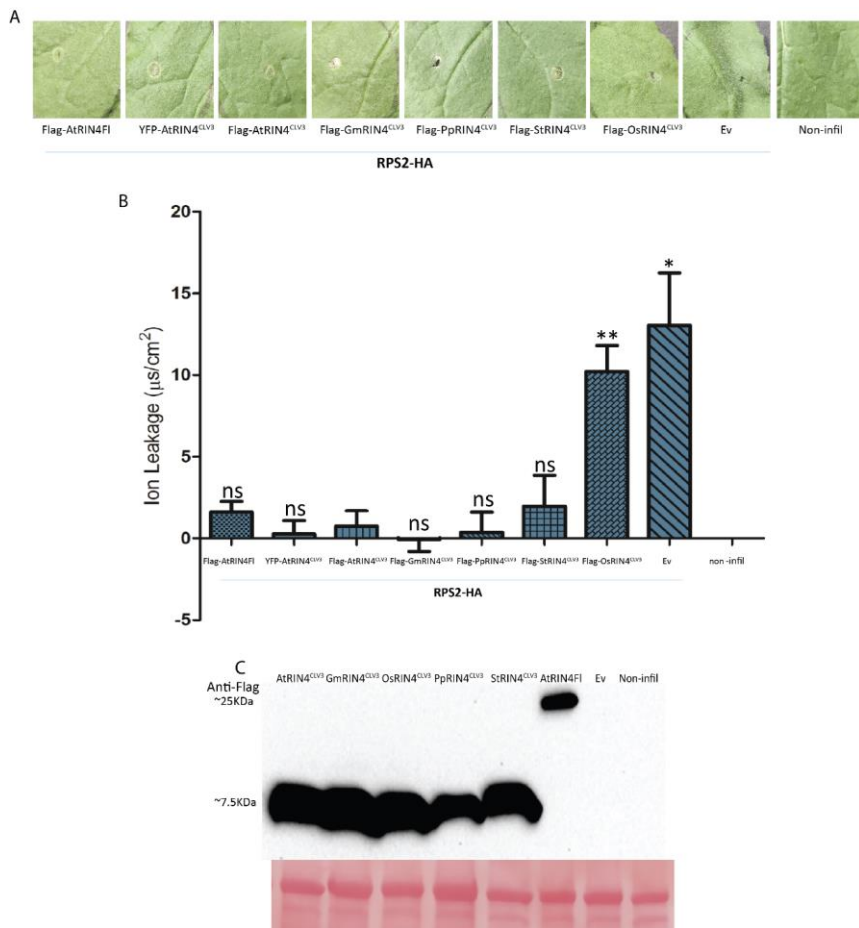


**Figure 4.8. The Flag-RIN4<sup>CLV3</sup> fragments are capable of suppressing RPS2 in *N. benthamiana*.** (A) Similar to Flag-AtRIN4Fl, Co-infiltration of Flag-RIN4<sup>CLV3</sup> fragments (OD<sub>600</sub> 1.0) from Arabidopsis, soybean, peach, and potato suppressed macroscopic cell death induced by RPS2-HA (OD<sub>600</sub> 0.04) at 48 HPI in *N. benthamiana*. Empty vector and YFP-OsRIN4<sup>CLV3</sup> failed to suppress RPS2-HA. (B) Cell death was quantified based on electrolyte leakage. Three leaf discs for the indicated combinations were collected, immersed in sterile water, and conductivity of the bath solution was measured at 72 HPI. Data was collected from 3 independent experiments. Error bars represent SEM. Student's t-test, at 95% confidence limits, was used for comparison with Flag-AtRIN4<sup>CLV3</sup> (ns, not significant; \*P>0.05; \*\*P>0.01). Anti-Flag immunoblot conducted on samples collected at 72 HPI shows that Flag-RIN4<sup>CLV3</sup> accumulate to comparable levels in *N. benthamiana*. Panel below show ponceau stain for RuBisCO used as loading control.

After establishing RPS2 suppression by Flag-RIN4<sup>CLV3</sup> fragments we next sought to determine whether co-expression of non-membrane tethered fragments of AtRIN4 would result in activation of Flag-RIN4<sup>CLV3</sup> suppressed RPS2. For this purpose RIN4 derivatives, homologous Flag-AtRIN4<sup>CLV3</sup> derivatives (OD<sub>600</sub> 0.6) were co-infiltrated with RPS2-HA (OD<sub>600</sub> 0.04) and either Flag-ACP2 or YFP-AcV5-AtRIN4<sup>INT</sup> (OD<sub>600</sub> 0.6) in *N. benthamiana* leaves (Figure 4.9a and b). Similar to Flag-AtRIN4Fl, the homologous Flag-RIN4<sup>CLV3</sup> fragments also suppressed RPS2, while both Flag-ACP2 and YFP-AcV5-AtRIN4<sup>INT</sup> failed to suppress RPS2. Both Flag-ACP2 and YFP-AcV5-AtRIN4<sup>INT</sup> activated RPS2 suppressed by Flag-AtRIN4<sup>CLV3</sup>; while they failed to activate RPS2 suppressed by YFP-AtRIN4<sup>CLV3</sup> (Figure 4.9a and b). Interestingly Flag-ACP2 and YFP-AcV5-AtRIN4<sup>INT</sup> failed to activate RPS2 suppressed by homologous Flag-RIN4<sup>CLV3</sup> derivatives. This indicates that even though the homologous derivatives are able to complement RPS2 suppression, they fail to complement RPS2 activation in the presence of the non-membrane tethered AtRIN4 fragments.

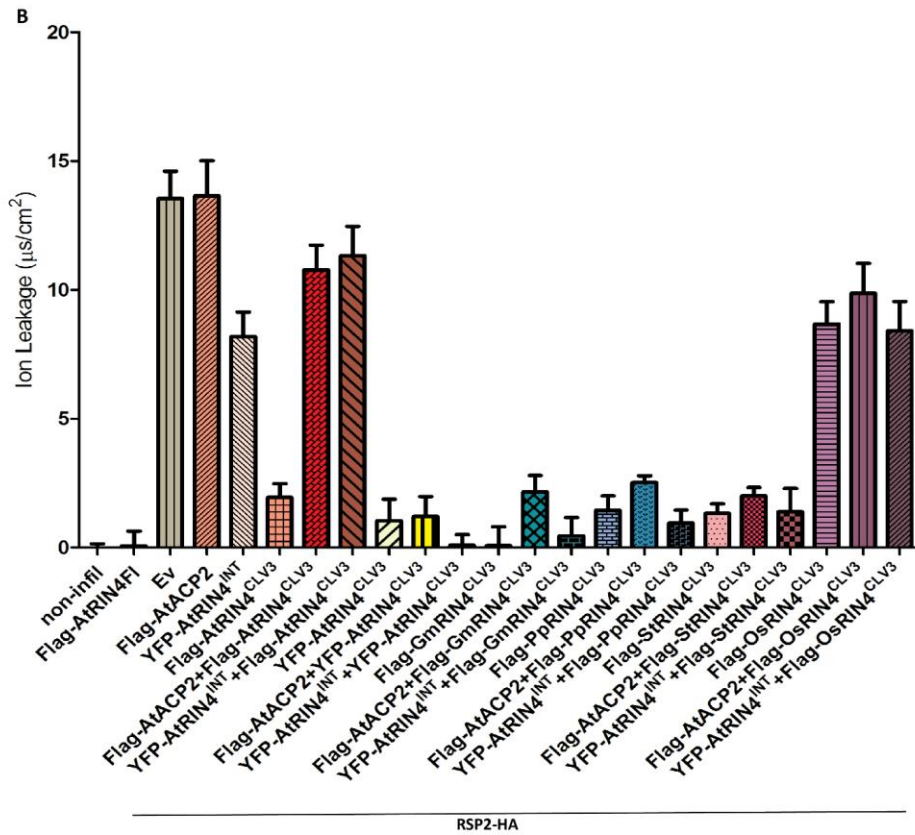


**Figure 4.9. Non-membrane tethered AtRIN4 fragments fail to activate RPS2 suppressed by homologous Flag-AtRIN4<sup>CLV3</sup> fragments.** (A) RIN4 derivatives (Flag-AtRIN4Fl, Flag-AtACP2, YFP-AcV5-AtRIN4<sup>INT</sup>, Flag-AtRIN4<sup>CLV3</sup>, YFP-AtRIN4<sup>CLV3</sup> or homologous Flag-RIN4<sup>CLV3</sup>) and empty vector (OD<sub>600</sub> 0.6) were co-infiltrated with RPS2-HA (OD<sub>600</sub> 0.04) in *N. benthamiana* leaves. Macroscopic cell death was observed at 48 HPI. Similar to Flag-AtRIN4Fl, YFP-AtRIN4<sup>CLV3</sup> and homologous Flag-RIN4<sup>CLV3</sup> derivatives also suppressed RPS2-HA, while Flag-AtACP2, YFP-AcV5-AtRIN4<sup>INT</sup> and empty vector failed to suppress RPS2-HA expressed in *N. benthamiana*. Co-infiltration of Flag-AtACP2 or YFP-AcV5-AtRIN4<sup>INT</sup> derivatives with Flag-RIN4<sup>CLV3</sup> failed to activate RPS2-HA suppressed by homologous Flag-RIN4<sup>CLV3</sup>. (B) Cell death was quantified based on electrolyte leakage. Three leaf discs for the indicated combination co-infiltrated with RPS2-HA were collected, immersed in sterile water, and conductivity of the bath solution was measured at 96 HPI. Data was collected from 5 independent experiments. Error bars represent SEM.

#### **4.2.4. Homologous RIN4<sup>INT</sup> derivatives are capable of activating RPS2-HA suppressed by Flag-AtRIN4<sup>CLV3</sup>.**

The observation that RIN4<sup>CLV3</sup> weakly suppressed RPS2 led us to speculate that the homologous RIN4<sup>INT</sup> fragments might be able to overcome the RIN4<sup>CLV3</sup> mediated RPS2 suppression. To test this we co-expressed Flag-AtRIN4<sup>CLV3</sup> (OD<sub>600</sub> 0.6) with the homologous YFP-AcV5-RIN4<sup>INT</sup> (OD<sub>600</sub> 0.6) fragments and RPS2-HA (OD<sub>600</sub> 0.04). Figure 4.10 shows that while AtRIN4<sup>CLV3</sup> was able to suppress RPS2-HA, both Flag-ACP2 and YFP-AcV5-AtRIN4<sup>INT</sup> were able to activate Flag-AtRIN4<sup>CLV3</sup> suppressed RPS2. Interestingly the homologous YFP-AcV5-RIN4<sup>INT</sup> also resulted in the activation of AtRIN4<sup>CLV3</sup> suppressed RPS2 (Figure 4.10a and b). This indicated that the non-membrane tethered derivatives from the homologs under study were sufficient to activate RPS2 suppressed by Flag-AtRIN4<sup>CLV3</sup>. Results from this experiment are consistent with our proposed model for RPS2 activation which states that AvrRpt2 activates RPS2 through the generation of the non-membrane tethered fragment ACP2.

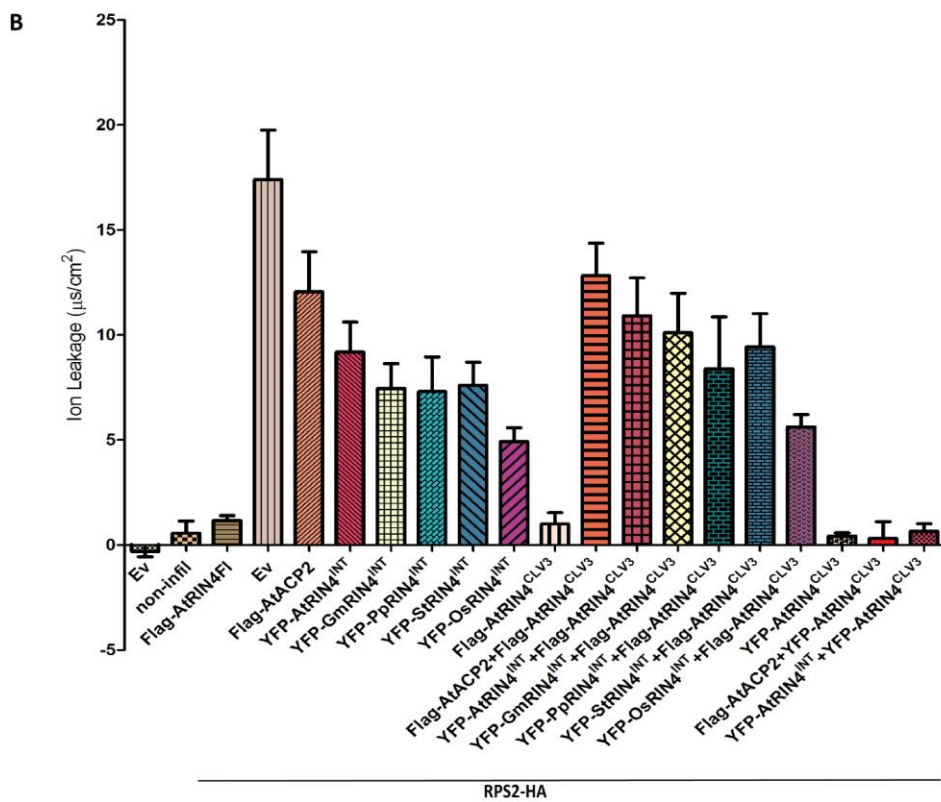
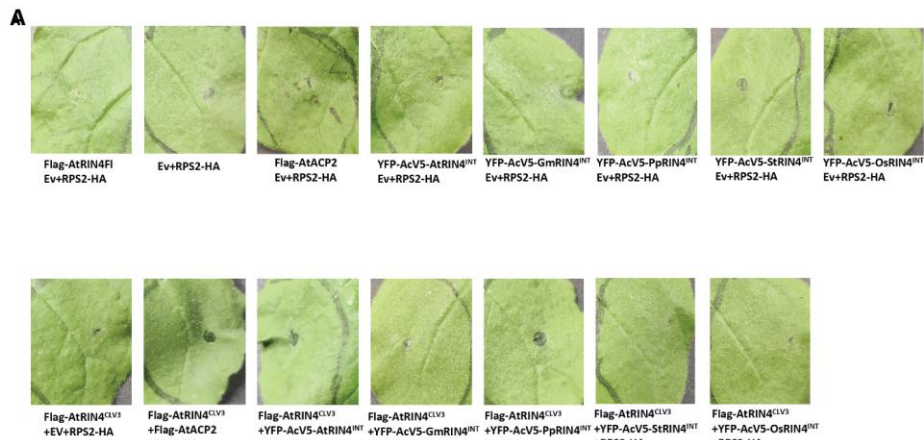


**Figure 4.10. Homologous RIN4<sup>INT</sup> derivatives are capable of activating RPS2-HA suppressed by Flag-AtRIN4<sup>CLV3</sup>.** (A) RIN4 derivatives (Flag-AtRIN4Fl, Flag-AtACP2, Flag-AtRIN4<sup>CLV3</sup> or homologous YFP-AcV5-RIN4<sup>INT</sup>) and empty vector (OD<sub>600</sub> 0.6) were co-infiltrated with RPS2-HA (OD<sub>600</sub> 0.04) in *N. benthamiana* leaves. Macroscopic cell death was observed at 48 HPI. Similar to Flag-AtRIN4Fl, Flag-AtRIN4<sup>CLV3</sup> also suppressed RPS2-HA, while Flag-AtACP2, homologous YFP-AcV5-RIN4<sup>INT</sup> and empty vector failed to suppress RPS2-HA expressed in *N. benthamiana*. Co-infiltration of Flag-AtACP2 or homologous YFP-AcV5-RIN4<sup>INT</sup> derivatives with Flag-AtRIN4<sup>CLV3</sup> resulted in RPS2-HA activation. (B) Cell death was quantified based on electrolyte leakage. Three leaf discs for the indicated combination co-infiltrated with RPS2-HA were collected, immersed in sterile water, and conductivity of the bath solution was measured at 96 HPI. Data was collected from 3 independent experiments. Error bars represent SEM.

#### **4.2.5. Homologous RIN4<sup>INT</sup> derivatives are capable of activating RPS2-HA suppressed by homologous Flag-RIN4<sup>CLV3</sup>.**

In order to determine whether homologous YFP-AcV5-RIN4<sup>INT</sup> derivatives could activate Flag-RIN4<sup>CLV3</sup> suppressed RPS2, we co-infiltrated these constructs in *N. benthamiana* leaves (Figure 4.11). Similar to Flag-AtRIN4Fl, YFP-AtRIN4<sup>CLV3</sup> and homologous Flag-RIN4<sup>CLV3</sup> also suppressed RPS2-HA, while Flag-AtACP2, homologous YFP-AcV5-RIN4<sup>INT</sup> and empty vector failed to suppress RPS2-HA expressed in *N. benthamiana* (Figure 4.11). Co-infiltration of Flag-AtACP2 or YFP-AcV5-AtRIN4<sup>INT</sup> derivatives with Flag-AtRIN4<sup>CLV3</sup> resulted in RPS2-HA activation. While co-infiltration of either Flag-AtACP2 or YFP-AcV5-AtRIN4<sup>INT</sup> derivatives with YFP-AtRIN4<sup>CLV3</sup> failed to activate RPS2. Similar to non-membrane tethered derivatives AtRIN4, co-infiltration of homologous YFP-AcV5-RIN4<sup>INT</sup> derivatives with homologous Flag-RIN4<sup>CLV3</sup> resulted in RPS2-HA activation (Figure 4.11). Results from our experiment are consistent with a model where cleavage of RIN4 by AvrRpt2 activates RPS2 through the generation of the non-membrane tethered fragment of RIN4.



and empty vector failed to suppress RPS2-HA expressed in *N. benthamiana*. Co-infiltration of Flag-AtACP2 or YFP-AcV5-AtRIN4<sup>INT</sup> derivatives with Flag-AtRIN4<sup>CLV3</sup> resulted in RPS2-HA activation. Similarly, co-infiltration of homologous YFP-AcV5-RIN4<sup>INT</sup> derivatives with homologous Flag-RIN4<sup>CLV3</sup> resulted in RPS2-HA activation. Cell death was quantified based on electrolyte leakage. Three leaf discs for the indicated combination co-infiltrated with RPS2-HA were collected, immersed in sterile water, and conductivity of the bath solution was measured at 96 HPI. Data was collected from 5 independent experiments. Error bars represent SEM.

### 4.3. Discussion:

Multiple effectors target important immune regulators such as RIN4 to promoter bacterial virulence (Lee et al. 2015; Mackey et al. 2003; Mackey et al. 2002; Redditt et al. 2019; Wilton et al. 2010). The effector dependent post translational modifications are recognized by NLR proteins which in turn activates an appropriate immune response. For example, AvrRpt2 mediated cleavage of RIN4 results in the activation of RPS2 (Axtell and Staskawicz 2003; Day et al. 2005; Mackey et al. 2003). The generally accepted model for RPS2 activation stated that AvrRpt2 mediated elimination of RIN4 results in RPS2 activation (Axtell and Staskawicz 2003; Day et al. 2005; Mackey et al. 2003). Our lab has recently demonstrated that two of the cleavage fragments, ACP2 and ACP3, persist post cleavage and are involved in the regulation of RPS2 activation (Chapter 2). Thus, we propose a new model for RPS2 activation, in which cleavage of RIN4 by AvrRpt2 generates two fragments with ACP3 capable of maintaining RPS2 in a repressed state and ACP2 capable of overcoming that suppression to activate RPS2. Interestingly AvrRpt2 mediated cleavage of RIN4 homologs from soybean, peach and potato also resulted in RPS2 activation. To gain insight into the AvrRpt2-RIN4-RPS2 defense-activation module, we compared the function of AtRIN4 fragments with the homologous RIN4 fragments present in a diverse range of plant species

Proteolysis of the YFP-AcV5-RIN4<sup>1ARCS1</sup> derivatives by the effector, AvrRpt2, resulted in the generation of RIN4<sup>INT</sup> and RIN4<sup>CLV3</sup> fragments (Chapter 3). We have demonstrated that these two cleavage fragments differ with respect to regulation of RPS2. The cytosolic RIN4<sup>INT</sup> fragments are unable to suppress RPS2, while the membrane-tethered RIN4<sup>CLV3</sup> fragment retain the ability to prevent ectopic activity of RPS2.

AtRIN4<sup>INT</sup> is able to complement AtACP2 fragment in its ability to activate AtACP3 or AtRIN4<sup>CLV3</sup> suppressed RPS2. Interestingly, addition of a bulky tag at the N-terminus of the membrane-tethered AtRIN4<sup>CLV3</sup> fragment hindered RPS2 activation by the non-membrane tethered AtRIN4 fragments. We have previously demonstrated that while soluble fragment, ACP2, is able to activate RIN4<sup>CLV3</sup> suppressed RPS2, it fails to activate RPS2 suppressed by a RIN4 derivative that has an intact C-terminal NOI domain, 142-211. Taken together these results indicate that additional residues at the N-terminus of RIN4<sup>CLV3</sup> hinder the ability of the soluble fragments to cause activation of RPS2.

The homologous RIN4<sup>INT</sup> were able to activate AtRIN4<sup>CLV3</sup> suppressed RPS2. This indicates that suppression of RPS2 by AtRIN4<sup>CLV3</sup> is weak and can be activated by a non-membrane tethered RIN4 derivative. Both AtRIN4<sup>INT</sup> and AtACP2 failed to activate RPS2 suppressed by homologous RIN4<sup>CLV3</sup> fragments. While the respective homologous RIN4<sup>INT</sup> fragments were able to activate homologous RIN4<sup>CLV3</sup> suppressed RPS2. This indicates that, at least for the homologs, activation of RIN4<sup>CLV3</sup> suppressed RPS2 required the respective non-membrane tethered fragments for interaction within the protein complex required for RPS2 activation. These observations further support the possibility that RPS2 activation results from the combined activity of the RIN4 cleavage fragments, rather than simply the elimination of full-length RIN4.

AvrRpt2 homologs are present in a number of bacterial pathogens and are reported to play a role in promoting pathogenesis (Eschen-Lippold et al. 2016; Mazo-Molina et al. 2020; Prokchorchik et al. 2020). For example an AvrRpt2 homolog from *Erwinia amylovora* is the causal agent of bacterial fire blight in apple and pear (Prokchorchik et al. 2020). In case of apple, an NLR protein MR5, provides resistance against AvrRpt2 (Prokchorchik et al. 2020). Similar to RPS2, MdrIN4 cleavage by AvrRpt2 is sufficient for MR5 activation (Prokchorchik et al. 2020). However, in this case the membrane tethered fragment, MdACP3, was sufficient to cause MR5 activation in *N. benthamiana* (Prokchorchik et al. 2020).

Suppression of RPS2 by AtRIN4<sup>CLV3</sup> and homologous equivalent fragments is in contrast to regulation of Mr5 in apple. Rather than suppressing Mr5, AvrRpt2-induced MdACP3 is required for its activation. And, in the absence of AvrRpt2, MdACP3 is sufficient to activate MR5 (Prokchorchik et al. 2020). Even though RPS2 and MR5 belong to the same CC-NLR class of proteins and recognize AvrRpt2-mediated cleavage of RIN4, they evolved independently (Mazo-

Molina et al. 2020; Prokchorchik et al. 2020). It is apparent that the RPS2 and Mr5 NLR-proteins differ in how they are regulated by full-length and AvrRpt2-generated fragments of RIN4. Another NLR-protein, Ptr1 from tomato, has also been shown to respond to the AvrRpt2-mediated cleavage of SIRIN4. It will be of interest to compare the role of AvrRpt2-generated fragments of RIN4 in the regulation of Ptr1 activity. Collectively, these findings indicate that a variety of NLR-proteins distinctly monitor the status of RIN4.

## Chapter 5. RPS2 remains at the membrane during ectopic and AvrRpt2-induced activation

This chapter is adapted from Alam, et al., 2021 RIN4 homologs from important crop species differentially regulate the Arabidopsis NB-LRR immune receptor, RPS2. *Plant cell reports*. In press

### 5.1. Introduction:

In order to deal with the pressure of infection, plants have developed a sophisticated innate immune system. Plant *Resistance (R)* genes are the key players in the defense response mounted against the virulence factors secreted by pathogens (Dangl and Jones 2001). *R* genes in the plant cell encode for proteins that belong to the intracellular nucleotide binding leucine rich repeat (NBLRR or NLR) family of receptors (Bonardi et al. 2012; Chiang and Coaker 2015; Dangl and Jones 2001). NLR proteins are characterized by the presence of a highly conserved central nucleotide binding (NB) site and a variable C-terminal leucine rich repeat (LRR) domain (Figure 5.1) (Chiang and Coaker 2015; Monteiro and Nishimura 2018). The NB domain is responsible for nucleotide binding and exchange which leads to conformational changes within the protein resulting in NLR activation; whereas the LRR domain is involved in both negative, (auto-inhibition) and positive regulation (detection of pathogen effectors) of NBLRRs (Figure 1.1). NBLRRs, based on their N-terminal domain, can be further subdivided into either the toll/interleukin-1 receptor (TIR), or coiled-coiled (CC) NBLRR receptors (Bonardi et al. 2012; Chiang and Coaker 2015; Grund et al. 2019; Monteiro and Nishimura 2018). The N-terminal domains of NLR proteins mediate signaling post activation (Monteiro and Nishimura 2018).

At least two modes of effector recognition by the NLR proteins have been reported (Jones and Dangl 2006). NLR proteins can either directly interact with the corresponding effector (Chiang and Coaker 2015; Jones and Dangl 2006; Monteiro and Nishimura 2018); or they can indirectly detect the effector through the cooperation of an additional host protein (Jones and Dangl 2006) (Figure 1.1). The indirect mode of detection is explained by the guard hypothesis which states that the secreted pathogen targets and modifies a host protein (gaurdee) guarded by an NLR protein (Figure 1.1) (Jones and Dangl 2006). The NLR protein then detects the effector mediated modification of the gaurdee and activates an immune response (Figure 1.1) (Jones and Dangl 2006). The host protein or gaurdee can either be a *bona fide* effector virulence target or can act as

a decoy (van der Hoorn and Kamoun 2008). In latter case the host protein does not play a role in plant immunity but only serves to interact with the secreted effector by mimicking the bona fide effector target (van der Hoorn and Kamoun 2008). The detection of the effectors by the NLR proteins results in the activation of ETI which usually culminates in programmed cell death at the site of infection (Figure 1.1) (Chiang and Coaker 2015; Jones and Dangl 2006). Even though NLRs are key regulator of ETI response in plants, the molecular mechanism of NLR activation and NLR mediated immune signaling remains poorly understood.

Prior to their activation, NBLRR proteins are present in diverse locations within the cell including the plasma membrane, cytosol and the nucleus (Chiang and Coaker 2015). A few NLRs have been reported to re-localize post activation (Chiang and Coaker 2015; Elmore et al. 2011; Gao et al. 2011). In some cases the nucleo-cytoplasmic trafficking of the NLR proteins is reported to be sufficient for ETI activation (Chiang and Coaker 2015; Elmore et al. 2011). While re-localization has been reported for NLR's belonging to both the TIR and CC-NLR group, to this date there is no generalization regarding NLR localization post activation.

RPM1 and RPS2 are two CC-NBLRR proteins present in Arabidopsis (Mackey et al. 2003; Mackey et al. 2002). Both these proteins are known to physically interact with a membrane localized protein, RPM1 interacting protein 4 (RIN4) (Figure 1.2 and 1.3) (Day et al. 2005; Mackey et al. 2003; Mackey et al. 2002). Even though, RPM1 and RPS2 lack a predicted transmembrane domain, both these protein localize at the membrane (Afzal et al. 2011; Axtell and Staskawicz 2003; Gao et al. 2011). In case of RPM1, both the inactive and active versions of the protein were reported to be membrane localized (El Kasmi et al. 2017; Gao et al. 2011). In the absence of the pathogen, inactive RPM1 is localized at the membrane (El Kasmi et al. 2017; Gao et al. 2011). RPM1 provides resistance against *P. syringae* expressing the effectors AvrB and AvrRPM1 (Chung et al. 2011; Gao et al. 2011; Mackey et al. 2002). Both AvrB and AvrRPM1 localize at the membrane where they induce phosphorylation of RIN4 which in turn leads to the activation of RPM1 (Gao et al. 2011; Nimchuk et al. 2000). Effector activated RPM1 also remained membrane localized (Gao et al. 2011). It was further demonstrated that tethering RPM1 to the plasma membrane did not hinder its ability to induce HR in the presence of the effector (Gao et al. 2011). This indicated that re-localization of RPM1 is not required for its function. Similar to RPM1, RPS2 has also been reported to localize at the membrane (Axtell and Staskawicz 2003). In

the absence of the pathogen, RPS2 is maintained in a signaling competent state and is suppressed through its interaction with RIN4 at the plasma membrane (Day et al. 2005; Mackey et al. 2003). Absence of RIN4 in *Arabidopsis* results in constitutive activation of RPS2 leading to seedling lethality (Mackey et al. 2003). RPS2 provides resistance against *P. syringae* expressing the effector AvrRpt2 (Axtell and Staskawicz 2003; Day et al. 2005; Mackey et al. 2003). AvrRpt2, once activated in the plant cytosol, most likely also localizes at the membrane where it causes the cleavage of RIN4 which results in the activation of RPS2 (Figure 4.1) (Afzal et al. 2011; Axtell and Staskawicz 2003; Coaker et al. 2006; Mackey et al. 2003). Effector activated RPS2 is also reported to localize at the membrane (Axtell and Staskawicz 2003). Whether activated RPS2 re-localizes to initiate downstream defense signaling remains to be determined.

The generally accepted model for RPS2 activation states that RPS2 activates signaling upon perception of AvrRpt2 mediated elimination of RIN4 (Axtell and Staskawicz 2003; Day et al. 2005; Mackey et al. 2003). Cleavage of RIN4 by AvrRpt2 results in the generation of three fragments, AvrRpt2-cleavage product 1 (ACP1, AtRIN4<sup>1-10</sup>), ACP2 (AtRIN4<sup>11-152</sup>) and ACP3 (AtRIN4<sup>153-211</sup>) (Afzal et al. 2011; Kim et al. 2005a). We have recently demonstrated that the soluble fragment, ACP2 generated post AvrRpt2 mediated cleavage of RIN4, is responsible for RPS2 activation. This led us to speculate that AvrRpt2 activated RPS2 might interact with ACP2 and/or re-localize in the soluble fraction to mediate immune signaling.

In order to test our hypothesis, we made an RPS2 derivative with a C-terminal YFP tag and co-expressed it with AcV5-AtRIN4 and AvrRpt2-HA in *N. benthamiana*. We then observed the localization pattern of ectopically and effector activated RPS2 in *N. benthamiana* cells. In this chapter we have demonstrated that similar to the membrane suppressed RPS2, the ectopically active RPS2 also remains membrane localized. We further demonstrated the AvrRpt2 triggers RPS2-YFP-HA activation, however activated RPS2 was predominantly membrane localized. Taken together these results indicate that the plasma membrane localization of RPS2 is unaffected by its suppression/activation status.

## 5.2. Results:

**5.2.1. RPS2-YFP-HA and RPS2-HA are functionally comparable for cell death induction and RIN4-suppression in *Nicotiana benthamiana*.**

To determine the localization of RPS2 when it is ectopically active (expressed in *N. benthamiana* without RIN4) and when it is activated by AvrRpt2 (expressed in *N. benthamiana* with RIN4 and AvrRpt2), we used the fluorescent-protein tagged, RPS2-YFP-HA, derivative of RPS2 (Figure 5.1a).

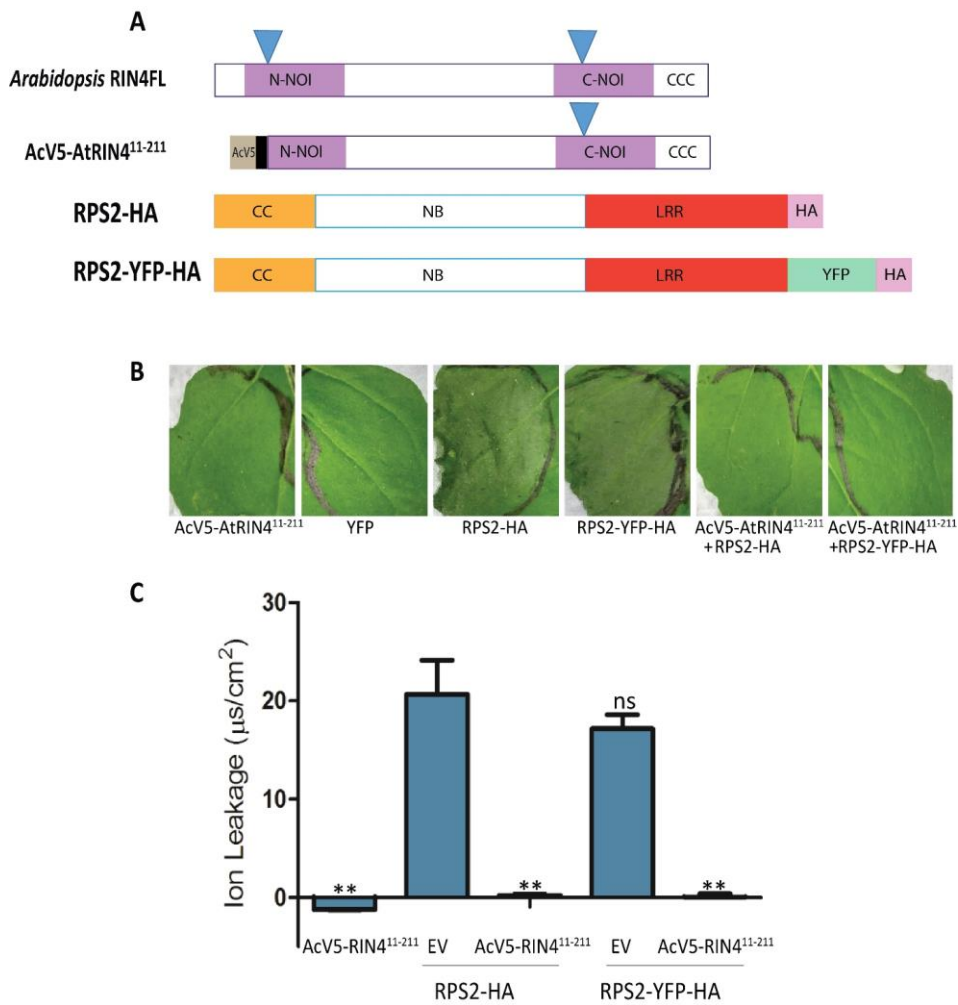


**Figure 5.1. RPS2-YFP-HA and RPS2-HA are functionally comparable for cell death induction and RIN4-suppression in *N. benthamiana*.** (A) Schematic diagram of RIN4 and RPS2 derivatives used in this chapter. Within RIN4 derivatives: brown squares indicate AcV5 epitopes, purple rectangles indicate NOI domains, and blue triangles indicate RCS2. Within RPS2 derivatives: orange rectangles indicate coiled coil domains, blue border rectangles indicate NB domains, red rectangles indicate LRR domains, light purple squares indicate HA epitopes, and the green rectangle indicates YFP. (B) RPS2-YFP-HA (OD<sub>600</sub> 0.1) and RPS2-HA (OD<sub>600</sub> 0.1) were co-infiltrated with AcV5-AtRIN4<sup>11-211</sup> (OD<sub>600</sub> 1.0) in *N. benthamiana*. Macroscopic RPS2-induced cell death was observed at 48 HPI. Empty vector failed to suppress either RPS2-HA or RPS2-YFP-HA; while co-infiltration with AcV5-AtRIN4<sup>11-211</sup> resulted in suppression of RPS2 activation. (C) Cell death was quantified based on electrolyte leakage. Three leaf discs for each combination, in panel A, were collected at 48 HPI, immersed in sterile water, and conductivity of the bath solution was measured. Data was collected from 3 independent experiments. Error bars represent SEM. Student's t-test, at 95% confidence limits, was used for comparison with RPS2:HA (ns, not significant;\*\*P < 0.05)

In order to test whether the RPS2-YFP-HA derivative was functionally active, we initially expressed the construct in, the absence and presence of AcV5-AtRIN4<sup>11-211</sup>, in *N. benthamiana*. Figure 5.1b and c show that similar to RPS2-HA, expression of RPS2-YFP-HA with *Agrobacterium* at an OD<sub>600</sub> of 0.1 resulted in a cell death phenotype and this ectopic activity of RPS2 could be suppressed by expression of AtRIN4<sup>11-211</sup>. Thus, the RPS2-YFP-HA was functional.

### 5.2.2. RPS2 remains at the membrane during ectopic and AvrRpt2-induced activation

After confirming the functionality of RPS2-YFP-HA, we next sought to determine the localization of RIN4-suppressed and AvrRpt2-activated RPS2. In the absence of AvrRpt2, RPS2 is localized at the plasma membrane where it interacts with RIN4 (Axtell and Staskawicz 2003; Belkhadir et al. 2004; Mackey et al. 2003). Some R-proteins re-localize upon activation (Burch-Smith et al. 2007; Deslandes et al. 2003). The ectopic activation of RPS2-YFP-HA (OD<sub>600</sub> of 0.2) resulted in a cell death phenotype at 42 HPI (Figure. 5.2a).

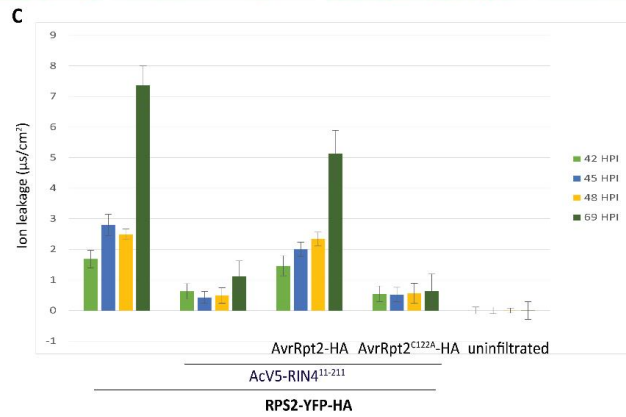
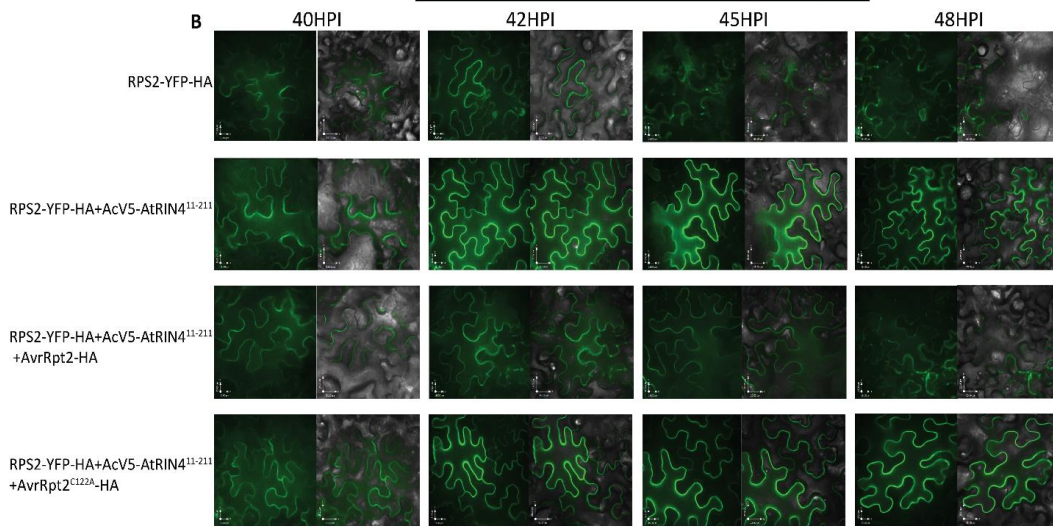
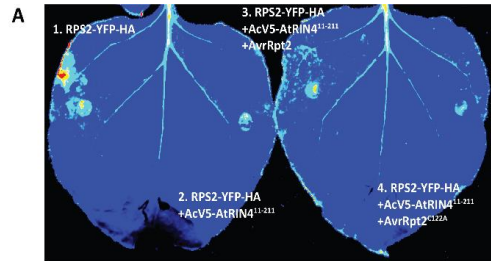


**Figure 5.2. RPS2 remains membrane-localized during ectopic and AvrRpt2-induced activation.** RPS2-YFP-HA (OD<sub>600</sub> 0.2) and P19 (OD<sub>600</sub> 0.3) were co-infiltrated with the indicated combinations of AcV5-AtRIN4<sup>11-211</sup> (OD<sub>600</sub> 0.6) and AvrRpt2-HA or AvrRpt2<sup>C122A</sup>-HA (OD<sub>600</sub> 0.01) in *N. benthamiana* plants. **(A)** RPS2 induced cell death at 42 HPI in *N. benthamiana* leaves was detected via leaf auto-fluorescence. The signal observed in section 1 and 3 corresponds to the onset of cell death. **(B)** Localization of the fluorescent signal was observed at the indicated time points using confocal-microscopy (Scale bar: 15 μM). **(C)** Cell death was quantified based on electrolyte leakage. Five leaf discs for each combination, as in panel **B**, were taken at the indicated time points, immersed in sterile water, and conductivity of the bath solution was measured. Data collected from 3 independent experiments where n=15. Error bars represent SEM

Ectopically expressed RPS2-YFP-HA predominantly remained localized at the plasma membrane at 40–48 HPI (Figure. 5.2b). The shape of the epidermal cells remained largely unchanged at these time points (Figure. 5.2b). By 45 HPI, RPS2-YFP-HA caused significant cell death and even though there was a reduction in the levels of RPS2-YFP-HA, it was still predominately localized at the plasma membrane (Figure. 5.2b). Notably, RPS-YFP-HA remained membrane localized even in epidermal cells that the bright field imaging indicated were dead or dying (Figure. 5.2b). As expected, when suppressed by co-expressed AtRIN4<sup>11-211</sup>, no cell death was apparent (Figure. 5.2a and 5.2c), and RPS2-YFP-HA remained localized at the membrane (Figure. 5.2b). We observed similar patterns of membrane localization for ectopically active and RIN4-suppressed RPS2-YFP-HA (OD<sub>600</sub> of 0.1 and 0.4) at time points when cell death became apparent (Figure. 5.3a and b).

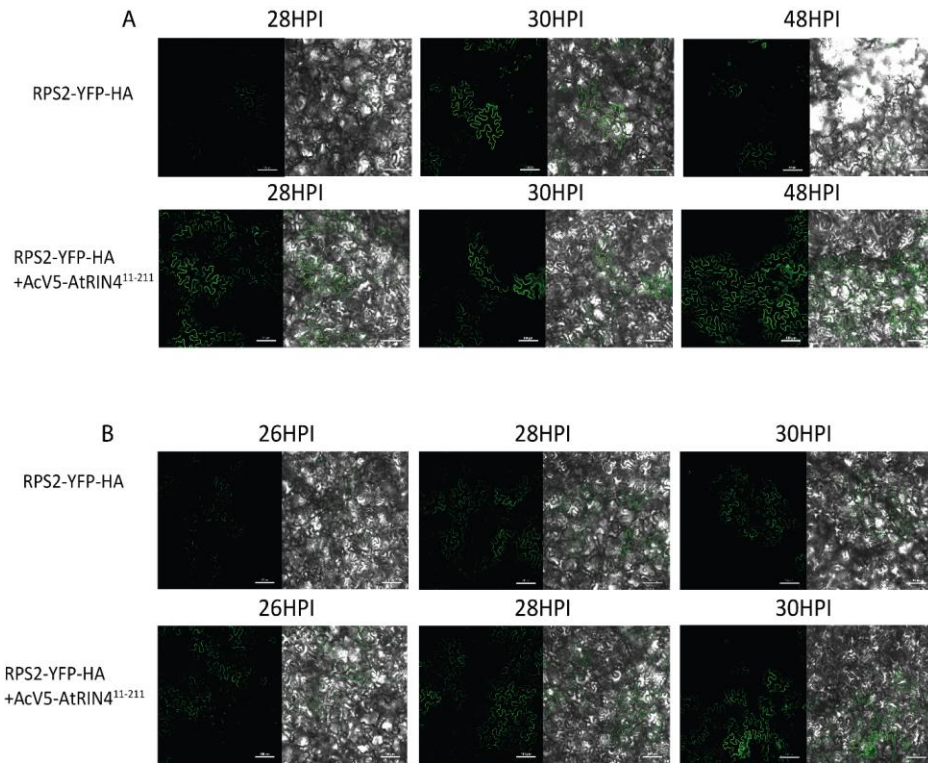


**Figure 5.3. Ectopically active and AcV5-AtRIN4<sup>11-211</sup> suppressed RPS2-YFP-HA are predominantly membrane localized in *N. benthamiana* cells.** Localization of the fluorescent signal was observed at the indicated time points using confocal-microscopy (Scale bar: 100  $\mu$ M). **(A)** RPS2-YFP-HA (OD<sub>600</sub> 0.1) was co-expressed in *N. benthamiana* with either empty vector (top panel) or AcV5-RIN4<sup>11-211</sup> (OD<sub>600</sub> 1.0) (bottom panel). **(B)** RPS2-YFP-HA (OD<sub>600</sub> 0.4) was co-expressed in *N. benthamiana* with empty vector (top panel) or AcV5-RIN4<sup>11-211</sup> (OD<sub>600</sub> 1.0) (bottom panel)

We next examined the localization of RPS2-YFP-HA following its activation by AvrRpt2. When co-infiltrated with AcV5-AtRIN4<sup>11-211</sup> and AvrRpt2, RPS2-YFP-HA triggered weak cell death at 42 HPI (Figure. 5.2a and c). Notably, similar to when it is ectopically active, AvrRpt2-activated RPS2-YFP-HA remained detectable and was predominantly present at the plasma membrane at 40–48 HPI (Figure. 5.2b). Collectively, our results indicate that the plasma membrane localization

of RPS2 is unaffected by its suppression/activation state and that it is thus likely to elicit defense responses, including cell death, at the plasma membrane.

### 5.3. Discussion:

NLR-proteins localize to a variety of subcellular compartment prior to their activation (Caplan et al. 2008; Gao et al. 2011). In some cases, activation of NLR-proteins results in their re-localization (Burch-Smith et al. 2007; Caplan et al. 2008; Deslandes et al. 2003). For example the TIR-NLR protein, N, present in tobacco recognizes the effector released by *Tobacco mosaic virus* in the cytoplasm and subsequently re-localizes to the nucleus to initiate the defense response (Burch-Smith et al. 2007; Caplan et al. 2008). Another example of a TIR-NLR protein that maintains a nucleocytoplasmic localization is the SNC1 protein present in Arabidopsis (Cheng et al. 2009). SNC1 contains both the Nuclear localization signal (NLS) and nuclear exclusion sequence (NES), and it was determined that the nuclear pool of SNC1 is required for mediating downstream immune signaling (Cheng et al. 2009). Another example of a protein that re-localizes upon effector detection is the RRS1 protein present in Arabidopsis. It has been reported that RRS1 contains several putative nuclear localization sequences (NLS) and re-localizes from the cytosol to the nucleus in the presence of the effector PopP2 (Deslandes et al. 2003). A CC-NLR protein from potato, Rx1, is also reported to maintain a nucleocytoplasmic localization (Slootweg et al. 2010). Rx1 is activated in the cytoplasm, however both nuclear and cytoplasmic pools of this protein are required for mediating the immune response against *Potato virus X* (Slootweg et al. 2010). Taken together these findings indicate the importance of the appropriate localization of the NLR proteins for mediating downstream signaling during pathogen invasion. While re-localization has been reported for a few NLR's, other NLR's, post effector activation, remain localized at the plasma or endo-membrane and disruption of their proper localization affects their function.

RPS2 is a CC-NLR protein that is reported to physically associate with RIN4 in Arabidopsis plants (Day et al. 2005). Based on the analysis of its primary sequence, RPS2 was predicted to be a largely hydrophilic protein and it lacked motifs that might suggest a distinctive sub-cellular localization (Axtell and Staskawicz 2003; Mindrinos et al. 1994). However, RPS2 was also predicted to have a membrane spanning hydrophobic motif at the N-terminal region and was later demonstrated to localize at the membrane (Axtell and Staskawicz 2003; Mindrinos et al. 1994).

RPS2 provides resistance against *P. syringae* effector AvrRpt2 (Axtell and Staskawicz 2003; Mackey et al. 2003). Due to its acylation after delivery into a plant cell, AvrRpt2 is also localized at the plasma membrane where it cleaves RIN4 leading to the activation of RPS2 (Coaker et al. 2006). While RPS2 gets activated at the membrane, whether it re-localizes to regulate downstream signaling was unknown.

We have recently determined that the non-membrane tethered derivative of RIN4, CCC>AAA, in the presence of full length RIN4 was able to activate RPS2 in Arabidopsis. We have also determined that the soluble fragment, ACP2, generated after AvrRpt2 mediated cleavage of RIN4 is sufficient for RPS2 activation. Based on our findings we speculated that activated RPS2 might interact with the non-membrane tethered derivative and/or re-localize in the soluble fraction to mediate immune signaling. However in this chapter we have demonstrated that ectopically and effector activated RPS2 remains membrane localized. We tracked the expression of RPS2-YFP-HA at different time points to determine the localization of RPS2 before and after the onset of HR. We observed that activated RPS2, at different time points still remained membrane localized. Even though there was a decrease in the YFP signal after the onset of HR, RPS2 still remained membrane localized. Therefore, we concluded that downstream signaling regulation by activated RPS2 does not depend on its re-localization.

## Conclusion:

The current study focuses on understanding the AvrRpt2-RIN4-RPS2 defense-activation module. It has been demonstrated that expression of non-membrane-tethered derivatives of RIN4 in *Arabidopsis* activates RPS2 and, notably, this activation occurred in the presence of native RIN4. The expression of these non-membrane tethered derivatives in the presence of wild type RIN4 resembles the scenario where both the soluble, ACP2, and membrane tethered, ACP3, fragments are generated by AvrRpt2. We have demonstrated that membrane tethered fragment of RIN4 (ACP3) can suppress the activation of RPS2 while the soluble fragment, ACP2, overcomes this suppression. Therefore we propose a new model for RPS2 activation, where the *presence* of a RIN4 derivative, in this case ACP2, triggers RPS2 activation. On the whole this model best fits to the guard hypothesis that the virulence promoting perturbation of RIN4 by AvrRpt2 results in the activation of RPS2.

Further insight into the AvrRpt2-RIN4-RPS2 defense-activation module was gained by comparing the function of AtRIN4 with RIN4 homologs present in a diverse range of plant species. We identified a set of RIN4 homologs, from soybean, peach and potato, that like RIN4 from *Arabidopsis* and apple are able to regulate RPS2-mediated immune responses against AvrRpt2. We speculate that the homologs under study might interact with RPS2-like proteins in their respective host species. Alternatively, these homologs could effectively regulate AtRPS2 introduced into those plant species. We also determined that in addition to their role as negative regulators of basal defenses, the two RIN4 cleavage fragments, RIN4<sup>INT</sup> and RIN4<sup>CLV3</sup>, play contrasting roles in the regulation of RPS2. Interestingly similar to AtRIN4, the homologous RIN4<sup>INT</sup> activated RPS2 suppressed by RIN4<sup>CLV3</sup>. These observations further support the possibility that RPS2 activation results from the combined activity of the RIN4 cleavage fragments, rather than simply the elimination of full-length RIN4.

## Chapter 6 Methodology

This chapter is adapted from Alam, et al., 2021 RIN4 homologs from important crop species differentially regulate the Arabidopsis NB-LRR immune receptor, RPS2. *Plant cell reports*. In press

### 6.1. Plants and growth conditions

*Arabidopsis thaliana* (Col-0, transgenic and mutants) plants were grown at 24°C (day) and 22°C (night) in a growth chamber under an 8-h-light/16-h-dark cycle. For *Agrobacterium* infiltrations, *Nicotiana benthamiana* seeds were sown in soil (Peat moss, Pindstrup færdigblanding substrate) and grown at 24°C (day) and 22°C (night) in a growth chamber under an 8h-light/16h-dark cycle. After 2 weeks of germination, seedlings were transferred to pots (one seedling per pot). The seedlings were further grown for 4 weeks after which they were ready for *Agrobacterium* infiltrations. Fully expanded *N. benthamiana* leaves were used to carry out bacterial infiltrations. To prepare RNA, *Arabidopsis thaliana* (Col-0), *Lactuca sativa* (Lettuce), *Oryza sativa* (Rice), *Malus domestica* (Apple), *Solanum lycopersicum* (tomato), *Solanum tuberosum* (potato), *Prunus persica* (peach), and *Glycine max* (soybean) seeds were also sown in soil (Peat moss, Pindstrup færdigblanding substrate) and grown at 24°C (day) and 22°C (night) in a growth chamber under an 8h-light/16h-dark cycle. Leaves were harvested from 4-week-old plants and were stored in a –80°C freezer.

### 6.2. Plasmid construction

The Arabidopsis RIN4 derivatives (chapter 2) were cloned using the Gateway system (Invitrogen, Carlsbad, CA). Constructs for Arabidopsis RIN4 derivatives were derived from pMAC100c vector containing full-length RIN4 (Afzal et al. 2011). AtRIN4 derivatives, including RIN4FI, CCC>AAA (mutation of acylation site cysteines to alanines) and 177Δ211 (deletion of 35 C-terminal residues of RIN4), were fused with an N-terminal T7 (MASMTGGQMG) tag. AtRIN4 derivatives including RIN4FI, ACP2 (11-152), ACP3 (153-211) and 142-211 were fused with an N-terminal Flag (DYKDDDDK) tag. ACP2 derivatives were fused with either an N-terminal Nuclear Localization Signal (NLS, PKKKRKVED) (Haasen et al. 1999), Nuclear Export Signal (NES, NELALKLAGLDINKT) (Gadal et al. 2001) or Shuffled Nuclear Export signal (SNE, NELALKAAGADINKT) tag. These derivatives were cloned into pENTR-D-TOPO and

subsequently moved into the gateway binary vectors pGWB12 (containing a 35S promoter) or pEarlyGate 104 (35S:N-YFP). Dexamethasone (dex)-inducible stable transgenic lines expressing derivatives of RIN4 (chapter 2) were generated as described (Afzal et al. 2011) in Col-0, *rpm1*, *rps2* or in the *rpm1rps2* background.

The homologous RIN4 constructs were also cloned using the Gateway system (Invitrogen, Carlsbad, CA). To prepare RNA, the harvested leaves were ground by mortar and pestle in liquid nitrogen. RNA was extracted using Trizol following the manufacturer's protocol (Invitrogen, Carlsbad, CA). The corresponding cDNAs were synthesized using M-MLV Reverse transcriptase following the manufacturer's protocol (Invitrogen Carlsbad, CA). Using cDNA as template, RIN4 homologs were amplified through polymerase chain reaction (PCR). All primers, used for the purpose of cloning, were designed in such a way that they incorporated a CACC tag at the 5' end of each construct (Supplemental Table 1). Primers used for the amplification of homologous RIN4<sup>1ΔRCS1</sup> and RIN4<sup>INT</sup> (Internal) equivalent fragments were specifically designed to introduce an AcV5 tag at the 5' end of each construct and to exclude the region corresponding to the first 12 or 13 amino acids or 1ΔRCS1 (RIN4 cleavage site 1). Sequence data from this study can be found in the accession numbers mentioned in Supplemental Table 1.

| Gene                     | Genbank ID/<br>NCBI reference<br>ID | Orientation | Sequence 5'-3'  | Source    |
|--------------------------|-------------------------------------|-------------|---|-----------|
| AiRIN4F1                 | NM_113411.3                         | Forward     | caccATGGCACGTTCCAATGTACCA   | This work |
| AiRIN4F1                 | NM_113411.3                         | Reverse     | TCATTTTCCTCCAAAGCCAAAGCAGC  | This work |
| AiRIN4 <sup>1ARCSI</sup> | NM_113411.3                         | Forward     | caccagctggaaggacgccagcgctgctgGAAAGTGGAGAGAATGTTCCCTACACAGCTTAC  | This work |
| AiRIN4 <sup>1ARCSI</sup> | NM_113411.3                         | Reverse     | TCATTTTCCTCCAAAGCCAAAGCAGC  | This work |
| AiRIN4 <sup>INT</sup>    | NM_113411.3                         | Reverse     | tcaACCGAATTTAGGCACCACTGTGACTTTTTCAG   | This work |
| AiRIN4 <sup>CLV3</sup>   | NM_113411.3                         | Forward     | caccGACTGGGACGAGAACAACCCGTCATC  | This work |
| GmRIN4 <sup>1ARCSI</sup> | MW438284                            | Forward     | caccagctggaaggacgccagcgctgctgGATAGTGGAGAGAATGTTCCCTATACAGCA   | This work |
| GmRIN4 <sup>1ARCSI</sup> | MW438284                            | Reverse     | TCATTTTTCCTCCAAAGCCAGC  | This work |
| GmRIN4 <sup>INT</sup>    | MW438284                            | Reverse     | tcaACCAAACTTTGGAACAGCTGCACCTTATC  | This work |
| GmRIN4 <sup>CLV3</sup>   | MW438284                            | Forward     | caccGACTGGGATGTGAATAACCCTGCA-3'   | This work |
| LSRIN4 <sup>1ARCSI</sup> | MW438288                            | Forward     | caccagctggaaggacgccagcgctgctgGAAAGCGAAGATAATGTTCCCTATACGGTT   | This work |
| LSRIN4 <sup>1ARCSI</sup> | MW438288                            | Reverse     | TCACTTCGACGATGGGAAGCA   | This work |
| OsRIN4 <sup>1ARCSI</sup> | MW438289                            | Forward     | CACCagctggaaggacgccagcgctgctgGAGGATGAAGACCGTGGTGAACACCTCTACACACAGTAT  | This work |
| OsRIN4 <sup>1ARCSI</sup> | MW438289                            | Reverse     | TCAGTTCCTTGAACCACTGAAGCATGAGCAGCCTG   | This work |
| OsRIN4 <sup>INT</sup>    | MW438289                            | Reverse     | tcaTCCAACCTTTGGCACGGCTGATCCTCTATCAGGCGT   | This work |
| OsRIN4 <sup>CLV3</sup>   | MW438289                            | Forward     | caccGAATGGGATGAGAAAGATCCCTTCTA  | This work |
| PpRIN4 <sup>1ARCSI</sup> | MW438286                            | Forward     | caccagctggaaggacgccagcgctgctgGAAAGTGAAGAAAAATGTTCCCTACACAG  | This work |
| PpRIN4 <sup>1ARCSI</sup> | MW438286                            | Reverse     | TCATTTTCTGCTCCATGGAAAAGCA   | This work |
| PpRIN4 <sup>INT</sup>    | MW438286                            | Reverse     | tcaGCCAAATTTGGAAACAGCAGCAC  | This work |
| PpRIN4 <sup>CLV3</sup>   | MW438286                            | Forward     | caccGAGTGGGATGAGAATGATCCTGCA  | This work |
| SIRIN4 <sup>1ARCSI</sup> | MW438290                            | Forward     | caccagctggaaggacgccagcgctgctgGAAATGAAGACAACACTCCTTACTGT   | This work |
| SIRIN4 <sup>1ARCSI</sup> | MW438290                            | Reverse     | TCACCACAAAGGAAAGCAGCAG  | This work |
| StRIN4 <sup>1ARCSI</sup> | MW438287                            | Forward     | caccagctggaaggacgccagcgctgctgGAAAATGACGATAACACGCCTTACTGT  | This work |
| StRIN4 <sup>1ARCSI</sup> | MW438287                            | Reverse     | TTACCAGGGACAACAACACCACTTCAT   | This work |
| StRIN4 <sup>INT</sup>    | MW438287                            | Reverse     | tcaCCCCAATCTTGGAACTGCAGCA   | This work |
| StRIN4 <sup>CLV3</sup>   | MW438287                            | Forward     | caccGAGTGGGACGAGAATGATCCTC  | This work |
| M13                      |                                     | Forward     | GTAAACAGCAGGCCAG  |           |
| M13                      |                                     | Reverse     | CAGGAAACAGCTATGAC   |           |
| AiRIN4 <sup>11-211</sup> | NM_113411.3                         | Forward     | <u>agctggaaggacgccagcgctgctg</u> aat gaa tta gcc tta aaa gca gca ggt gcc gat atc aac aag aca<br>AACTGGGAAGCTGAGGAGAATGT | This work |
| AiRIN4 <sup>11-211</sup> | NM_113411.3                         | Reverse     | TCATTTTCCTCCAAAGCCAAAGCAGC  | This work |

**Table 6.1 Oligonucleotides used in this study.** (Note that the nucleotides in lowercase are not a part of the RIN4 sequences. The AcV5 tag is underlined)

Phusion® DNA Polymerase (NEB, Ipswich, MA) was used for the gene-specific amplification of the homologous RIN4 constructs and RPS2. PCR amplified genes were cloned into the entry vector, pENTR™ Directional TOPO (D-TOPO) (Invitrogen, Carlsbad, CA). The gateway binary vector pEarley Gate 104 (35S promoter, YFP:N) was used as the destination vector for the homologous RIN4 derivatives; while pEarley Gate 101 (35S promoter, C:YFP-HA) was used as the destination vector for RPS2. Since the entry and the destination vector had the same antibiotic selection marker (Kanamycin), we followed the PCR amplification based (PAB) method to mobilize the inserts from the entry clones to the destination vector (Kumar et al. 2013). The insert was amplified from the entry vector using M13 primers (Supplemental Table 1) and was

subsequently cloned into the destination vector using LR Clonase™ (Invitrogen Carlsbad, CA). The destination vector was then transformed in *A. tumefaciens* GV3101 pMP90 cells. AtRIN4 derivative, RIN4<sup>11-211</sup> was amplified using primers that added an AcV5 tag and a sequence that encodes a 15 amino acid linker (NELALKAAGADINKT) at the 5' end of the insert. The chimeric insert was cloned into pENTR-D-TOPO and subsequently moved into the gateway binary vector pB2GW7 (containing a 35S promoter).

*A. tumefaciens* strain C58-C1 carrying RPS2-HA, expressed under the control of a promoter (pOCS:RPS2-HA), was a gift from Dr Brad Day and has been described previously (Day et al. 2005). AvrRpt2-HA and AvrRpt2<sup>C122A</sup>-HA, expressed under the control of a 35S promoter, were a gift from Dr Kee Hoon Sohn and have been described previously (Prokhorchik et al. 2020). p19 (silencing suppressor) expressed under the control of a 35S promoter has been described previously (Hamilton et al. 2002; Prado et al. 2019). RFP-OsRac1 expressed under the control of 35S promoter (pGDR vector backbone) was a gift from Dr Guo-Liang Wang. RFP fused OsRac1, a GTPase, has been used as a plasma membrane marker previously (Fan et al. 2018).

### 6.3. *Agrobacterium*-mediated transient expression

*A. tumefaciens* strains carrying the AtRIN4 derivatives (chapter 2), homologous 35S:YFP-AcV5-RIN4 derivatives, pOCS:RPS2-HA or 35S:RPS2-YFP-HA, 35S:AvrRpt2-HA or 35S:AvrRpt2<sup>C122A</sup>-HA were grown overnight at 28°C in Luria-Bertani (LB) media containing the appropriate antibiotics (100 µg/ml of kanamycin, 50 µg/ml of gentamycin, 100 µg/ml of rifampicin or 5 µg/ml of tetracycline). The overnight cultures were centrifuged at 4500 × g for 10 min. The pellet collected was re-suspended in induction media (10 mM MES PH5.6, 10 mM MgCl<sub>2</sub> and 200 µM acetosyringone). The OD<sub>600</sub> (optical density) of the cultures, as required for each assay, was adjusted using the induction media. For all infiltrations, the final OD<sub>600</sub> of *A. tumefaciens* strains carrying the desired construct(s), was adjusted to a constant total OD<sub>600</sub> using *A. tumefaciens* strain GV3101. *A. tumefaciens* strain(s) were infiltrated into *N. benthamiana* leaves as described previously (Day et al. 2005; Tai et al. 1999).

### 6.4. Confocal microscopy analysis

The localization of homologous YFP-AcV5-RIN4 derivatives and RPS2-YFP-HA was observed at the indicated time points. Leaf discs from the infiltrated area were obtained and the YFP signal was observed using a confocal microscope (Nikon Eclipse Ti/C2/C2Si) (Nikon, Foster City, CA)

using an excitation wavelength of 514 nm and an emission wavelength of 530 nm. Nuclei in the infiltrated region, were stained by infiltrating 1 µg/ml DAPI D3571 dye (Invitrogen, Eugene, OR) into *N. benthamiana* leaves, 6 hours before imaging. The fluorescence from the DAPI stained nuclei was observed using an excitation wavelength of 358 nm and an emission wavelength of 461 nm. Co-localization of YFP-RIN4 derivatives and RFP-OsRac1 was observed at the indicated time points. RFP signal was observed using an excitation wavelength of 561 nm and an emission wavelength of 575 nm.

### **6.5. Protein extraction and SDS-PAGE**

To determine expression of the transiently expressed YFP-AcV5-RIN4 derivatives, total protein was extracted from the plant tissue as described previously (Afzal et al. 2011). Briefly, 0.1 gram (g) leaf tissue was homogenized in 300 µl of extraction buffer, 20 mM Tris, 150 mM NaCl, 1 mM EDTA, 1% TritonX-100, 0.1% SDS, 5 mM DTT and 10X plant protease inhibitor cocktail (Sigma-Aldrich, Saint Louis, MO). The samples were centrifuged at  $13,523 \times g$  for 20 min at 4°C to remove the insoluble debris. To 100 µl of the collected supernatant (total protein), 5X SDS-PAGE loading dye was added, and the samples were heated at 65°C for 10 min. The protein samples were resolved on 12% (w/v) SDS-PAGE gels and were subsequently transferred to nitrocellulose membrane. The membrane was probed with 1:5000 dilution of anti-GFP antibody (Abcam, Cambridge, UK) to detect YFP-tagged RIN4 derivatives. For detecting AtRIN4 derivatives, Anti-RIN4 sera (Mackey et al., 2002), anti-T7 monoclonal antibody (Novagen, Madison, Wisconsin) and anti-Flag antibody (Sigma-Aldrich, Taufkirchen, Germany) were used at dilutions of 1:5000, 1:10,000, or 1:5000, respectively. For protein detection, the blot was probed with ECL following manufacturer's protocol (GE Healthcare Amersham, Buckinghamshire, UK) and chemiluminescence was observed using the ChemiDoc XRS system (Bio-Rad, Hercules, CA).

### **6.6. Subcellular fractionation**

In order to separate membrane proteins from soluble proteins, 0.1 g leaf tissue was ground in liquid nitrogen and resuspended in 700 µl of homogenization buffer (30 mM Tris PH 8.3, 150 mM NaCl, 1 mM EDTA, 20% glycerol, 5 mM DTT, 10X protease inhibitor and 10 mM PMSF). The samples were centrifuged at  $13,523 \times g$  for 10 min at 4°C to remove insoluble debris. The "total" fraction consisted of the supernatant from this first spin combined directly with the SDS-PAGE loading dye and heated at 65°C for 10 min. For fractionation of the microsomal fraction, 600 µl of

supernatant from the first spin was combined with 20  $\mu$ l of 1M CaCl<sub>2</sub> and incubated on ice for 90 min prior to centrifugation at 21,130  $\times$  g for 90 min at 4°C. The “soluble” fraction (supernatant from the second spin) was combined with the loading dye and heated at 65°C for 10 min. The pellet from the second spin was re-suspended in 100  $\mu$ l of resuspension buffer (10 mM Tris pH 7.6, 150 mM NaCl, 0.1 mM EDTA, 10% glycerol, 10X protease inhibitor, 10 mM PMSF) and centrifuged again at 21,130  $\times$  g for 60 min at 4°C. The “microsomal membrane” fraction (the final pellet) was resuspended in 90  $\mu$ l of 1X SDS-PAGE loading dye and heated at 65°C for 15 min. The subcellular fractions were resolved on either 12% (w/v) SDS-PAGE or 4-20% (w/v) precast TGX (Bio-Rad, Hercules, CA) gels and were subsequently transferred to nitrocellulose membrane. The membrane was probed with 1:5000 dilution of anti-GFP antibody (Abcam, Cambridge, UK) to detect YFP-tagged RIN4 derivatives. A 1:600 dilution of H<sup>+</sup>-ATPase (Agrisera, Vannas, SE) was used as a plasma membrane marker.

### **6.7. Quantification of hypersensitive response**

To quantify the Hypersensitive Response, ion leakage from leaf discs corresponding to the agro-infiltrated area of *N. benthamiana* leaves was measured. Leaf discs were submerged in 15 ml of water for 1 hour and cell death was quantified with the aid of a conductivity meter (WTW, Weilheim, Germany). For each construct, ion leakage data were generated from three to five biological replicates (three technical replicates per biological replicate). Background correction was based on the conductivity from leaf discs corresponding to un-infiltrated *N. benthamiana* leaves. Cell death in intact leaves was detected by observing leaf auto-fluorescence using the ChemiDoc XRS Imager (Bio-Rad, Hercules, CA).

### **6.8. Protein alignment**

The homologous RIN4 protein sequences were aligned by ClustalW using MEGA-X. Alignments were generated with a reduced Gap penalty (4.0) for both pairwise and multiple sequence alignments. Pairwise sequence similarity and identity for the multiple sequence alignments was calculated by the BLOSUM 62 scoring Matrix with the SIAS (sequence identity and similarity) tool.

### **6.9. Palmitoylation prediction**

Putative palmitoylation residues in the homologous RIN4 sequences were predicted using CSS-Palm 4.0 (Zhou et al. 2006) with the threshold stringency set to medium

(<http://csspalm.biocuckoo.org>). The software employs a clustering and scoring strategy algorithm (CSS), a group-based prediction system (GPS) as well as a training dataset that comprises 277 proteins that contain 583 palmitoylation sites to accurately predict putative palmitoylation sites in query proteins (Ren et al. 2008; Weng et al. 2017).

## References:

- Afzal AJ, da Cunha L, Mackey D (2011) Separable fragments and membrane tethering of Arabidopsis RIN4 regulate its suppression of PAMP-triggered immunity. *The Plant cell* 23:3798-3811
- Afzal AJ, Kim JH, Mackey D (2013) The role of NOI-domain containing proteins in plant immune signaling. *BMC genomics* 14:327
- Ashfield T, Redditt T, Russell A, Kessens R, Rodibaugh N, Galloway L, Kang Q, Podicheti R, Innes RW (2014) Evolutionary relationship of disease resistance genes in soybean and Arabidopsis specific for the *Pseudomonas syringae* effectors AvrB and AvrRpm1. *Plant physiology* 166:235-251
- Axtell MJ, Staskawicz BJ (2003) Initiation of RPS2-Specified Disease Resistance in Arabidopsis Is Coupled to the AvrRpt2-Directed Elimination of RIN4. *Cell* 112:369-377
- Belkhadir Y, Nimchuk Z, Hubert DA, Mackey D, Dangl JL (2004) Arabidopsis RIN4 negatively regulates disease resistance mediated by RPS2 and RPM1 downstream or independent of the NDR1 signal modulator and is not required for the virulence functions of bacterial type III effectors AvrRpt2 or AvrRpm1. *The Plant cell* 16:2822-2835
- Bergelson J, Kreitman M, Stahl EA, Tian D (2001) Evolutionary dynamics of plant R-genes. *Science* 292:2281-2285
- Bonardi V, Cherkis K, Nishimura MT, Dangl JL (2012) A new eye on NLR proteins: focused on clarity or diffused by complexity? *Current opinion in immunology* 24:41-50
- Burch-Smith TM, Schiff M, Caplan JL, Tsao J, Czymmek K, Dinesh-Kumar SP (2007) A novel role for the TIR domain in association with pathogen-derived elicitors. *PLoS biology* 5:e68
- Caplan J, Padmanabhan M, Dinesh-Kumar SP (2008) Plant NB-LRR immune receptors: from recognition to transcriptional reprogramming. *Cell host & microbe* 3:126-135
- Caplan JL, Mamillapalli P, Burch-Smith TM, Czymmek K, Dinesh-Kumar SP (2008) Chloroplastic protein NRIP1 mediates innate immune receptor recognition of a viral effector. *Cell* 132:449-462
- Chang JH, Urbach JM, Law TF, Arnold LW, Hu A, Gombar S, Grant SR, Ausubel FM, Dangl JL (2005) A high-throughput, near-saturating screen for type III effector genes from *Pseudomonas syringae*. *Proceedings of the National Academy of Sciences of the United States of America* 102:2549-2554

Cheng YT, Germain H, Wiermer M, Bi D, Xu F, Garcia AV, Wirthmueller L, Despres C, Parker JE, Zhang Y, Li X (2009) Nuclear pore complex component MOS7/Nup88 is required for innate immunity and nuclear accumulation of defense regulators in Arabidopsis. *The Plant cell* 21:2503-2516

Chiang Y-H, Coaker G (2015) Effector Triggered Immunity: NLR Immune Perception and Downstream Defense Responses. *The Arabidopsis Book* 13:e0183

Chisholm ST, Coaker G, Day B, Staskawicz BJ (2006) Host-microbe interactions: shaping the evolution of the plant immune response. *Cell* 124:803-814

Chisholm ST, Dahlbeck D, Krishnamurthy N, Day B, Sjolander K, Staskawicz BJ (2005) Molecular characterization of proteolytic cleavage sites of the *Pseudomonas syringae* effector AvrRpt2. *Proceedings of the National Academy of Sciences of the United States of America* 102:2087-2092

Chung EH, da Cunha L, Wu AJ, Gao Z, Cherkis K, Afzal AJ, Mackey D, Dangl JL (2011) Specific threonine phosphorylation of a host target by two unrelated type III effectors activates a host innate immune receptor in plants. *Cell host & microbe* 9:125-136

Chung EH, El-Kasmi F, He Y, Loehr A, Dangl JL (2014) A plant phosphoswitch platform repeatedly targeted by type III effector proteins regulates the output of both tiers of plant immune receptors. *Cell host & microbe* 16:484-494

Coaker G, Zhu G, Ding Z, Van Doren SR, Staskawicz B (2006) Eukaryotic cyclophilin as a molecular switch for effector activation. *Molecular microbiology* 61:1485-1496

Cui F, Wu S, Sun W, Coaker G, Kunkel B, He P, Shan L (2013) The *Pseudomonas syringae* type III effector AvrRpt2 promotes pathogen virulence via stimulating Arabidopsis auxin/indole acetic acid protein turnover. *Plant physiology* 162:1018-1029

Dangl JL, Horvath DM, Staskawicz BJ (2013) Pivoting the plant immune system from dissection to deployment. *Science* 341:746-751

Dangl JL, Jones JD (2001) Plant pathogens and integrated defence responses to infection. *Nature* 411:826-833

Dangl JL, McDowell JM (2006) Two modes of pathogen recognition by plants. *Proceedings of the National Academy of Sciences of the United States of America* 103:8575-8576

Day B, Dahlbeck D, Huang J, Chisholm ST, Li D, Staskawicz BJ (2005) Molecular basis for the RIN4 negative regulation of RPS2 disease resistance. *The Plant cell* 17:1292-1305

Deslandes L, Olivier J, Peeters N, Feng DX, Khounlotham M, Boucher C, Somssich I, Genin S, Marco Y (2003) Physical interaction between RRS1-R, a protein conferring resistance to bacterial wilt, and PopP2, a type III effector targeted to the plant nucleus. *Proceedings of the National Academy of Sciences of the United States of America* 100:8024-8029

Desveaux D, Singer AU, Wu AJ, McNulty BC, Musselwhite L, Nimchuk Z, Sondek J, Dangl JL (2007) Type III effector activation via nucleotide binding, phosphorylation, and host target interaction. *PLoS pathogens* 3:e48

Dodds PN, Lawrence GJ, Catanzariti AM, Teh T, Wang CI, Ayliffe MA, Kobe B, Ellis JG (2006) Direct protein interaction underlies gene-for-gene specificity and coevolution of the flax resistance genes and flax rust avirulence genes. *Proceedings of the National Academy of Sciences of the United States of America* 103:8888-8893

Dodds PN, Rathjen JP (2010) Plant immunity: towards an integrated view of plant-pathogen interactions. *Nature reviews Genetics* 11:539-548

El Kasmi F, Chung EH, Anderson RG, Li J, Wan L, Eitas TK, Gao Z, Dangl JL (2017) Signaling from the plasma-membrane localized plant immune receptor RPM1 requires self-association of the full-length protein. *Proceedings of the National Academy of Sciences of the United States of America* 114:E7385-E7394

Elmore JM, Lin ZJ, Coaker G (2011) Plant NB-LRR signaling: upstreams and downstreams. *Current opinion in plant biology* 14:365-371

Eschen-Lippold L, Jiang X, Elmore JM, Mackey D, Shan L, Coaker G, Scheel D, Lee J (2016) Bacterial AvrRpt2-Like Cysteine Proteases Block Activation of the Arabidopsis Mitogen-Activated Protein Kinases, MPK4 and MPK11. *Plant Physiol* 171:2223-2238

Fan J, Bai P, Ning Y, Wang J, Shi X, Xiong Y, Zhang K, He F, Zhang C, Wang R, Meng X, Zhou J, Wang M, Shirsekar G, Park CH, Bellizzi M, Liu W, Jeon JS, Xia Y, Shan L, Wang GL (2018) The Monocot-Specific Receptor-like Kinase SDS2 Controls Cell Death and Immunity in Rice. *Cell host & microbe* 23:498-510 e495

Gadal O, Strauss D, Kessler J, Trumppower B, Tollervey D, Hurt E (2001) Nuclear export of 60s ribosomal subunits depends on Xpo1p and requires a nuclear export sequence-containing factor, Nmd3p, that associates with the large subunit protein Rpl10p. *Molecular and cellular biology* 21:3405-3415

Gao Z, Chung EH, Eitas TK, Dangl JL (2011) Plant intracellular innate immune receptor Resistance to *Pseudomonas syringae* pv. *maculicola* 1 (RPM1) is activated at, and functions on, the plasma membrane. *Proceedings of the National Academy of Sciences of the United States of America* 108:7619-7624

Gill U, Nirmala J, Brueggeman R, Kleinhofs A (2012) Identification, characterization and putative function of HvRin4, a barley homolog of Arabidopsis Rin4. *Physiological and Molecular Plant Pathology* 80:41-49

Glowacki S, Macioszek VK, Kononowicz AK (2011) R proteins as fundamentals of plant innate immunity. *Cellular & molecular biology letters* 16:1-24

Grund E, Tremousaygue D, Deslandes L (2019) Plant NLRs with Integrated Domains: Unity Makes Strength. *Plant physiology* 179:1227-1235

Haasen D, Kohler C, Neuhaus G, Merkle T (1999) Nuclear export of proteins in plants: AtXPO1 is the export receptor for leucine-rich nuclear export signals in *Arabidopsis thaliana*. *The Plant Journal* 20:695-705

Hamilton A, Voinnet O, Chappell L, Baulcombe D (2002) Two classes of short interfering RNA in RNA silencing. *The EMBO journal* 21:4671-4679

Jeuken MJ, Zhang NW, McHale LK, Pelgrom K, den Boer E, Lindhout P, Michelmore RW, Visser RG, Niks RE (2009) Rin4 causes hybrid necrosis and race-specific resistance in an interspecific lettuce hybrid. *The Plant cell* 21:3368-3378

Jones JD, Dangl JL (2006) The plant immune system. *Nature* 444:323-329

Khan M, Subramaniam R, Desveaux D (2016) Of guards, decoys, baits and traps: pathogen perception in plants by type III effector sensors. *Current opinion in microbiology* 29:49-55

Kim HS, Desveaux D, Singer AU, Patel P, Sondek J, Dangl JL (2005a) The *Pseudomonas syringae* effector AvrRpt2 cleaves its C-terminally acylated target, RIN4, from Arabidopsis membranes to block RPM1 activation. *Proceedings of the National Academy of Sciences of the United States of America* 102:6496-6501

Kim MG, da Cunha L, McFall AJ, Belkhadir Y, DebRoy S, Dangl JL, Mackey D (2005b) Two *Pseudomonas syringae* type III effectors inhibit RIN4-regulated basal defense in Arabidopsis. *Cell* 121:749-759

Kim MG, Geng X, Lee SY, Mackey D (2009) The *Pseudomonas syringae* type III effector AvrRpm1 induces significant defenses by activating the Arabidopsis nucleotide-binding leucine-rich repeat protein RPS2. *The Plant journal : for cell and molecular biology* 57:645-653

Kumar K, Yadav S, Purayannur S, Verma PK (2013) An alternative approach in Gateway((R)) cloning when the bacterial antibiotic selection cassettes of the entry clone and destination vector are the same. *Molecular biotechnology* 54:133-140

Lee J, Manning AJ, Wolfgeher D, Jelenska J, Cavanaugh KA, Xu H, Fernandez SM, Michelmore RW, Kron SJ, Greenberg JT (2015) Acetylation of an NB-LRR Plant Immune-Effector Complex Suppresses Immunity. *Cell reports* 13:1670-1682

Liu J, Elmore JM, Lin ZJ, Coaker G (2011) A receptor-like cytoplasmic kinase phosphorylates the host target RIN4, leading to the activation of a plant innate immune receptor. *Cell host & microbe* 9:137-146

Luo Y, Caldwell KS, Wroblewski T, Wright ME, Michelmore RW (2009) Proteolysis of a negative regulator of innate immunity is dependent on resistance genes in tomato and *Nicotiana benthamiana* and induced by multiple bacterial effectors. *The Plant cell* 21:2458-2472

Macho AP, Zipfel C (2015) Targeting of plant pattern recognition receptor-triggered immunity by bacterial type-III secretion system effectors. *Current opinion in microbiology* 23:14-22

Mackey D, Belkhadir Y, Alonso JM, Ecker JR, Dangl JL (2003) Arabidopsis RIN4 Is a Target of the Type III Virulence Effector AvrRpt2 and Modulates RPS2-Mediated Resistance. *Cell* 112:379-389

Mackey D, Holt BF, Wiig A, Dangl JL (2002) RIN4 Interacts with *Pseudomonas syringae* Type III Effector Molecules and Is Required for RPM1-Mediated Resistance in Arabidopsis. *Cell* 108:743-754

Mazo-Molina C, Mainiero S, Haefner BJ, Bednarek R, Zhang J, Feder A, Shi K, Strickler SR, Martin GB (2020) Ptr1 evolved convergently with RPS2 and Mr5 to mediate recognition of AvrRpt2 in diverse solanaceous species. *The Plant journal : for cell and molecular biology* 103:1433-1445

Mindrinis M, Katagiri F, Yu G-L, Ausubel FM (1994) The *A. thaliana* disease resistance gene RPS2 encodes a protein containing a nucleotide-binding site and leucine-rich repeats. *Cell* 78:1089-1099

Monteiro F, Nishimura MT (2018) Structural, Functional, and Genomic Diversity of Plant NLR Proteins: An Evolved Resource for Rational Engineering of Plant Immunity. *Annual review of phytopathology* 56:243-267

Nimchuk Z, Marois E, Kjemtrup S, Leister RT, Katagiri F, Dangl JL (2000) Eukaryotic Fatty Acylation Drives Plasma Membrane Targeting and Enhances Function of Several Type III Effector Proteins from *Pseudomonas syringae*. *Cell* 101:353-363

Prado GS, Bamogo PKA, de Abreu JAC, Gillet FX, Dos Santos VO, Silva MCM, Brizard JP, Bemquerer MP, Bangratz M, Brugidou C, Sereme D, Grossi-de-Sa MF, Lacombe S (2019) *Nicotiana benthamiana* is a suitable transient system for high-level expression of an active inhibitor of cotton boll weevil alpha-amylase. *BMC biotechnology* 19:15

Prokchorchik M, Choi S, Chung EH, Won K, Dangl JL, Sohn KH (2020) A host target of a bacterial cysteine protease virulence effector plays a key role in convergent evolution of plant innate immune system receptors. *The New phytologist* 225:1327-1342

Redditt TJ, Chung EH, Karimi HZ, Rodibaugh N, Zhang Y, Trinidad JC, Kim JH, Zhou Q, Shen M, Dangl JL, Mackey D, Innes RW (2019) AvrRpm1 Functions as an ADP-Ribosyl Transferase to Modify NOI Domain-Containing Proteins, Including Arabidopsis and Soybean RPM1-Interacting Protein4. *The Plant cell* 31:2664-2681

Ren J, Wen L, Gao X, Jin C, Xue Y, Yao X (2008) CSS-Palm 2.0: an updated software for palmitoylation sites prediction. *Protein engineering, design & selection : PEDS* 21:639-644

Selote D, Kachroo A (2010a) RIN4-like proteins mediate resistance protein-derived soybean defense against *Pseudomonas syringae*. *Plant signaling & behavior* 5:1453-1456

Selote D, Kachroo A (2010b) RPG1-B-Derived Resistance to AvrB-Expressing *Pseudomonas syringae* Requires RIN4-Like Proteins in Soybean. *Plant physiology* 153:1199-1211

Slootweg E, Roosien J, Spiridon LN, Petrescu AJ, Tameling W, Joosten M, Pomp R, van Schaik C, Dees R, Borst JW, Smant G, Schots A, Bakker J, Govers A (2010) Nucleocytoplasmic distribution is required for activation of resistance by the potato NB-LRR receptor Rx1 and is balanced by its functional domains. *The Plant cell* 22:4195-4215

Sun X, Greenwood DR, Templeton MD, Libich DS, McGhie TK, Xue B, Yoon M, Cui W, Kirk CA, Jones WT, Uversky VN, Rikkerink EH (2014) The intrinsically disordered structural platform of the plant defence hub protein RPM1-interacting protein 4 provides insights into its mode of

action in the host-pathogen interface and evolution of the nitrate-induced domain protein family. *The FEBS journal* 281:3955-3979

Tahir J, Rashid M, Afzal AJ (2019) Post-translational modifications in effectors and plant proteins involved in host-pathogen conflicts. *Plant Pathology* 68:628-644

Tai TH, Dahlbeck D, Clark ET, Gajiwala P, Pasion R, Whalen MC, Stall RE, Staskawicz BJ (1999) Expression of the Bs2 pepper gene confers resistance to bacterial spot disease in tomato. *Proceedings of the National Academy of Sciences* 96:14153-14158

Takemoto D, Jones DA (2005) Membrane release and destabilization of Arabidopsis RIN4 following cleavage by *Pseudomonas syringae* AvrRpt2. *Molecular plant-microbe interactions : MPMI* 18:1258-1268

Toruno TY, Shen M, Coaker G, Mackey D (2019) Regulated Disorder: Posttranslational Modifications Control the RIN4 Plant Immune Signaling Hub. *Molecular plant-microbe interactions : MPMI* 32:56-64

Van der Hoorn R (2002) Balancing selection favors guarding resistance proteins. *Trends in Plant Science* 7:67-71

van der Hoorn RA, Kamoun S (2008) From Guard to Decoy: a new model for perception of plant pathogen effectors. *The Plant cell* 20:2009-2017

Weng SL, Kao HJ, Huang CH, Lee TY (2017) MDD-Palm: Identification of protein S-palmitoylation sites with substrate motifs based on maximal dependence decomposition. *PLoS one* 12:e0179529

Whalen MC, Innes RW, Bent AF, Staskawicz BJ (1991) Identification of *Pseudomonas syringae* pathogens of Arabidopsis and a bacterial locus determining avirulence on both Arabidopsis and soybean. *The Plant cell* 3:49-59

Wilton M, Subramaniam R, Elmore J, Felsensteiner C, Coaker G, Desveaux D (2010) The type III effector HopF2 Pto targets Arabidopsis RIN4 protein to promote *Pseudomonas syringae* virulence. *Proceedings of the National Academy of Sciences* 107:2349-2354

Zhou F, Xue Y, Yao X, Xu Y (2006) CSS-Palm: palmitoylation site prediction with a clustering and scoring strategy (CSS). *Bioinformatics* 22:894-896

Zipfel C (2014) Plant pattern-recognition receptors. *Trends in immunology* 35:345-351